Electronic Supplementary Material (ESI) for Organic & Biomolecular Chemistry.

Table of Contents

General synthetic methods
Chemicals were purchased from Sigma Aldrich Chemie GmbH (Steinheim, Germany), Carbolution Chemicals GmbH (St. Ingbert, Germany), or Carl Roth (Karlsruhe, Germany) and used without purification. Solvents for column chromatography were purchased in p.a. grade and purified by distillation. Thin-layer chromatography (TLC) was performed with 0.2 mm precoated plastic sheets Polygram Sil G/UV254 purchased from Machery-Nagel (Düren, Germany). Column chromatography was performed using silica gel 60 purchased from Merck (Darmstadt, Germany).

NMR spectroscopy
NMR spectra were recorded on a Bruker (Billerica, MA, USA) Avance I (300 MHz), Avance I (400 MHz), Avance I (500 MHz), Avance III HD Prodigy (500 MHz) or an Avance III HD Cryo (700 MHz) NMR spectrometer. Spectra were measured in C_6D_6 and referenced against solvent signals (^{1}H-NMR, residual proton signal: δ = 7.16; ^{13}C-NMR: δ = 128.06).[1]

GC/MS
GC/MS analyses were performed on a 5977A GC/MSD system (Agilent, Santa Clara, CA, USA) with a 7890B GC and a 5977A mass selective detector. The GC was equipped with a HP5-MS fused silica capillary column (30 m, 0.25 mm i. d., 0.50 μm film). Specific GC settings were 1) inlet pressure: 77.1 kPa, He at 23.3 mL min^{-1}, 2) injection volume: 1 μL, 3) temperature program: 5 min at 50 °C increasing at 10 °C min^{-1} to 320 °C, 4) 60 s valve time, and 5) carrier gas: He at 1.2 mL min^{-1}. MS settings were 1) source: 230 °C, 2) transfer line: 250 °C, 3) quadrupole: 150 °C and 4) electron energy: 70 eV. Retention indices (*I*) were determined from retention times in comparison to the retention times of *n*-alkanes (C_7-C_{40}).

HRMS
High resolution mass spectra were recorded with LTQ Orbitrap XL (Thermo Fisher Scientific, Waltham. Massachusetts, USA).

HPLC
Analytical scale HPLC seperation was carried out using a Azura series HPLC system (Knauer, Berlin, Germany), equipped with PAD-1 photodiode array detector (190–1000 nm) or Refractive index detector and a Daicel Industries Ltd., Japan Chiralpak IG-U column (1.6 μm; 3.0 mm × 100 mm). Preparative scale HPLC purification was performed on an Azura series HPLC system (Knauer, Berlin, Germany) with a multi wavelength detector MWL 2.1L (190 – 700 nm) using a Phenomenex - Lux i-Amylose 3 chiral column (5 µm; 21.2 x 250 mm) or Refractive index detector using YMC Europe - ChiralART Cellulose-SC chiral column (5 µm; 20 x 250 mm).

IR spectroscopy
IR spectra were recorded on a Bruker α infrared spectrometer with a diamond ATR probehead. Peak intensities are given as s (strong), m (medium), w (weak) and br (broad).

Optical rotations
Optical rotations were recorded on a Modular Compact Polarimeter MCP 100 (Anton Paar, Graz, Austria). The temperature setting was 25 °C; the wavelength of the light used was 589

nm (sodium D line); the path-length was 10 cm; the compound concentrations *c* are given in g 100 mL^{-1}.

X-ray crystallograpy

Crystals of **10** were obtained by recrystallisation from petrol ether / ethyl acetate (10:1), and crystals of **18**, *ent*-**18** and *ent*-**19** were obtained by recystallisation from pentane.

A clear colourless needle of **10** (0.30 x 0.10 x 0.06 mm), a clear colourless plank-like specimen of **18** (0.20 x 0.17 x 0.12 mm^3), a colourless plank-like specimen of *ent*-**18** (0.30 x 0.18 x 0.05 mm^3), and a colourless needle-like specimen of *ent*-**19** (0.60 x 0.16 x 0.04 mm^3) were mounted on a STOE STADIVARI Eulerian 4-circle diffractometer equipped with a low-temperature device (100(2)K, Oxford Cryostream 800er series, Oxford Cryosystems) by using Cu-*K*α-radiation (λ = 1.54186 Å, ASTIX++-optics) and a PILATUS 200K Pixel detector system. Intensities were measured by fine-slicing φ- and ω-scans and corrected for background, polarization and Lorentz effects. A semi-empirical absorption correction by scaling of reflection intensities with a subsequent spherical absorption correction was performed with LANA.[2]

Structure solutions were done using intrinsic phasing methods included in the SHELXT program system[3] and refined by full matrix least-squares/difference Fourier syntheses with ShelXL-2018/4).[4] All non-hydrogen atoms were refined anisotropically; hydrogen atoms were placed in geometrically calculated positions and included using a riding model on the bound carbon atoms and relative isotropic displacement parameters. Olex2 was used for graphical representations of the molecular structures.[5]

CCDC numbers 2356914 (**10**), 2356915 (**18**), 2356916 (*ent*-**18**), and 2356917 (*ent*-**19**) contain the supplementary crystallographic data for this paper, which can be obtained free of charge from the Cambridge Crystallographic Data Centre via http://www.ccdc.cam.ac.uk/data request/cif.

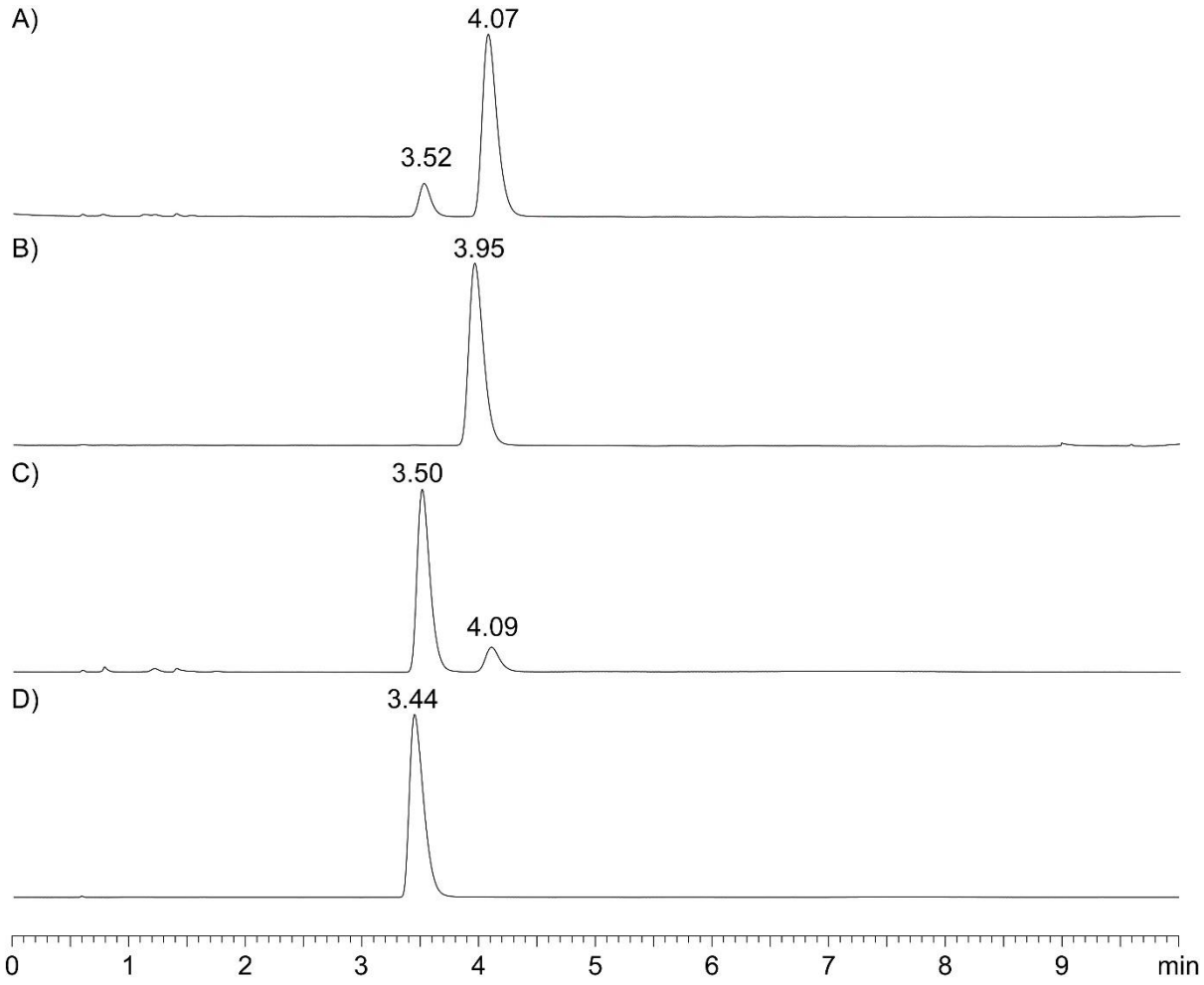

Figure S1. Determination of the enantiomeric purity of **18** and *ent*-**18** by HPLC using a chiral stationary phase. A) Synthetic **18** before repeated crystallisation (74% *ee*), and B) after repeated crystallisation. C) Synthetic *ent*-**18** before repeated crystallisation (73% *ee*), and D) after repeated crystallisation.

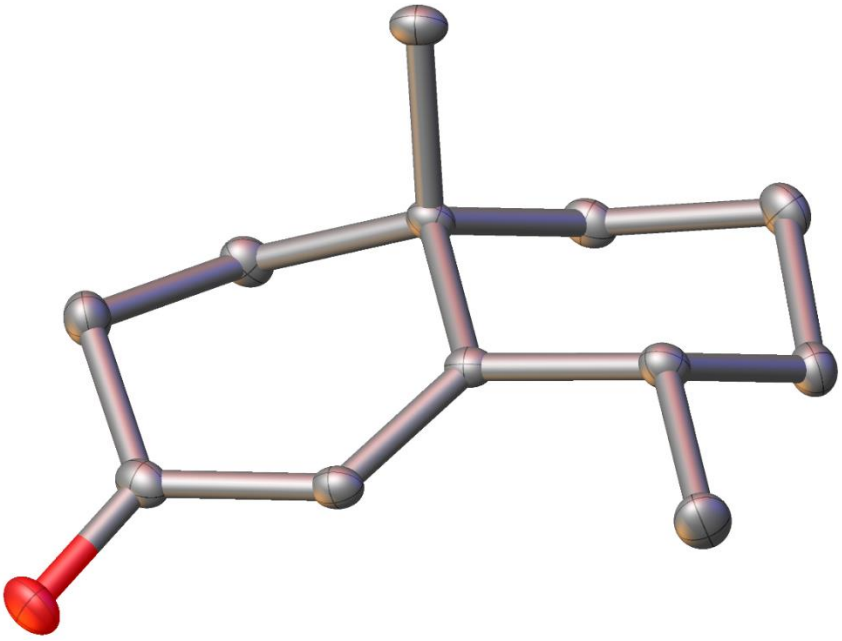

Figure S2. ORTEP illustration of **18**.

Table S1. Crystal data and structure refinement for **18**.

crystal habitus	clear colourless plank
device type	STOE STADIVARI
empirical formula	$C_{12}H_{18}O$
moiety formula	$C_{12}H_{18}O$
formula weight	178.26
temperature / K	100
crystal system	orthorhombic
space group	$P2_12_12_1$
a / Å	7.3252(3)
b / Å	9.8946(3)
c / Å	14.0386(4)
α = β = γ / °	90
volume / Å^3	1017.52(6)
Z	4
ρ_{calc} / g cm^{-3}	1.164
μ / mm^{-1}	0.55
F(000)	392
crystal size/mm^3	0.2 × 0.17 × 0.12
absorption correction	multi-scan
Tmin; Tmax	0.7561; 0.9299
radiation	Cu-*K*α (λ = 1.54186)
2Θ range for data collection	10.94° to 140.806°
completeness to Θ	1
index ranges	-8 ≤ h ≤ 7, -5 ≤ k ≤ 12, -16 ≤ l ≤ 16
reflections collected	8835
independent reflections	1918 [R_{int} = 0.0236, R_{sigma} = 0.0174]
data / restraints / parameters	1918/0/120
goodness-of-fit on F^2	1.037
final R indexes [I>=2σ (I)]	R_1 = 0.0317, wR_2 = 0.0802
final R indexes [all data]	R_1 = 0.0336, wR_2 = 0.0815
Largest diff. peak/hole / e Å^{-3}	0.12/-0.18
Flack parameter	0.01(17)
Bijvoet-pair Bayesian statistics	P2(true) = 1.000; P3(true) = 0.998; P3(rac-twin) = 0.002; P3(false) = $0.2 \cdot 10^{-10}$
CCDC accession no.	2356915

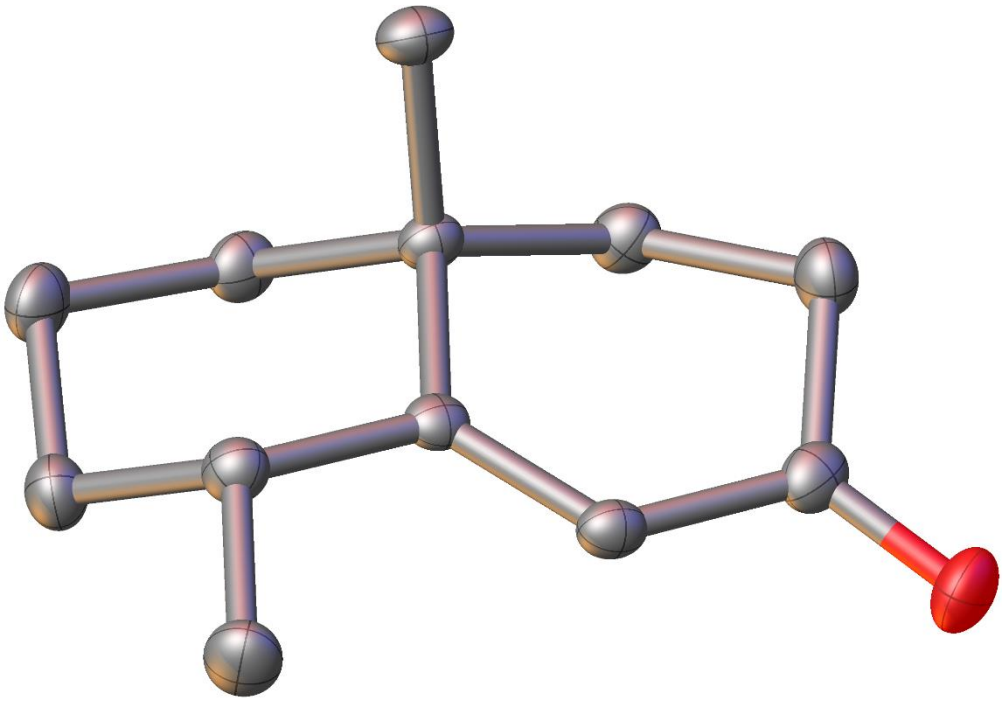

Figure S3. ORTEP illustration of *ent*-**18**.

Table S2. Crystal data and structure refinement for *ent*-**18**.

crystal habitus	clear colourless plank
device type	STOE STADIVARI
empirical formula	$C_{12}H_{18}O$
moiety formula	$C_{12}H_{18}O$
formula weight	178.26
temperature / K	100
crystal system	orthorhombic
space group	$P2_12_12_1$
a / Å	7.32486(22)
b / Å	9.9130(3)
c / Å	14.0128(6)
α = β = γ / °	90
volume / Å^3	1017.49(6)
Z	4
ρ_{calc} / g cm^{-3}	1.164
μ / mm^{-1}	0.55
F(000)	392
crystal size/mm^3	0.3 × 0.18 × 0.05
absorption correction	multi-scan
Tmin; Tmax	0.7672; 0.8823
radiation	Cu-*K*α (λ = 1.54186)
2Θ range for data collection	10.932° to 141.09°
completeness to Θ	1
index ranges	-8 ≤ h ≤ 2, -12 ≤ k ≤ 11, -16 ≤ l ≤ 16
reflections collected	9605
independent reflections	1918 [R_{int} = 0.0243, R_{sigma} = 0.0173]
data / restraints / parameters	1918/0/121
goodness-of-fit on F^2	1.048
final R indexes [I>=2σ (I)]	R_1 = 0.0294, wR_2 = 0.0739
final R indexes [all data]	R_1 = 0.0311, wR_2 = 0.0751
Largest diff. peak/hole / e Å^{-3}	0.13/-0.15
Flack parameter	0.1(3)
Bijvoet-pair Bayesian statistics	P2(true) = 1.000; P3(true) = 1.000; P3(rac-twin) = $0.2\cdot10^{-3}$; P3(false) = $0.4\cdot10^{-14}$
CCDC accession no.	2356916

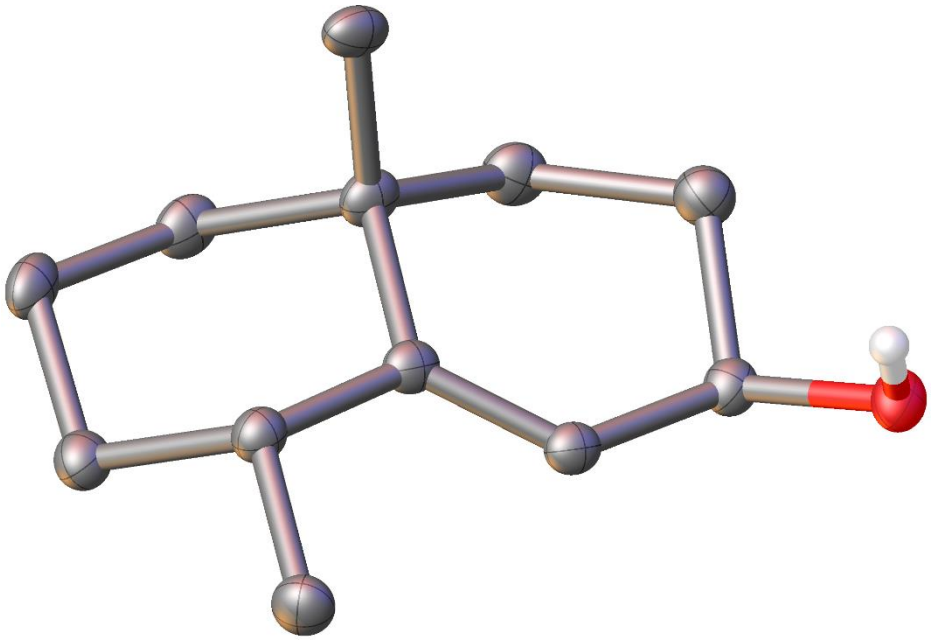

Figure S4. ORTEP illustration of *ent*-**19**.

Table S3. Crystal data and structure refinement for *ent*-**19**.

crystal habitus	clear colourless needle
device type	STOE Stadivari
empirical formula	$C_{12}H_{20}O$
moiety formula	$C_{12}H_{20}O$
formula weight	180.28
temperature / K	100
crystal system	orthorhombic
space group	$P2_12_12$
a / Å	36.7093(10)
b / Å	26.4549(9)
c / Å	6.8153(2)
α = β = γ / °	90
volume / Å^3	6618.6(3)
Z	24
ρ_{calc} / g cm^{-3}	1.086
μ / mm^{-1}	0.506
F(000)	2400
crystal size/mm^3	0.6 × 0.16 × 0.04
absorption correction	multi-scan
Tmin; Tmax	0.7149; 0.9742
radiation	Cu-*K*α (λ = 1.54186)
2Θ range for data collection	9.638° to 135.488°
completeness to Θ	0.997
index ranges	-43 ≤ h ≤ 44, -29 ≤ k ≤ 31, -4 ≤ l ≤ 8
reflections collected	77736
independent reflections	11933 [R_{int} = 0.0670, R_{sigma} = 0.0328]
data / restraints / parameters	11933/0/722
goodness-of-fit on F^2	1.027
final R indexes [I>=2σ (I)]	R_1 = 0.0766, wR_2 = 0.1929
final R indexes [all data]	R_1 = 0.0972, wR_2 = 0.2194
Largest diff. peak/hole / e Å^{-3}	0.46/-0.28
Flack parameter	0.1(3)
Bijvoet-pair Bayesian statistics	P2(true) = 1.000; P3(true) = 0.868; P3(rac-twin) = 0.132; P3(false) = $0.8 \cdot 10^{-4}$
CCDC accession no.	2356917

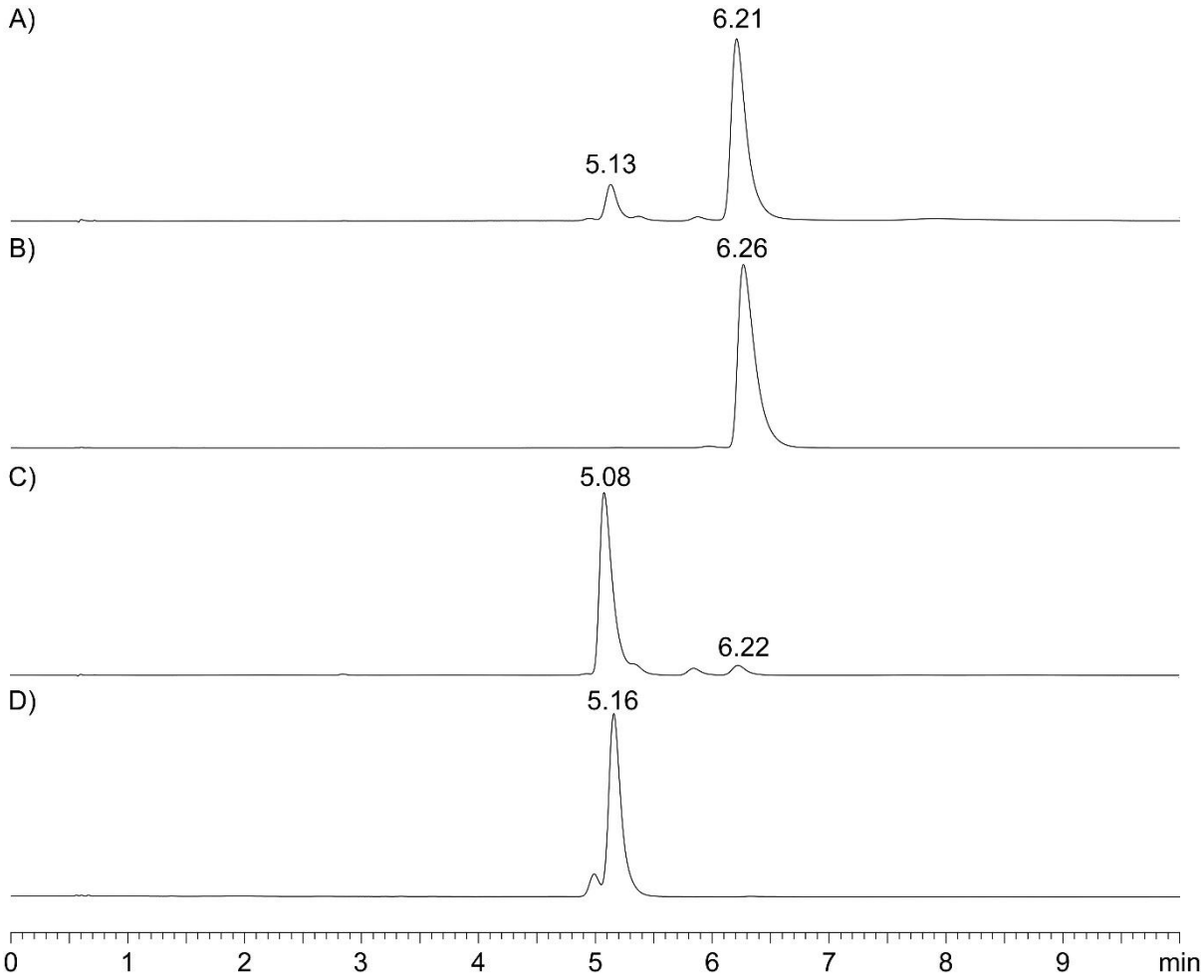

Figure S5. Determination of the enantiomeric purity of **23** and *ent*-**23** by HPLC using a chiral stationary phase. A) Synthetic **23** before repeated crystallisation (77% *ee*), and B) after repeated crystallisation. C) Synthetic *ent*-**23** before repeated crystallisation (88% *ee*), and D) after repeated crystallisation.

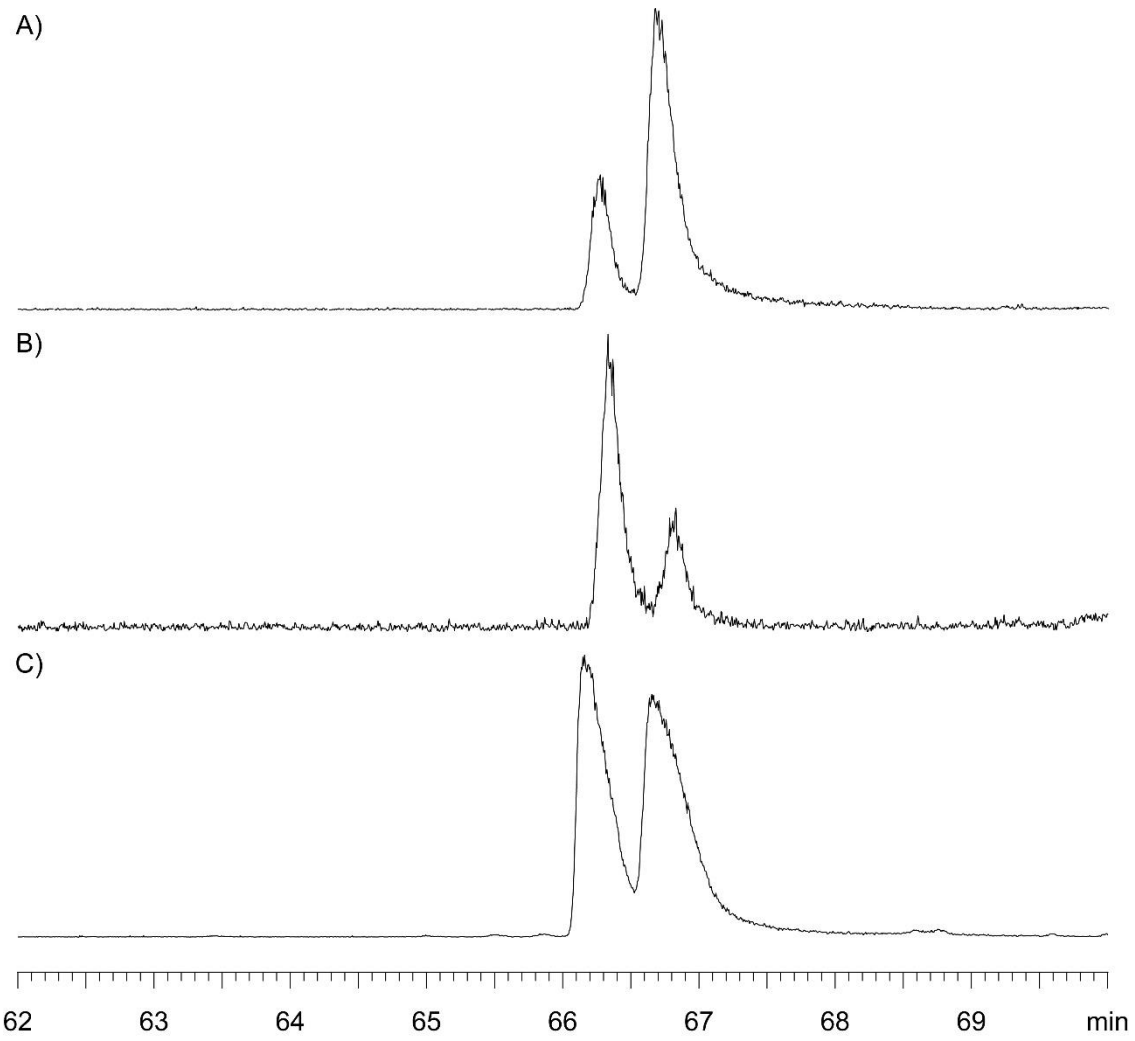

Figure S6. Determination of the enantiomeric purity of **34** and *ent*-**34** by GC using a chiral stationary phase. A) Synthetic **34** obtained from **29** using the chiral ligand (*S*)-*t*-Bu-PHOX (**30**), B) synthetic *ent*-**34** obtained from **29** using the chiral ligand (*R*)-*t*-Bu-PHOX (*ent*-**30**), C) racemic **34**.

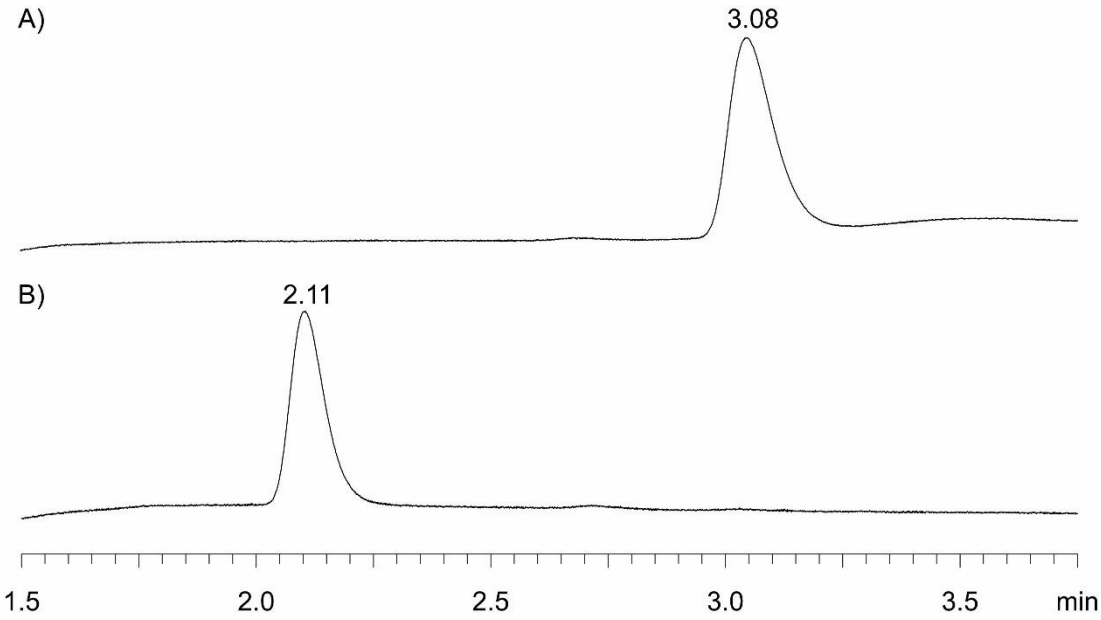

Figure S7. Determination of the enantiomeric purity of **34** and *ent*-**34** by HPLC using a chiral stationary phase. A) Synthetic **34** after HPLC, B) Synthetic *ent*-**34** after HPLC.

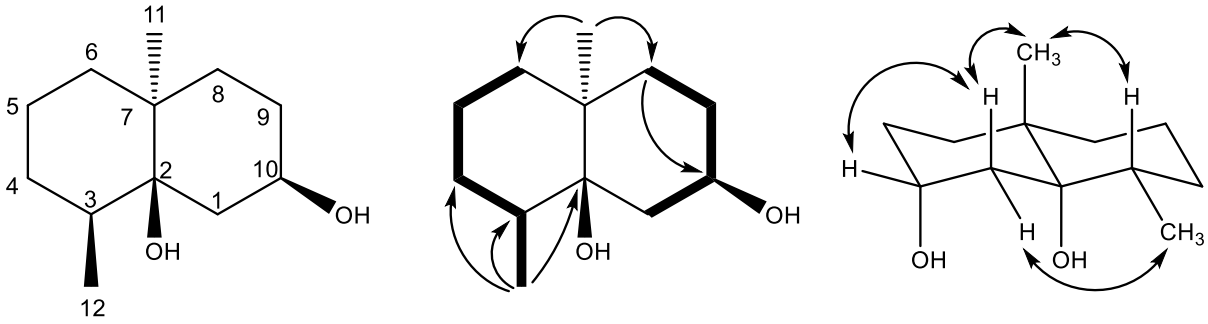

Figure S8. Structure elucidation of synthetic **10**. Bold: ^{1}H,^{1}H-COSY, single headed arrows: key HMBC, and double headed arrows: NOESY correlations.

Table S4. NMR data of **10** in $CDCl_3$ recorded at 298 K.

C[a]	type	^{13}C[b]	^{1}H[b]	^{13}C[c]
1	CH_2	35.1	1.92 (m, H_β) 1.53 (dd, *J* = 14.8, 3.2, H_α)	34.8
2	C	76.7		76.4
3	CH	34.2	1.66 (m)	34.0
4	CH_2	29.9	1.39 (m)	29.7
5	CH_2	34.8	1.66 (m, H_α) 1.03 (m, H_β)	34.6
6	CH_2	20.8	1.66 (m, H_α) 1.47 (m, H_β)	20.6
7	C	37.7		37.5
8	CH_2	30.5	1.97 (ddd, *J* = 13.6, 13.6, 3.9, H_β) 0.95 (ddd, *J* = 13.2, 4.5, 2.1, H_α)	30.3
9	CH_2	29.0	1.91 (m, H_α) 1.71 (m, H_β)	28.7
10	CH	68.3	4.12 (br s)	68.0
11	CH_3	20.2	1.01 (s)	20.0
12	CH_3	15.1	0.84 (d, *J* = 6.6)	14.9

[a] Carbon numbering as shown in Figure S8 indicates the origin of each carbon from FPP by same number. [b] Chemical shifts δ in ppm. Multiplicity: s = singlet, d = doublet, m = multiplet, br = broad. Coupling constants *J* are given in Hertz. [c] Reference data from the literature recorded in $CDCl_3$.[2]

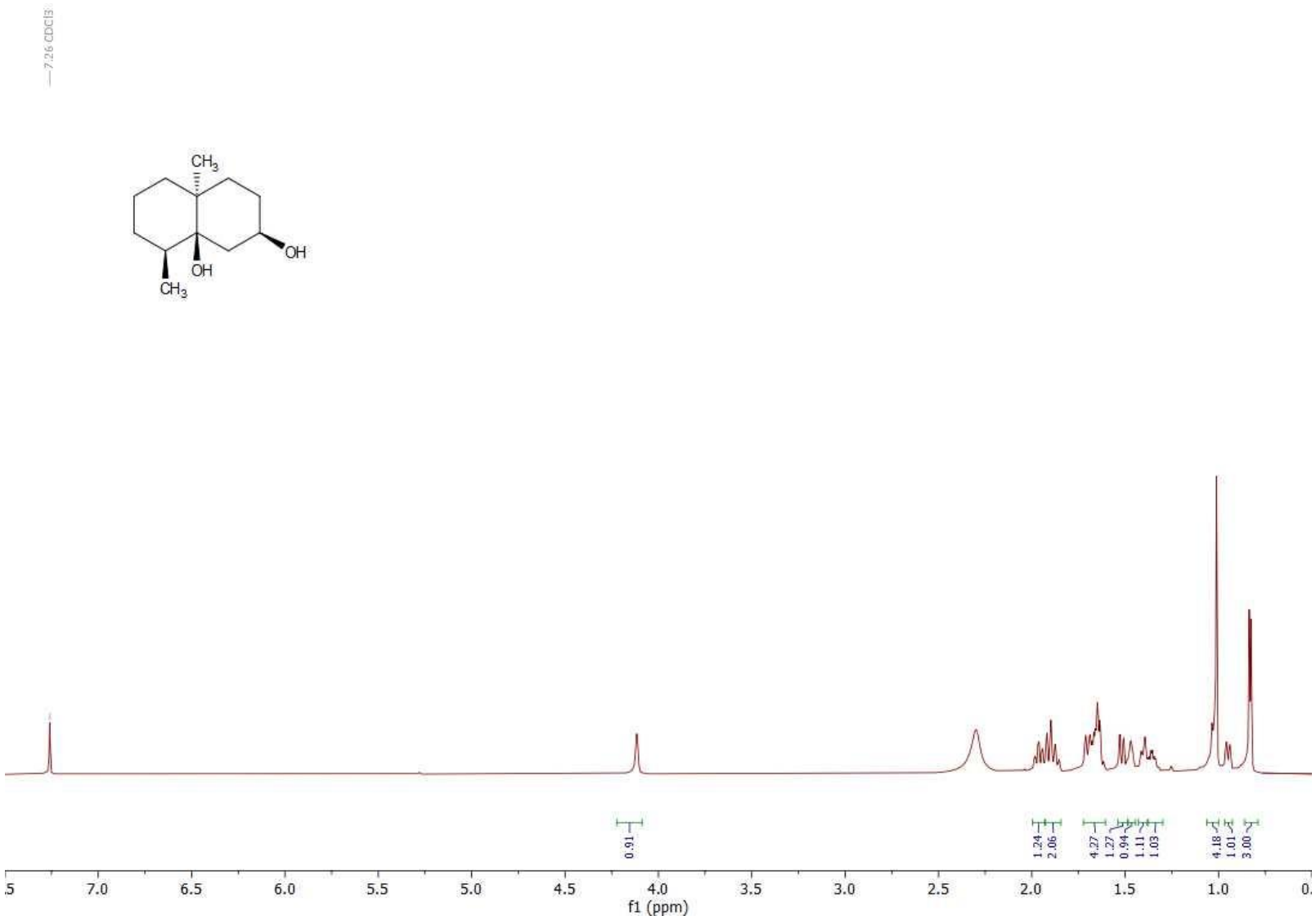

Figure S9. ^{1}H-NMR spectrum of **10** (700 MHz, $CDCl_3$).

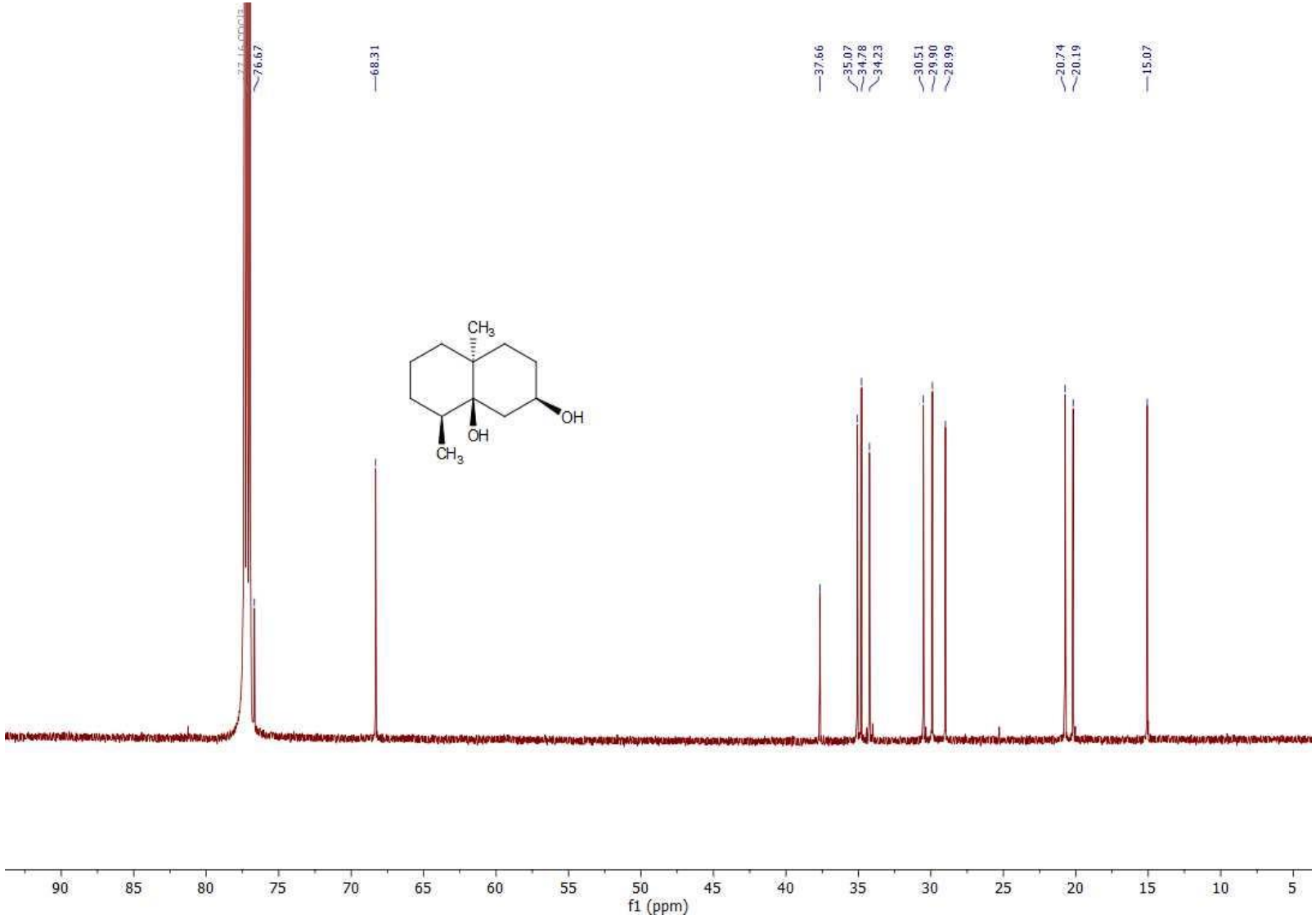

Figure S10. ^{13}C-NMR spectrum of **10** (176 MHz, $CDCl_3$).

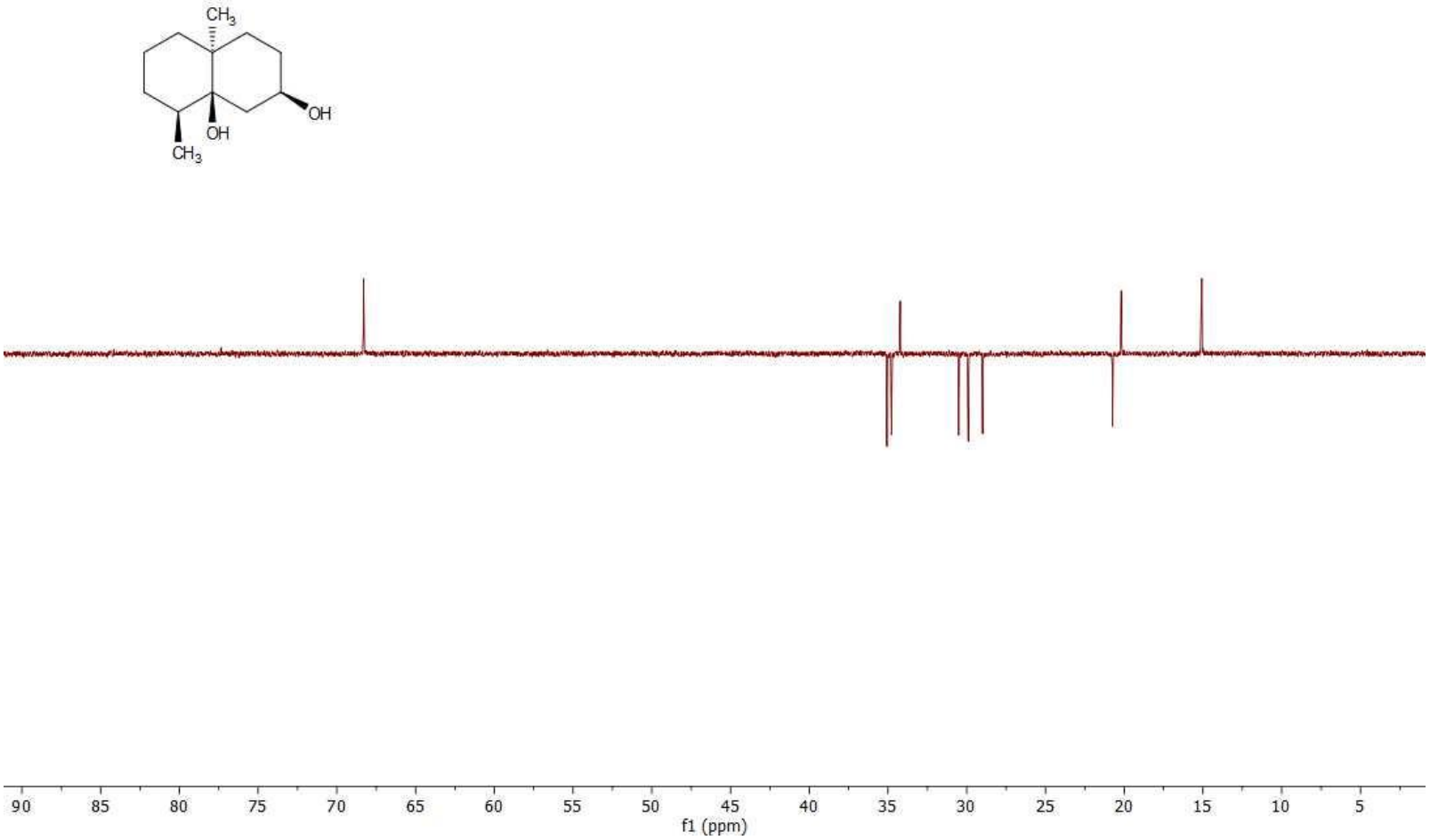

Figure S11. ^{13}C-DEPT135 spectrum of **10** (176 MHz, $CDCl_3$).

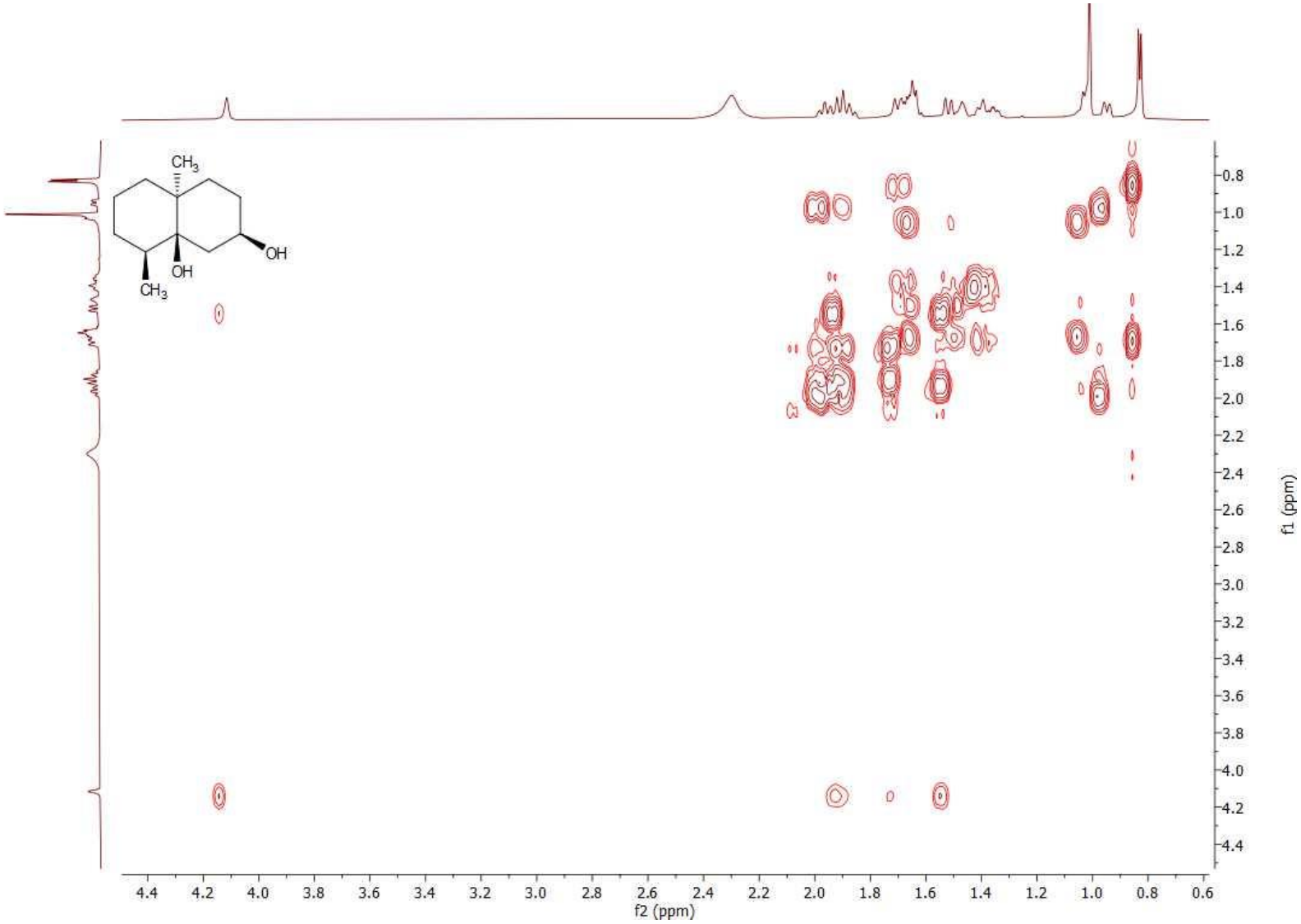

Figure S12. ^{1}H-^{1}H-COSY spectrum ($CDCl_3$) of **10**.

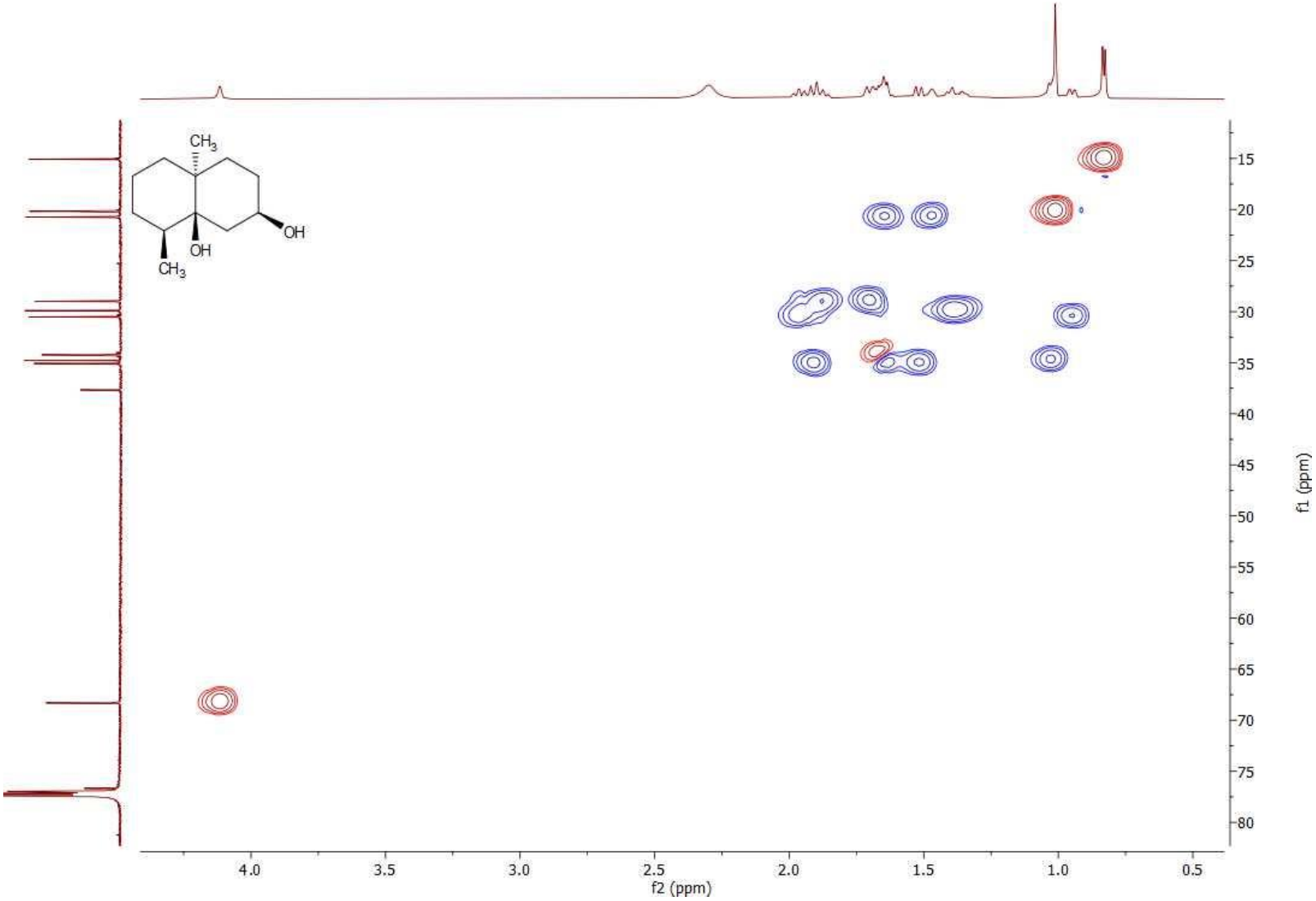

Figure S13. HSQC spectrum ($CDCl_3$) of **10**.

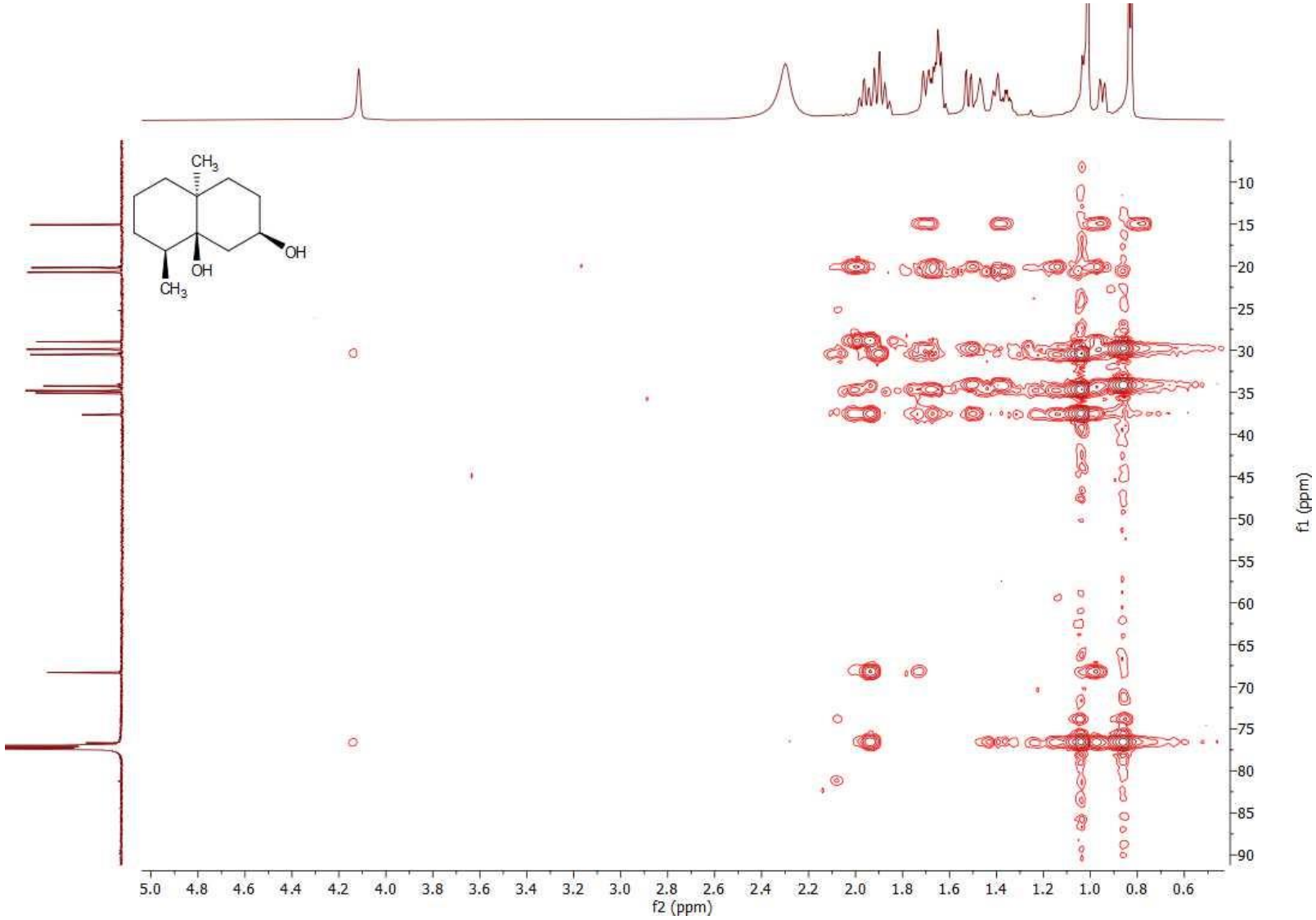

Figure S14. HMBC spectrum ($CDCl_3$) of **10**.

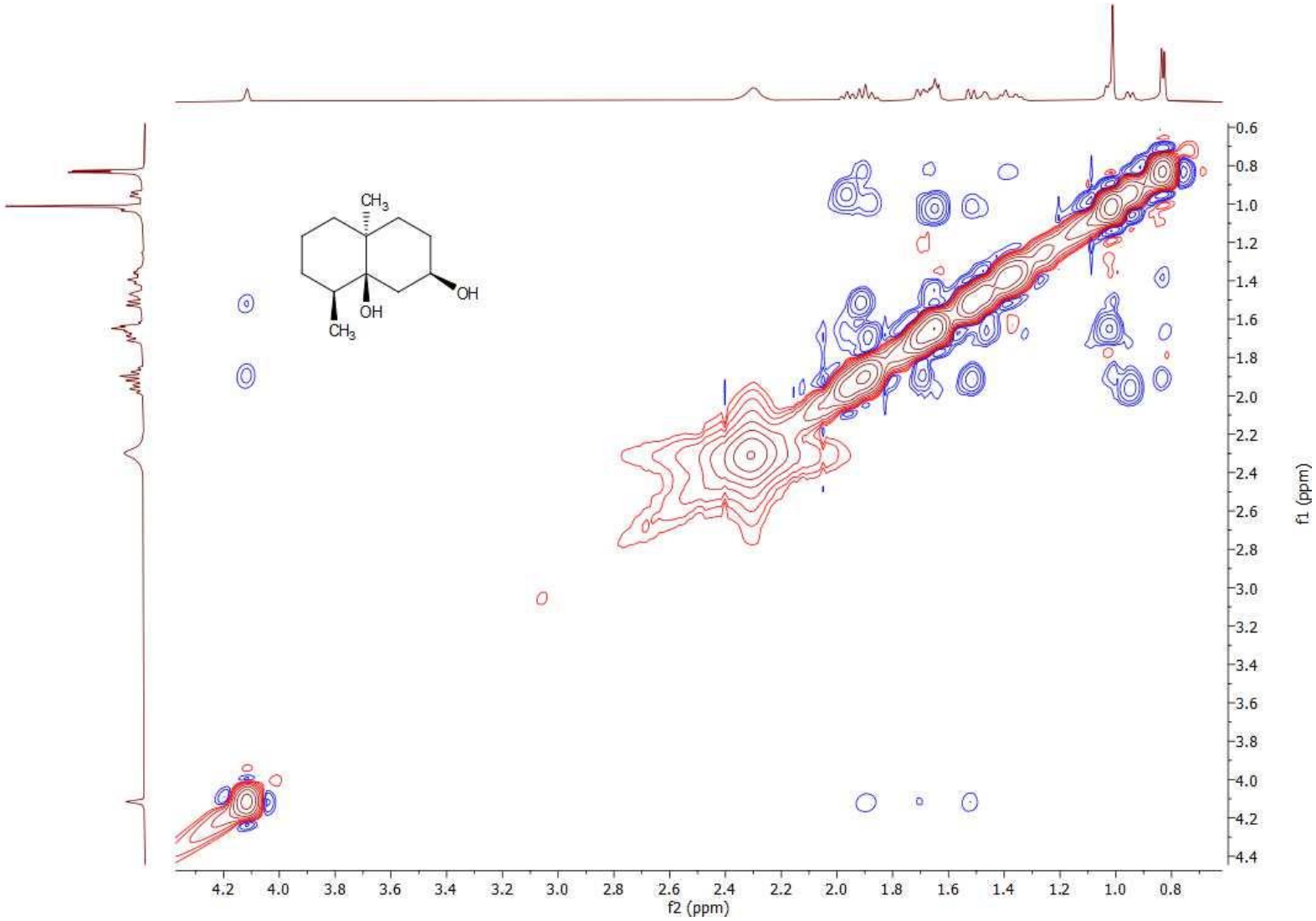

Figure S15. NOESY spectrum ($CDCl_3$) of **10**.

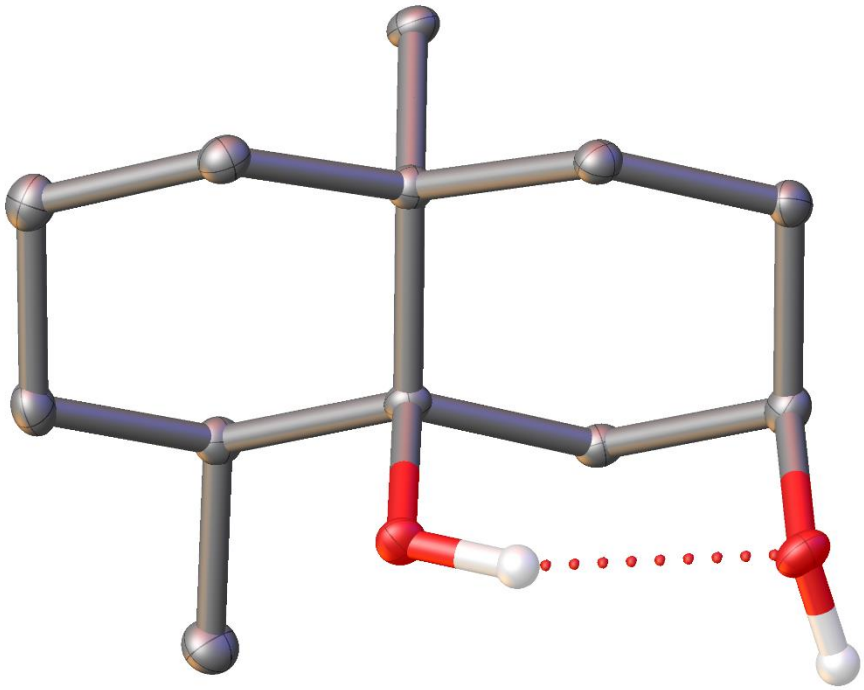

Figure S16. ORTEP illustration of **10**.

Table S5. Crystal data and structure refinement for **10**.

crystal habitus	clear colourless needle
device type	STOE STADIVARI
empirical formula	$C_{12}H_{22}O_2$
moiety formula	$C_{12}H_{22}O_2$
formula weight	198.3
temperature / K	100
crystal system	orthorhombic
space group	$P2_12_12_1$
a / Å	6.3202(3)
b / Å	11.5648(5)
c / Å	15.4255(9)
α = β = γ / °	90
volume / Å^3	1127.48(10)
Z	4
ρ_{calc} / g cm^{-3}	1.168
μ / mm^{-1}	0.6
F(000)	440
crystal size/mm^3	0.3 × 0.1 × 0.06
absorption correction	multi-scan
Tmin; Tmax	0.7297; 0.9228
radiation	Cu-*K*α (λ = 1.54186)
2Θ range for data collection	9.558° to 141.062°
completeness to Θ	1
index ranges	-7 ≤ h ≤ 4, -11 ≤ k ≤ 14, -18 ≤ l ≤ 18
reflections collected	14494
independent reflections	2141 [R_{int} = 0.0598, R_{sigma} = 0.0371]
data / restraints / parameters	2141/0/131
goodness-of-fit on F^2	1.051
final R indexes [I>=2σ (I)]	R_1 = 0.0387, wR_2 = 0.0911
final R indexes [all data]	R_1 = 0.0473, wR_2 = 0.0958
Largest diff. peak/hole / e Å^{-3}	0.20/-0.22
Flack parameter	-0.12(18)
Bijvoet-pair Bayesian statistics	P2(true) = 1.000; P3(true) = 1.000; P3(rac-twin) = $0.5\cdot10^{-4}$; P3(false) = $0.2\cdot10^{-13}$
CCDC accession no.	2356914

Strains and culture conditions

Streptomyces ambofaciens ATCC 23877 and *Streptomyces reticuli* DSM 101095 were grown in medium 65 (4.0 g glucose, 4.0 g yeast extract, 10.0 g malt extract, 1 L water, pH 7.2) at 30 °C, *E. coli* BL21 (DE3) was grown in LB medium at 37 °C, and *Saccharomyces cerevisiae* was grown in YPAD medium (20 g glucose, 10 g yeast extract, 20 g peptone, 40 mg adenine sulfate, 1 L water) at 30 °C.

CLSA headspace analysis

Streptomyces ambofaciens ATCC 23877 and *Streptomyces reticuli* DSM 101095 were grown on 65 agar medium at 28 °C for two days and then subjected for headspace extraction to a CLSA[6] for 24 h. The released volatiles were collected on charcoal filters (Chromtech, Idstein, Germany), followed by extraction of the filters with dichloromethane (50 μL) and analysis of the extracts by GC/MS.

Gene cloning

The gene sequence encoding the geosmin synthase from *Streptomyces ambofaciens* ATCC 23877 (accession number WP_053138925)[7] was cloned into the pYE-Express expression vector[8] through homologous recombination in yeast. For this purpose, the geosmin synthase gene was amplified from gDNA using the short primers listed in Table S6, followed by a second PCR using the PCR product as a template and the long primers listed in Table S6 containing homology arms with homologous sequences to the end sequences of the linearised pYE-Express vector (EcoRI and HindIII digestion). Q5 High-fidelity DNA polymerase (New England Biolabs, Ipswich, MA, USA) was used for all PCRs. PCR conditions were: initial denaturation at 98 °C, 1 min; 3-step cycle: 98 °C, 10 sec; 64.5 °C, 30 sec; 72 °C, 60 sec; repeated 35 times; final elongation at 72 °C, 2 min.

The PCR products together with the linearised pYE-Express shuttle vector (EcoRI and HindIII digestion) were used for a yeast homologous recombination through a standard protocol using PEG, LiOAc and salmon sperm DNA.[9] Cells were plated on YPAD medium and the cultures were grown at 28 °C for 2 days. Plasmid DNA was isolated using the Zymoprep™ Kit (Yeast Plasmid Miniprep) and then shuttled into *E. coli* electrocompetent cells by electroporation. Cells were grown overnight at 37 °C on LB agar plates (kanamycin 50 μg mL^{-1}). Single colonies were selected to inoculate LB medium (10 mL) with kanamycin (10 μL; 50 mg mL^{-1}), followed by culturing for 12 h and isolation of plasmid DNA. The sequence of the cloned gene was verified by DNA sequencing. The plasmid was named pYE-GeoS (*Streptomyces ambofaciens* ATCC 23877 geosmin synthase).

Table S6. Primers used in this study.

Primer	Nucleotide sequence (5'→3')[a]
WP_053138925_Fw	atgacgcaacagcccttcgaac
WP_053138925_Rv	tcaggccgtcggcacgg
WP_053138925_LFw	GGCAGCCATATGGCTAGCATGACTGGTGGAatgacgcaacagcccttcgaac
WP_053138925_LRv	TCTCAGTGGTGGTGGTGGTGGTGCTCGAGTtcaggccgtcggcacgg

[a] Sequences of homology arms for homologous recombination in yeast are indicated by capital letters, priming sequences for the target genes are indicated by small letters.

Gene expression and protein purification

E. coli BL21 (DE3) cells harboring the expression plasmid (pYE-GeoS) were used to inoculate a starter culture in LB medium (10 mL) supplied with kanamycin (50 μg/mL), which was grown

with shaking at 37 °C overnight. The starter culture was used to inoculate the expression culture (1/100 v/v) in LB medium (1 L) with kanamycin and the cells were grown with shaking at 37 °C until OD_{600} = 0.4 – 0.6 was reached. The culture was cooled to 18 °C, before IPTG (0.4 mM final concentration) was added to induce expression. The culture was shaken at the same temperature overnight and then centrifuged (3500 x g, 40 min, 4 °C).
For the preparation of geosmin synthase the medium was discarded and the cell pellet was resuspended in binding buffer (10 mL L^{-1} culture; 20 mM Na_2HPO_4, 500 mM NaCl, 20 mM imidazole, 1 mM $MgCl_2$, pH 7.4, 4 °C).[10] The cells were lysed by ultrasonication (10 x 1 min) under ice cooling. The cell debris was spun down (14600 x g, 10 min, 4 °C), the protein solution was filtered with disposable syringe filter (MACHEREY-NAGEL GmbH & Co. KG), and loaded onto a Ni^{2+}-NTA affinity chromatography column (10 mL column volume; Ni-NTA superflow, Qiagen, Venlo, Netherlands). The column was washed with two column volumes of binding buffer (10 mL L^{-1} culture) to elute non-binding proteins, followed by desorption of the target protein from the stationary phase with two column volumes of elution buffer (10 mL L^{-1} culture; 20 mM Na_2HPO_4, 500 mM NaCl, 500 mM imidazole, 1 mM $MgCl_2$, pH 7.4, 4 °C) with fractionation. The fractions were analysed by SDS-PAGE and fractions containing pure protein were pooled (Figure S17) and used for incubation experiments. The protein concentration was determined through Bradford assay[11] and adjusted to 1.6 mg/mL.

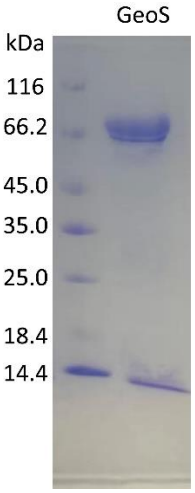

Figure S17. SDS-PAGE analysis of purified recombinant GeoS from *Streptomyces ambofaciens* ATCC 23877.

Small scale incubation of FPP with recombinant GeoS
Analytical scale incubations were performed with substrate (FPP, 0.5 mg) dissolved in substrate buffer (0.1 mL, 25 mM NH_4HCO_3). After dilution with incubation buffer (0.5 mL, 50 mM Tris, 10 mM $MgCl_2$, 20% glycerol, pH = 7.1), enzyme elution fraction (0.4 mL, containing 1.6 mg mL^{-1} enzyme) was added. The reaction mixture was incubated at 30 °C with shaking for 15 h, followed by extraction with hexane (200 µL). The organic layer was dried with $MgSO_4$ and analysed by GC/MS (Figure S18).

Preparative scale incubation of FPP with recombinant GeoS and isolation of 38
For a preparative scale incubation, FPP (100 mg) was dissolved in substrate buffer (20 mL), followed by addition of incubation buffer (155 mL, pH = 7.1). The reaction was started by addition of enzyme elution fraction (25 mL containing 1.6 mg mL^{-1} enzyme) from 8 L of expression culture and incubated at 30 °C with stirring overnight. The reaction mixture was then extracted with pentane (3 x 50 mL). The organic layers were dried with $MgSO_4$ and

concentrated under reduced pressure. Compounds **1** (5.0 mg), **3** (0.8 mg), and **5** (2.0 mg) were obtained by using column chromatography on silica gel with pentane and Et_2O.

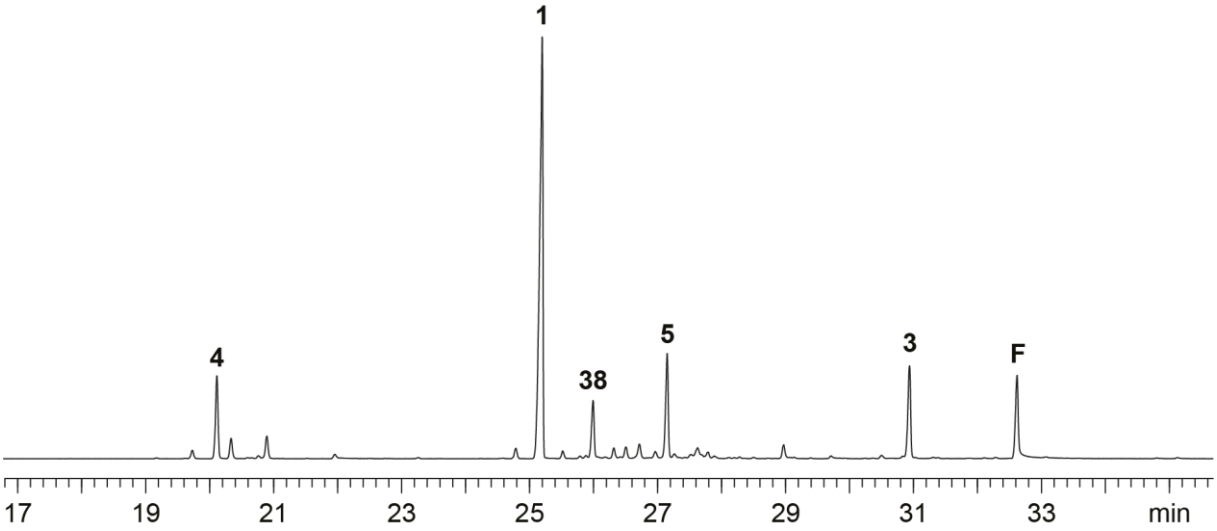

Figure S18. Total ion chromatogram of an extract from an enzyme incubation of FPP with GeoS. Peak labels refer to the compounds listed in Table S7.

Table S7. Identification of terpenes formed from FPP by GeoS.

Compound	*I*[a]	*I* (lit.)[b]	MS match[c]
(8*S*,9*R*,10*S*)-8,10-dimethyl-1-octalin (**4**)	1220	1224	907
geosmin (**1**)	1399	1399	925
isogeosmin (**38**)	1432		
germacrene D (**5**)	1477	1480	935
(1(10)*E*,5*E*)-germacradien-11-ol (**3**)	1634	1638	929
farnesol (**F**)	1708	1710	920

[a] Retention index on a HP5-MS GC column. [b] Retention index data from the literature on the same or a similar GC column. [c] Mass spectral match factor (0 – 999, 999 indicates identical mass spectra).

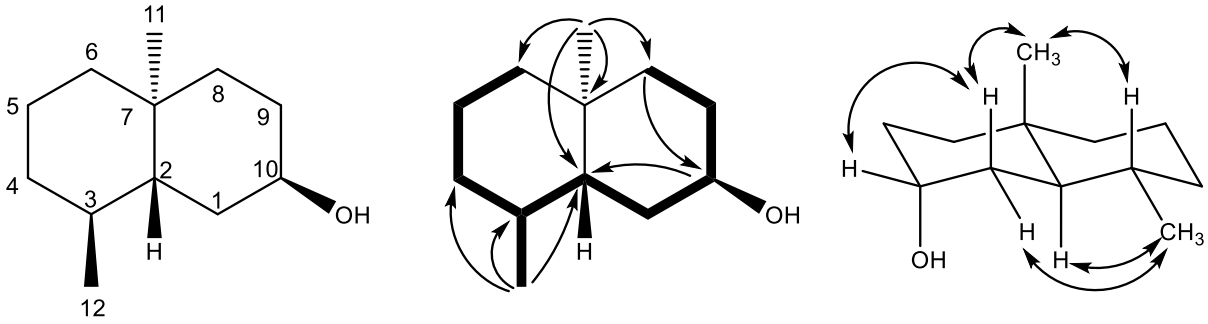

Figure S19. Structure elucidation of **38** isolated from the incubation of FPP with GeoS. Bold: ^{1}H,^{1}H-COSY, single headed arrows: key HMBC, and double headed arrows: NOESY correlations.

Table S8. NMR data of **38** in C_6D_6 recorded at 298 K.

C[a]	type	^{13}C[b]	^{1}H[b]
1	CH_2	32.2	1.58 (m, H_β)
			0.98 (m, H_α)
2	CH	44.2	1.22 (ddd, *J* = 13.1, 8.1, 2.9)
3	CH	31.5	1.12 (m, H)
4	CH_2	37.1	1.60 (m, H_β)
			0.94 (m, H_α)
5	CH_2	22.1	1.53 (m, H_α)
			1.43 (m, H_β)
6	CH_2	42.2	1.27 (br d, *J* = 13.7)
			1.12 (m, H_α)
7	C_q	34.0	–
8	CH_2	36.1	1.55 (m, H_α)
			1.02 (m, H_β)
9	CH_2	29.0	1.55 (m, H_α)
			1.43 (m, H_β)
10	CH	66.6	3.80 (br s)
11	CH_3	15.9	0.73 (s)
12	CH_3	20.3	0.78 (d, *J* = 6.3)

[a] Carbon numbering as shown in Figure S19 indicates the origin of each carbon from GFPP by same number. [b] Chemical shifts δ in ppm. Multiplicity: s = singlet, d = doublet, m = multiplet, br = broad. Coupling constants *J* are given in Hertz.

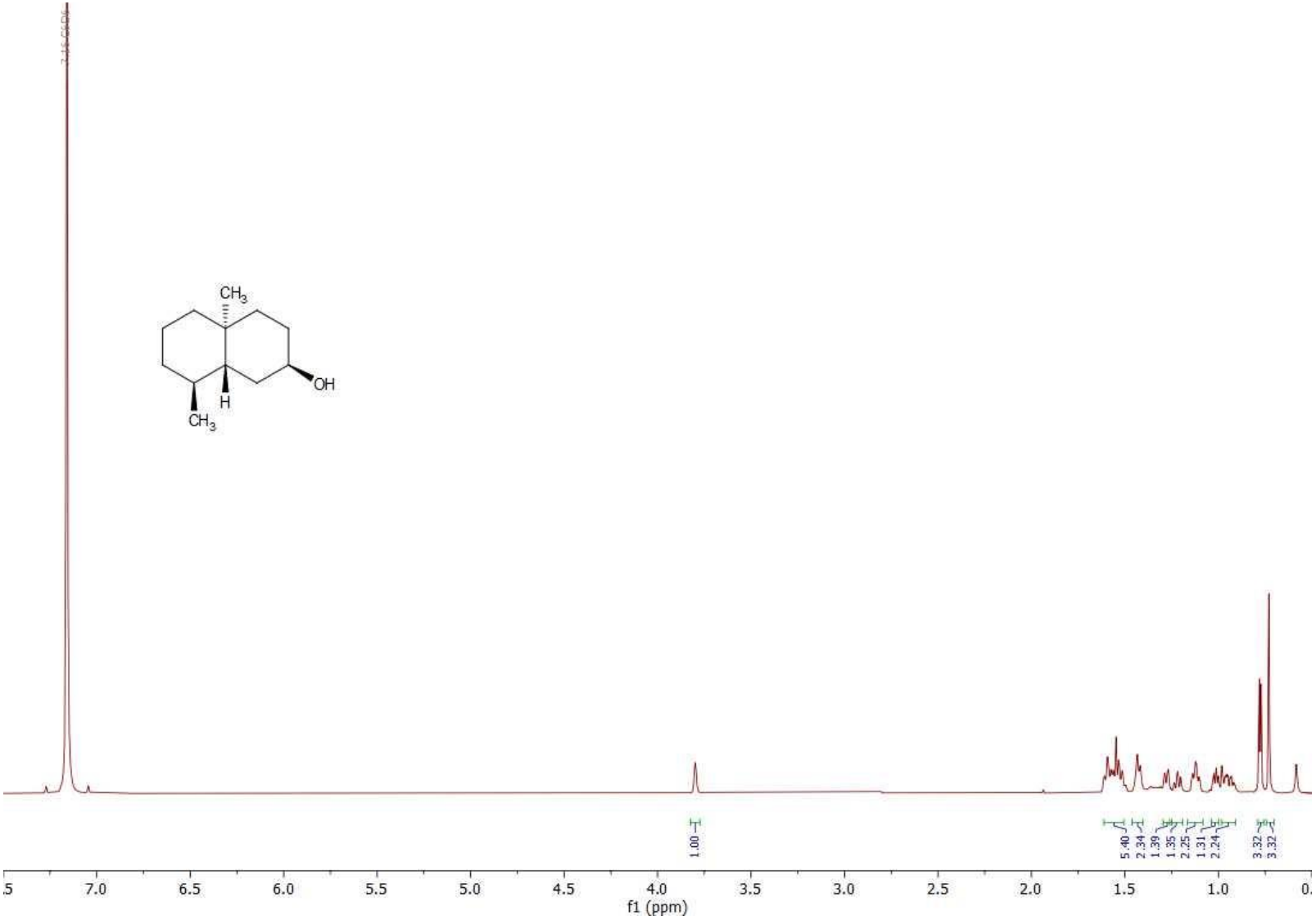

Figure S20. ^{1}H-NMR spectrum of **38** (700 MHz, C_6D_6).

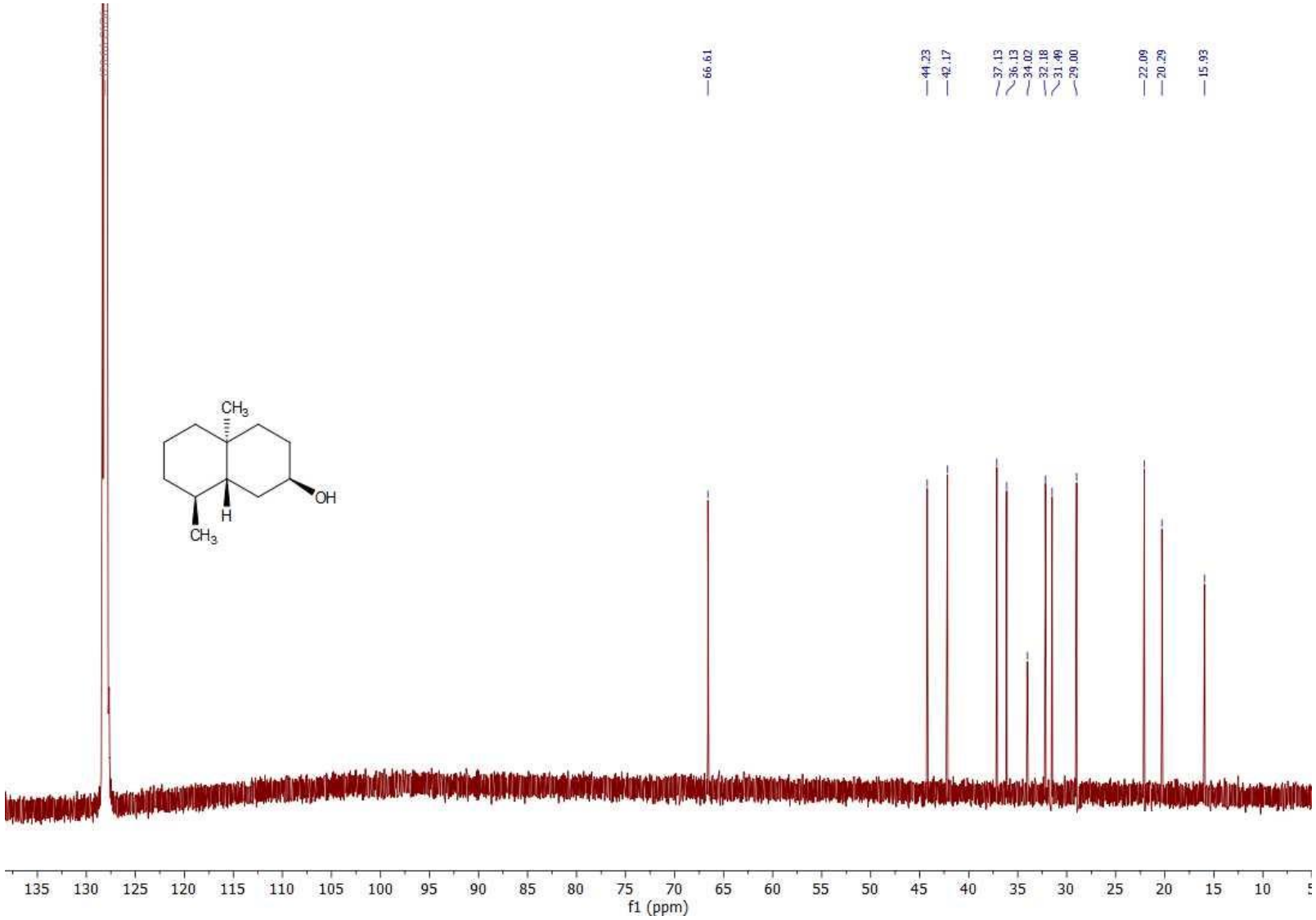

Figure S21. ^{13}C-NMR spectrum of **38** (176 MHz, C_6D_6).

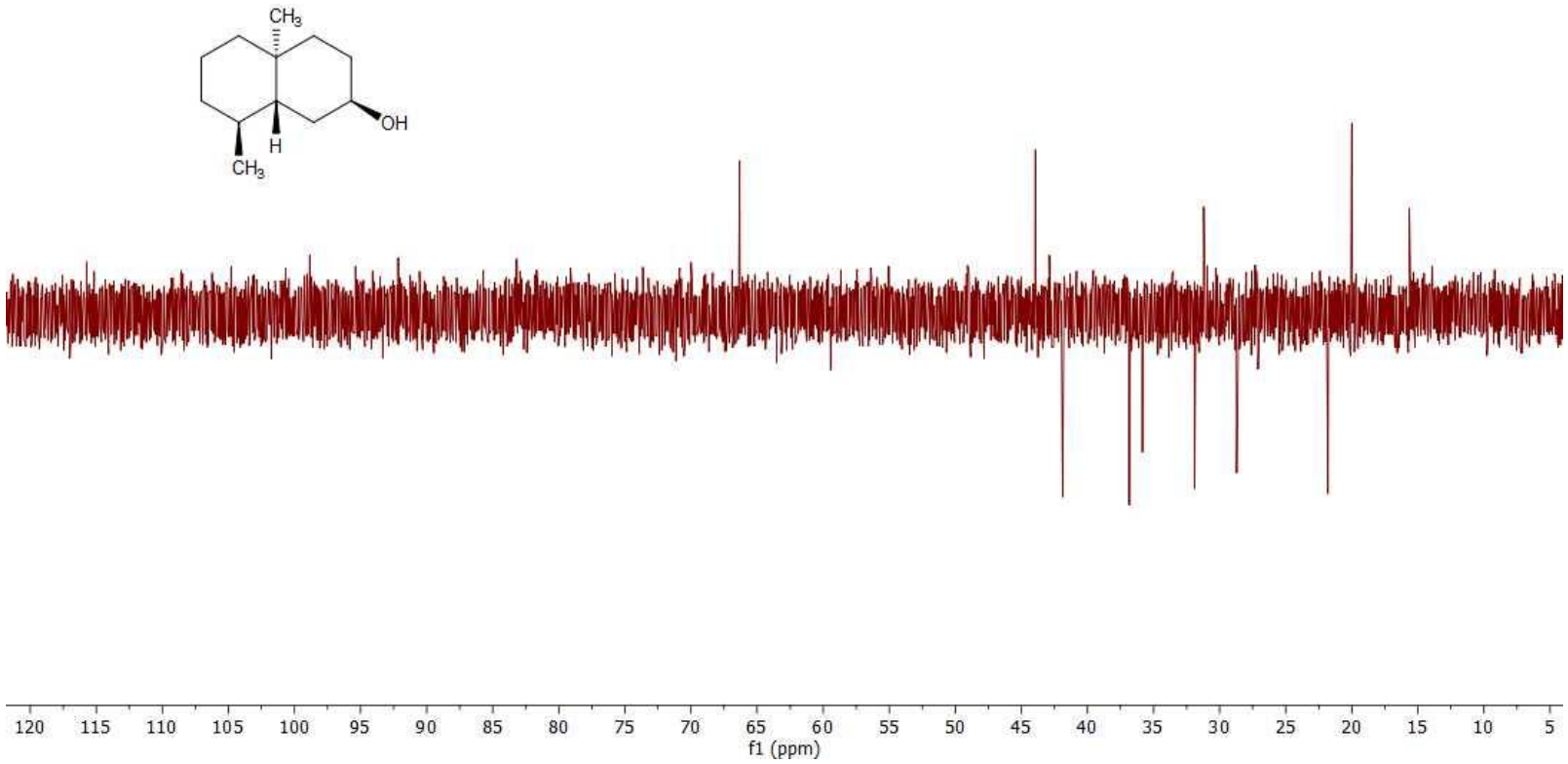

Figure S22. ^{13}C-DEPT135 spectrum of **38** (176 MHz, C_6D_6).

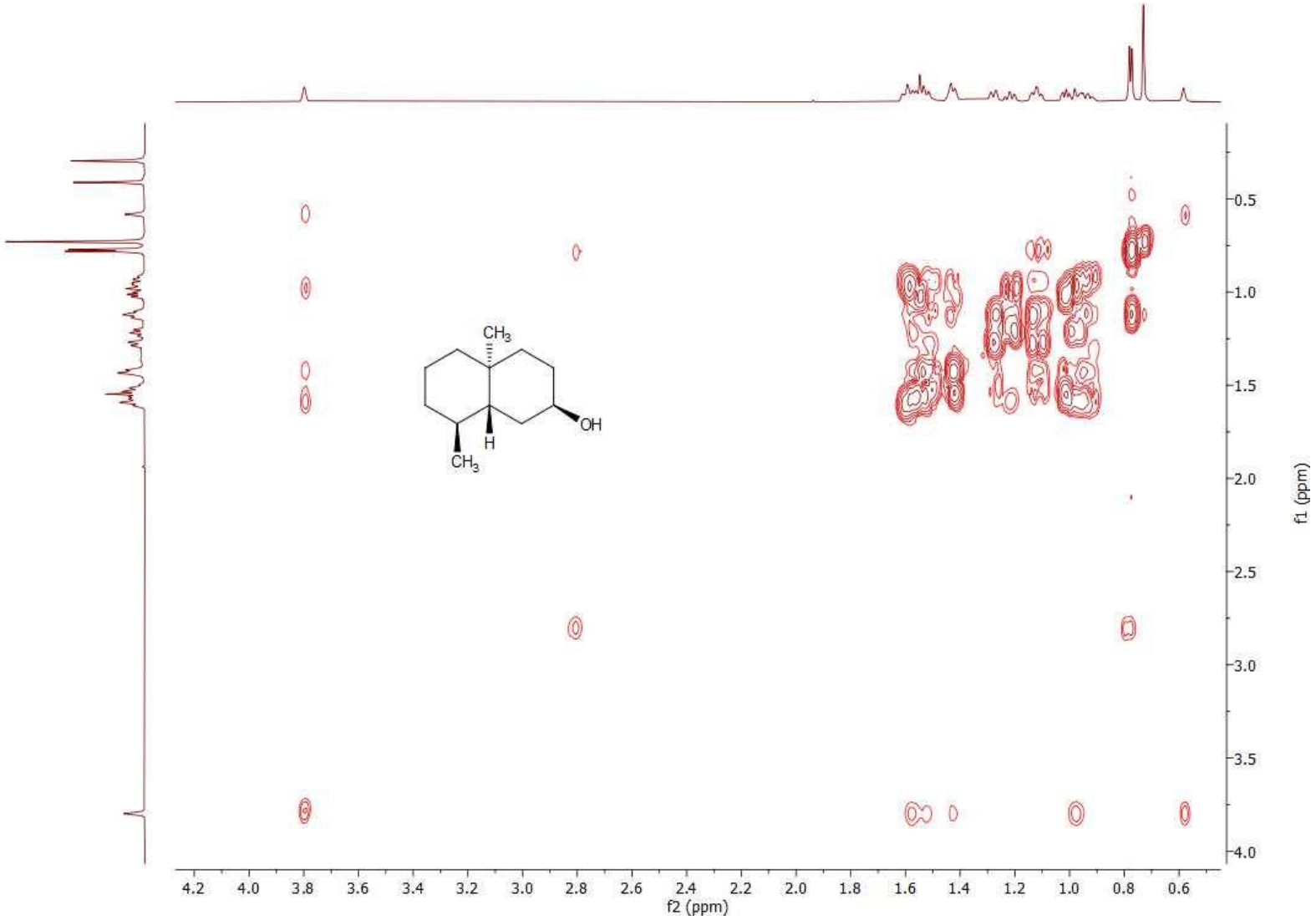

Figure S23. ^{1}H-^{1}H-COSY spectrum (C_6D_6) of **38**.

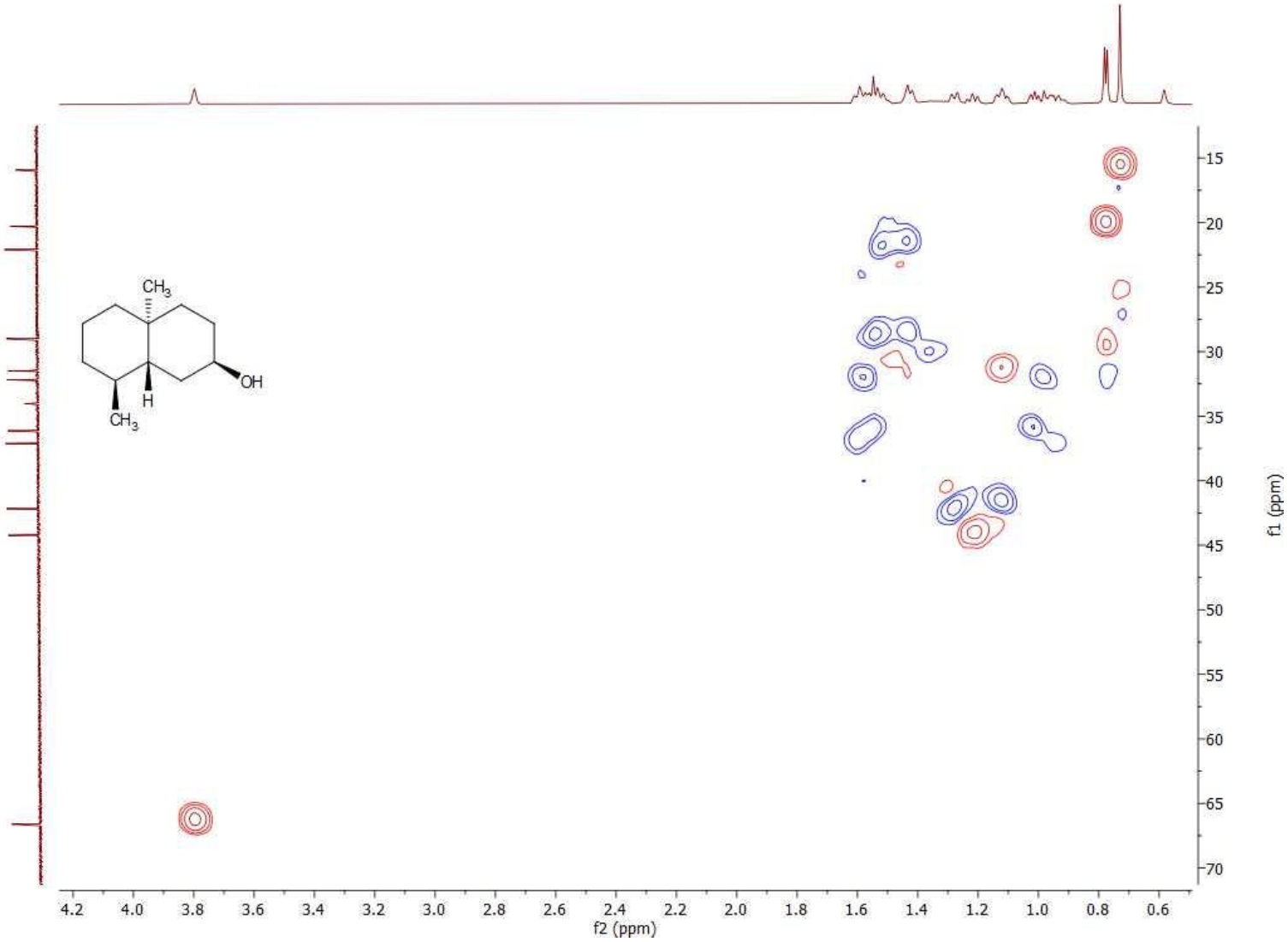

Figure S24. HSQC spectrum (C_6D_6) of **38**.

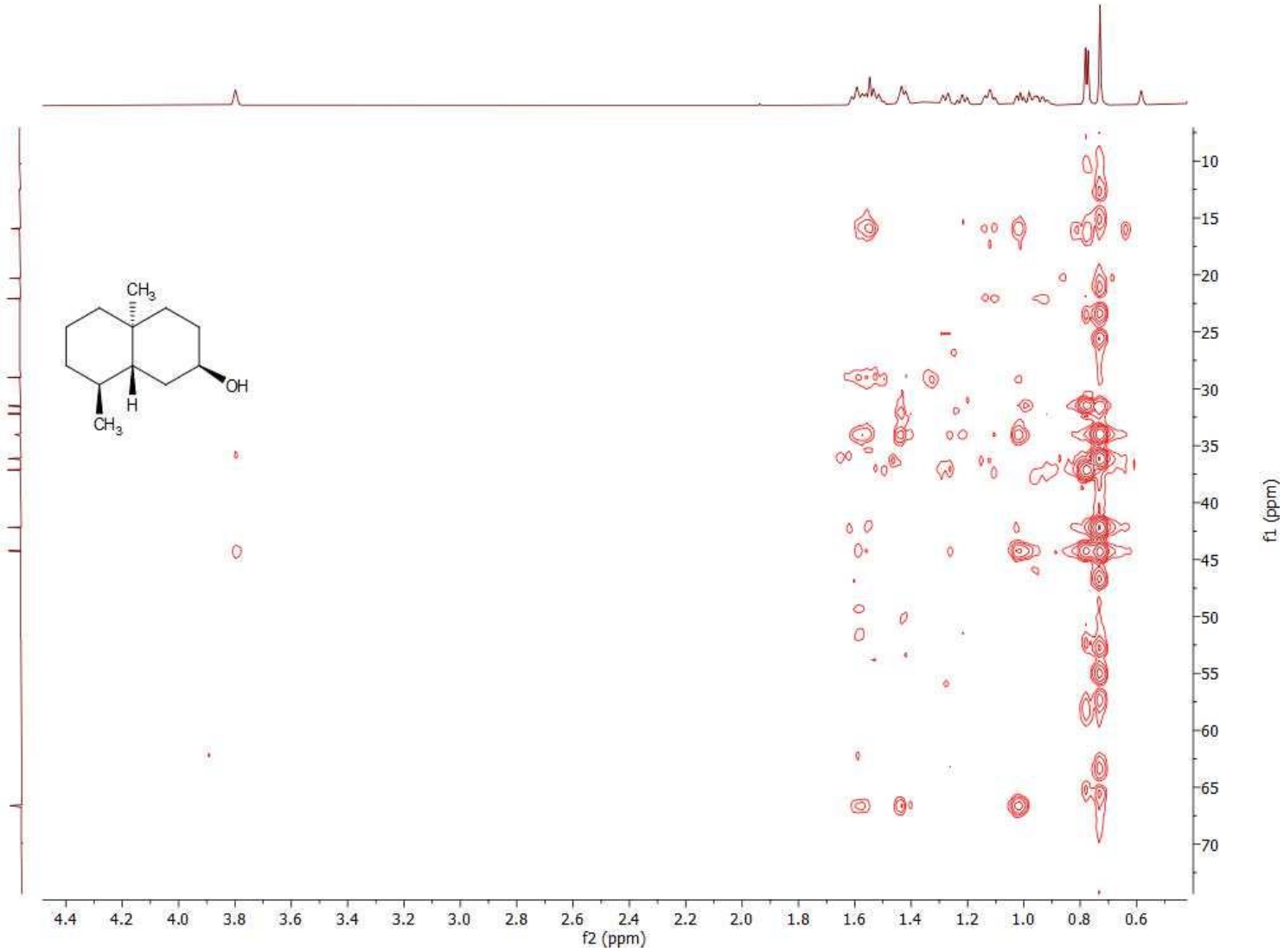

Figure S25. HMBC spectrum (C_6D_6) of **38**.

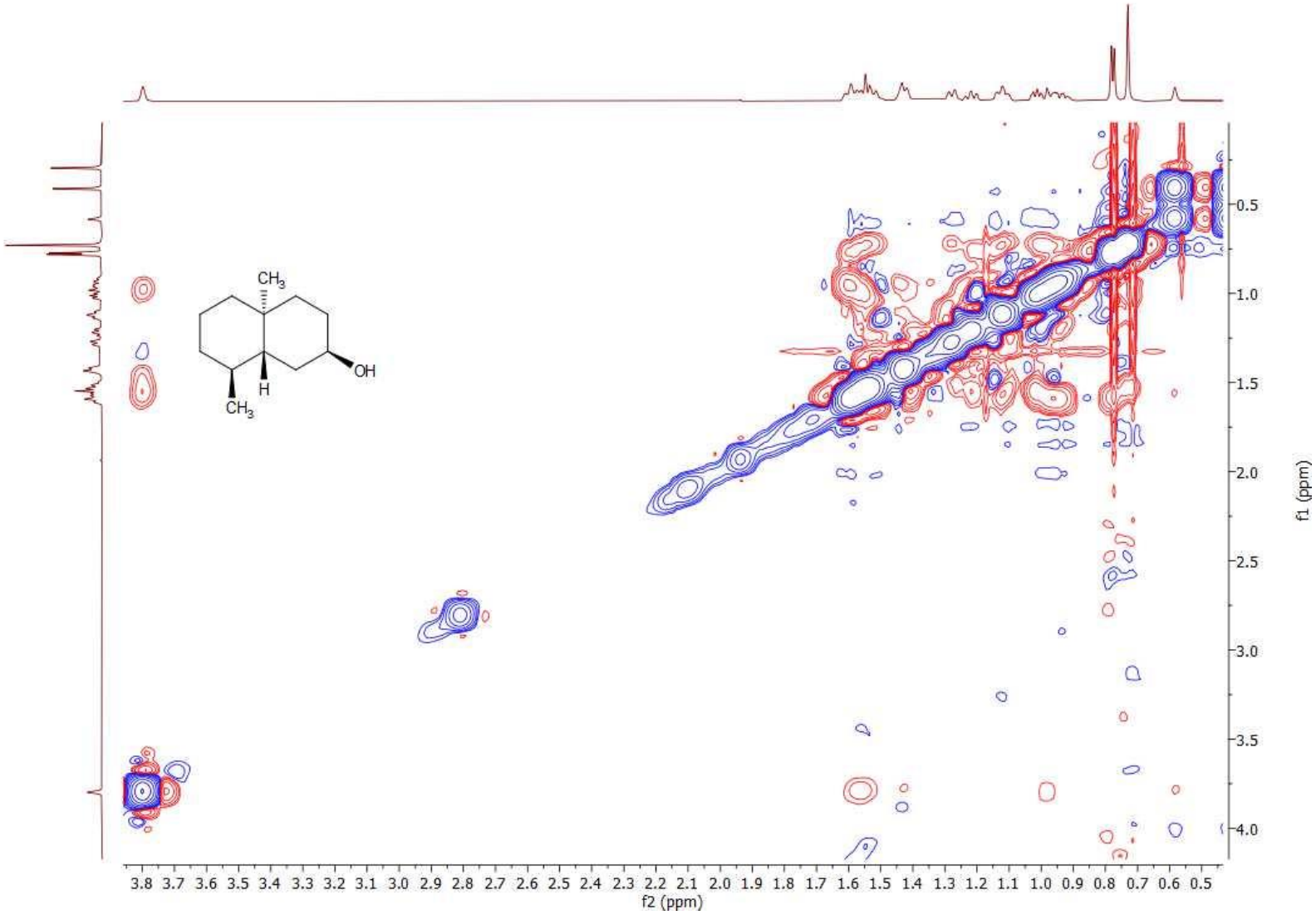

Figure S26. NOESY spectrum (C_6D_6) of **38**.

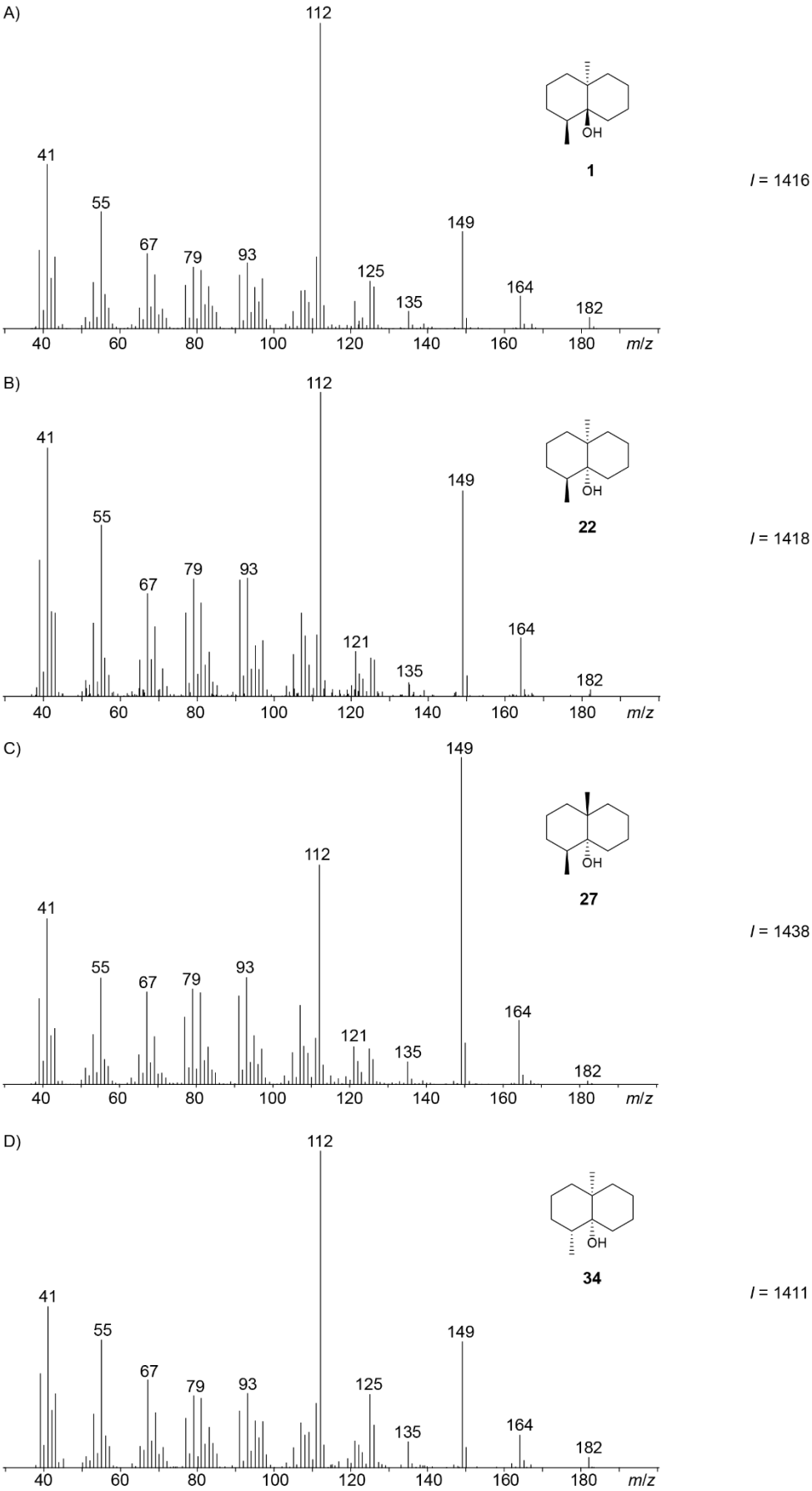

Figure S27. EI mass spectra and retention indices of A) geosmin (**1**), B) 5-*epi*-geosmin (**22**), C) 5,10-*diepi*-geosmin (**27**), and D) 4,5-*diepi*-geosmin (**34**).

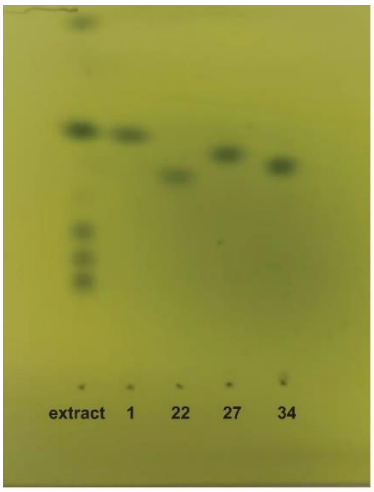

Figure S28. TLC analysis of an extract from an enzyme incubation of FPP with GeoS against authentic reference standards of geosmin (**1**) and its stereoisomers (**22**, **27** and **34**).

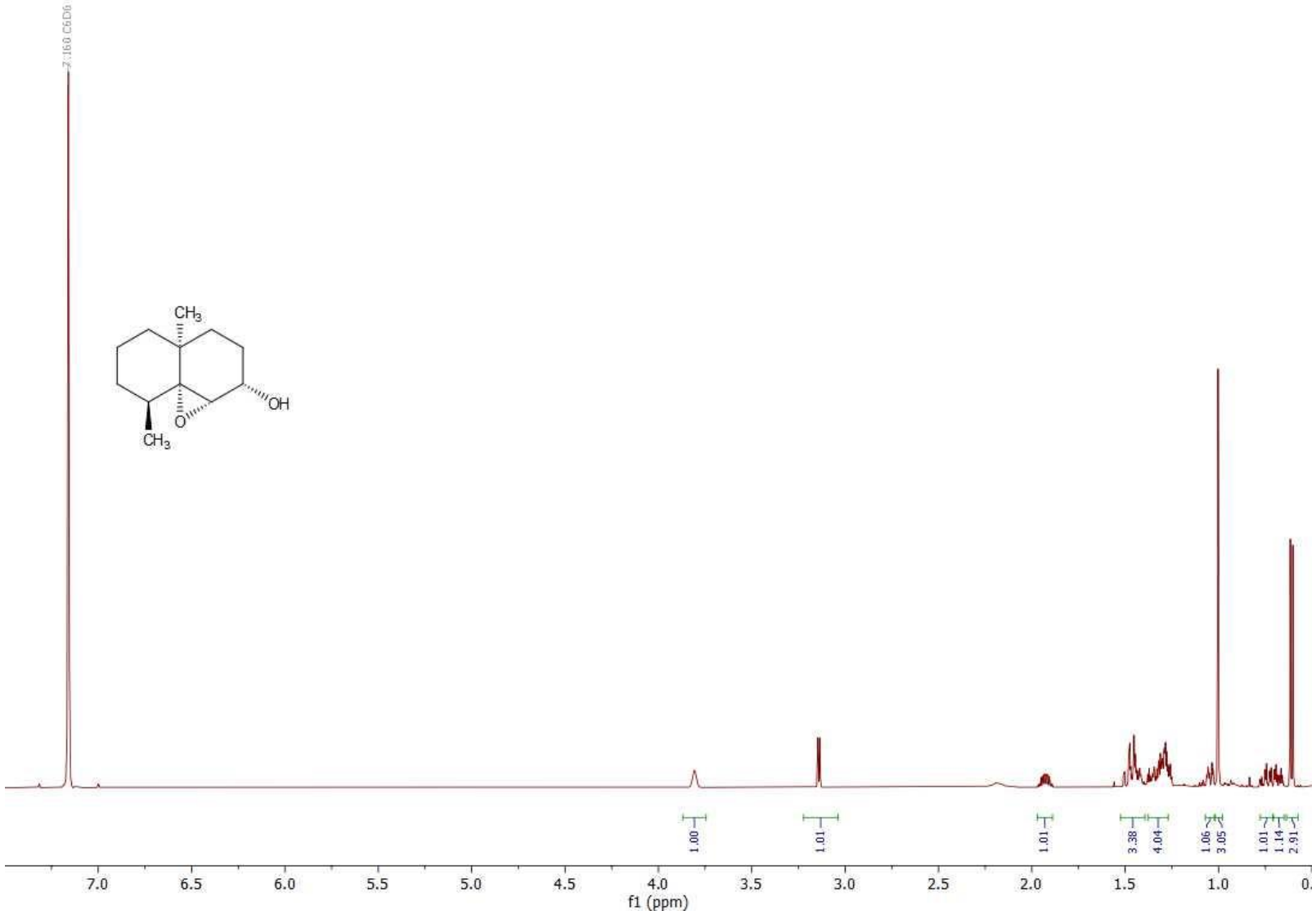

Figure S29. ^{1}H-NMR spectrum of synthetic **20a** (500 MHz, C_6D_6).

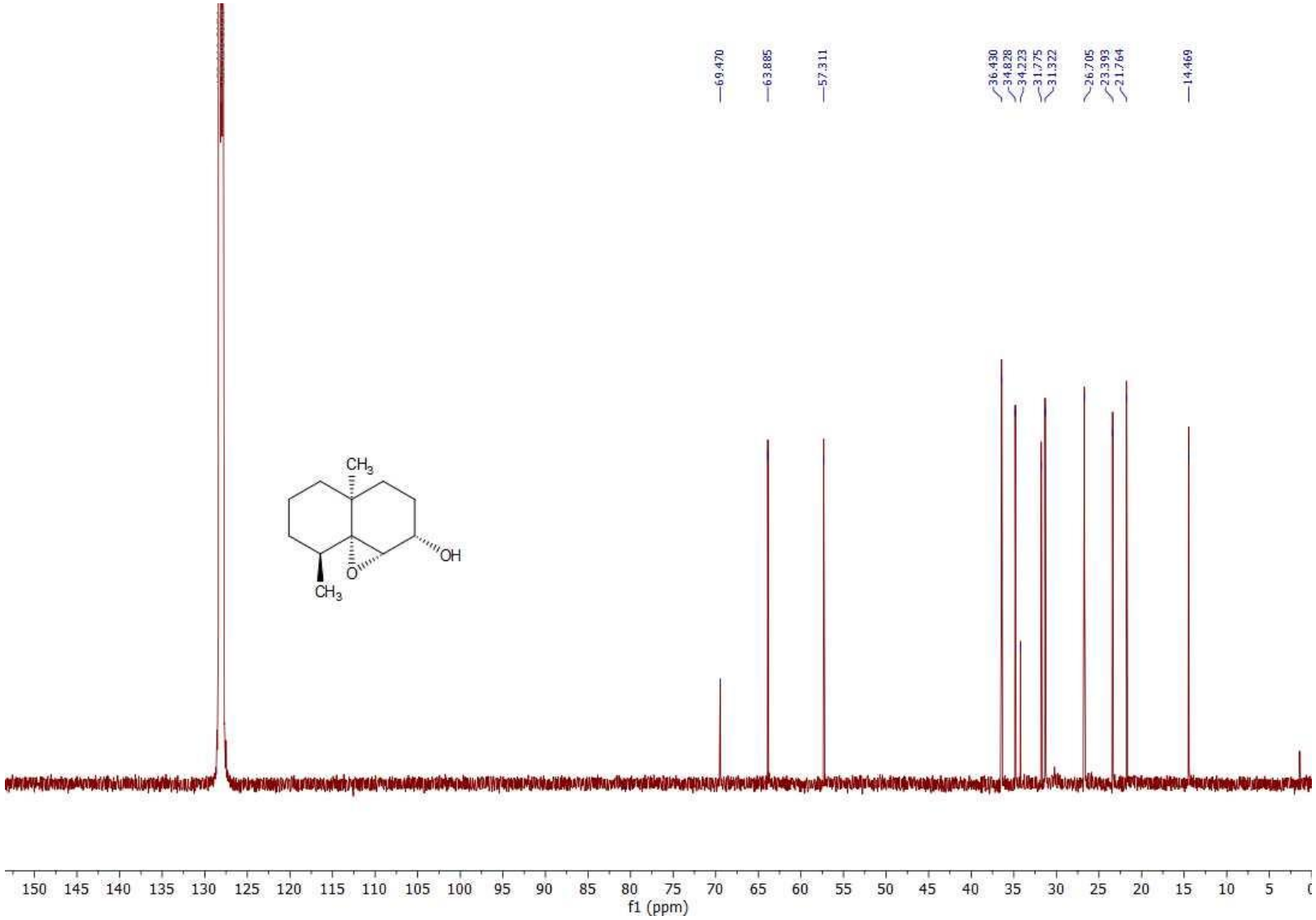

Figure S30. ^{13}C-NMR spectrum of synthetic **20a** (126 MHz, C_6D_6).

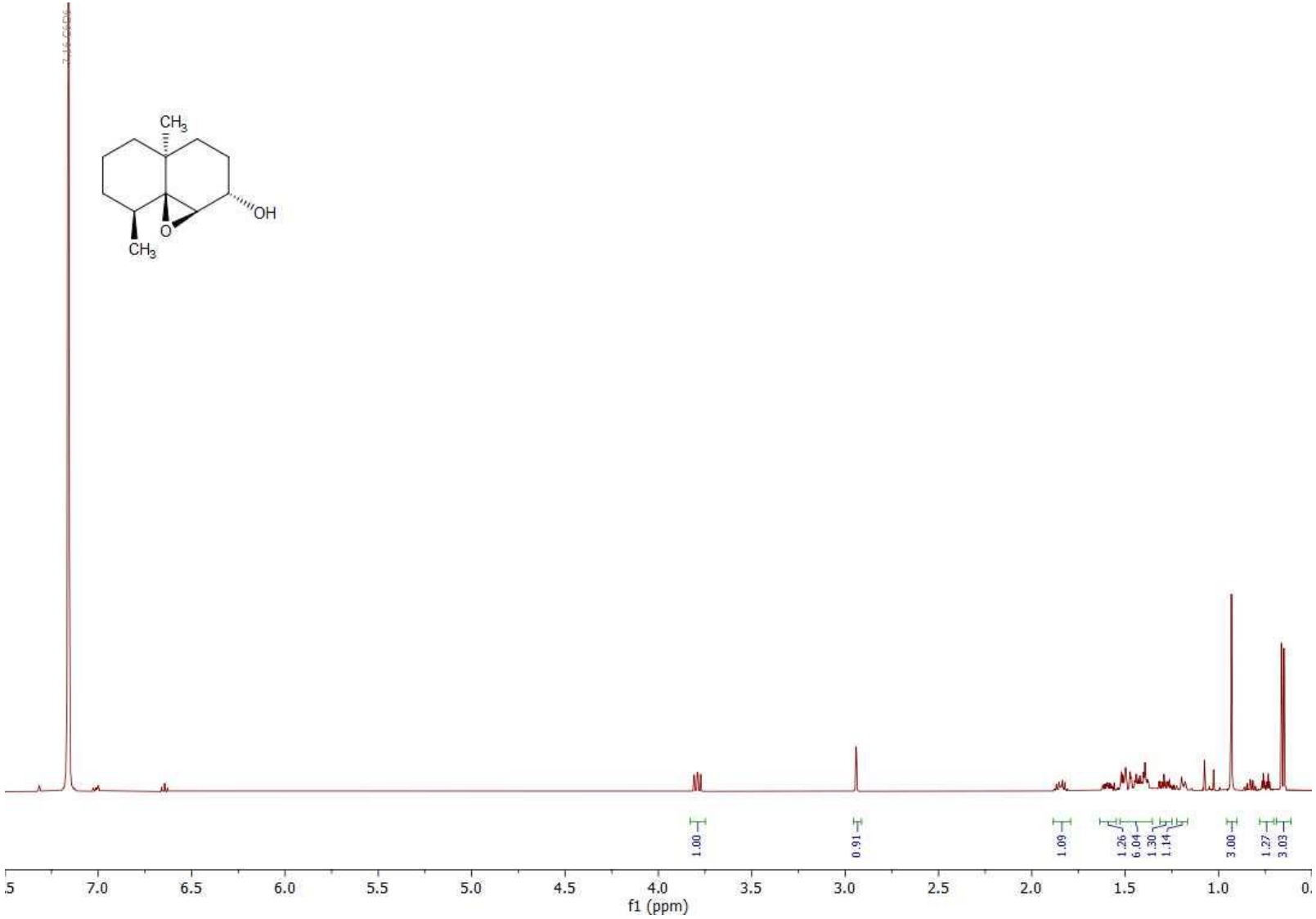

Figure S31. ^{1}H-NMR spectrum of synthetic **20b** (500 MHz, C_6D_6).

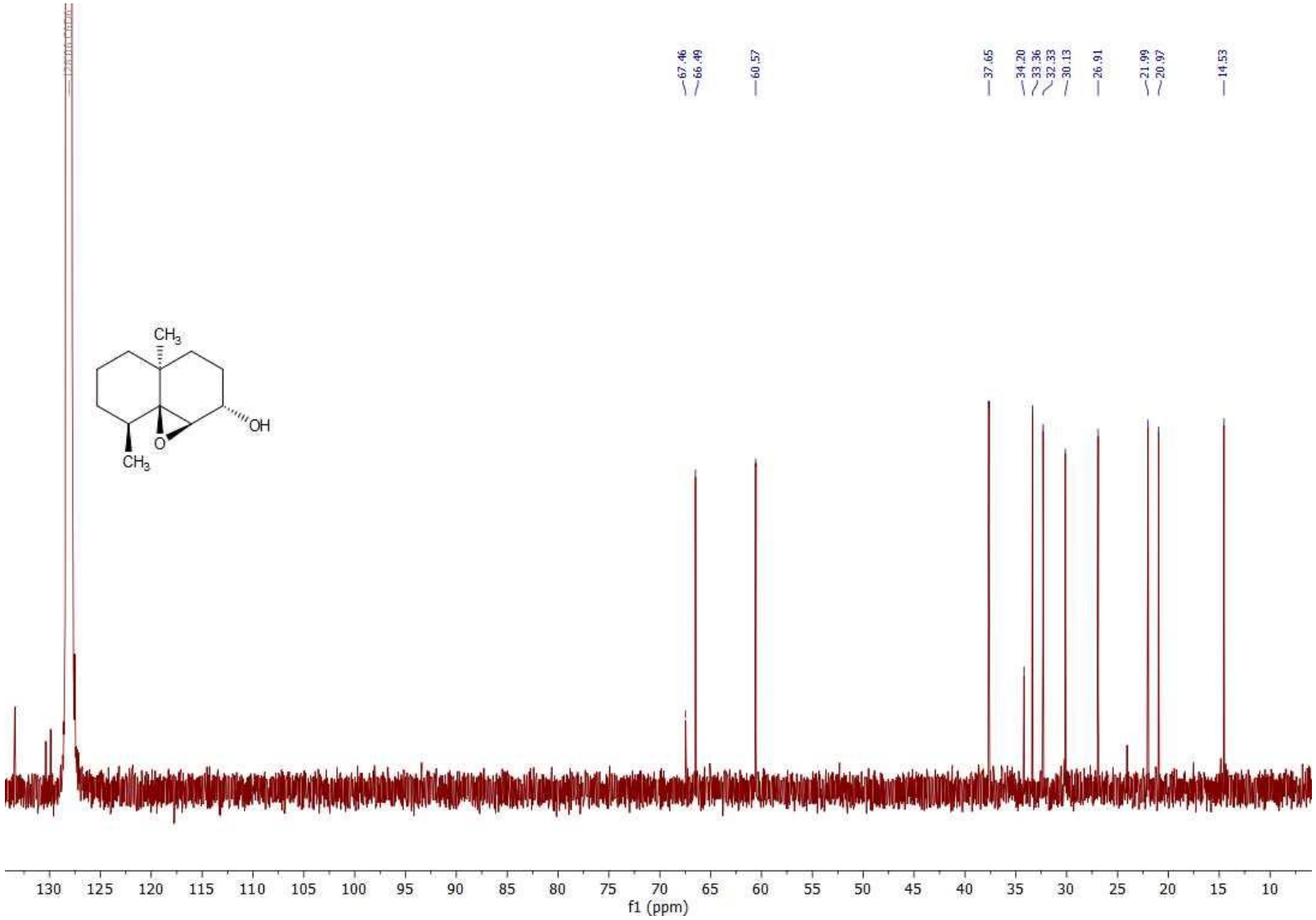

Figure S32. ^{13}C-NMR spectrum of synthetic **20b** (126 MHz, C_6D_6).

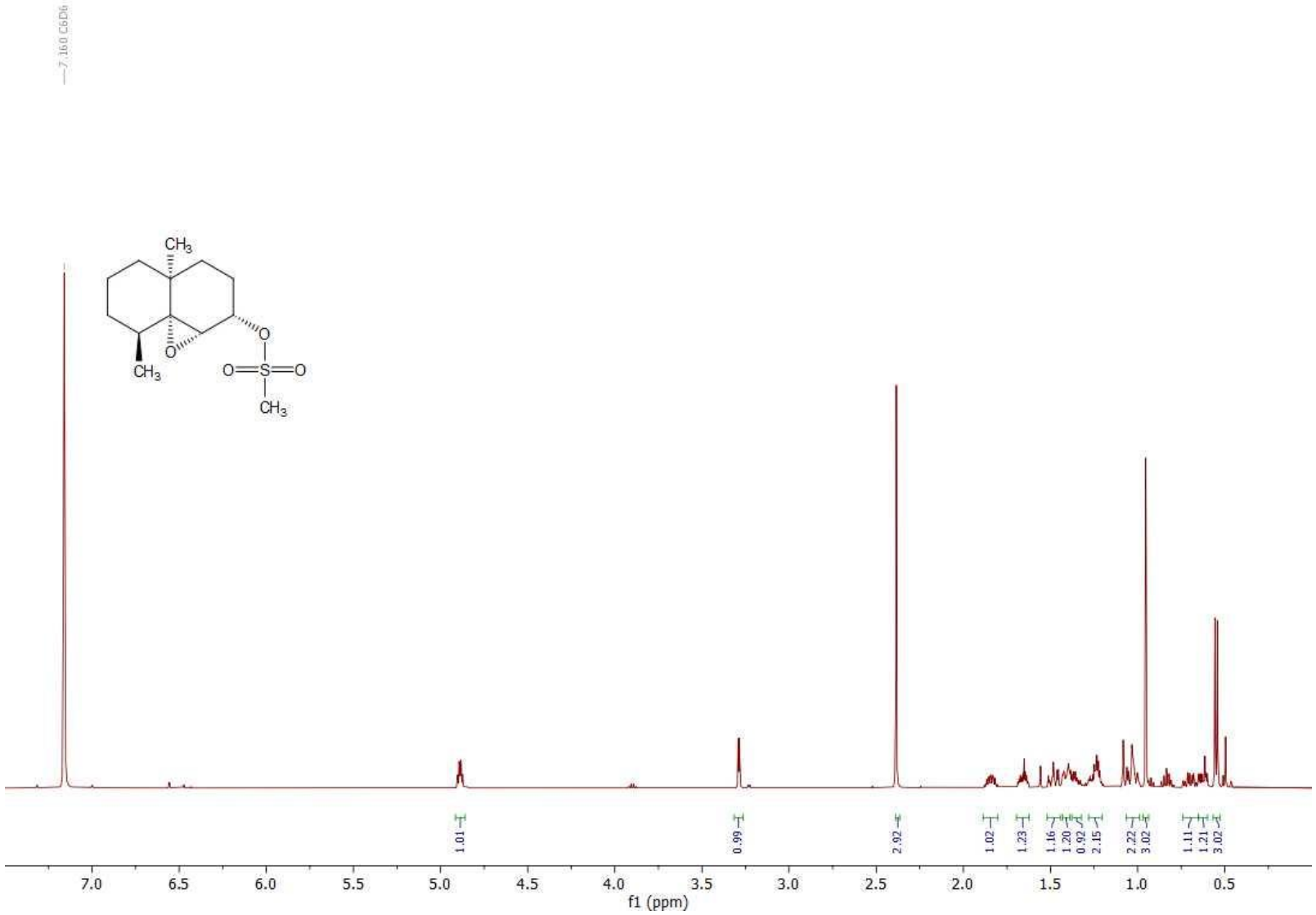

Figure S33. ^{1}H-NMR spectrum of synthetic **21** (500 MHz, C_6D_6).

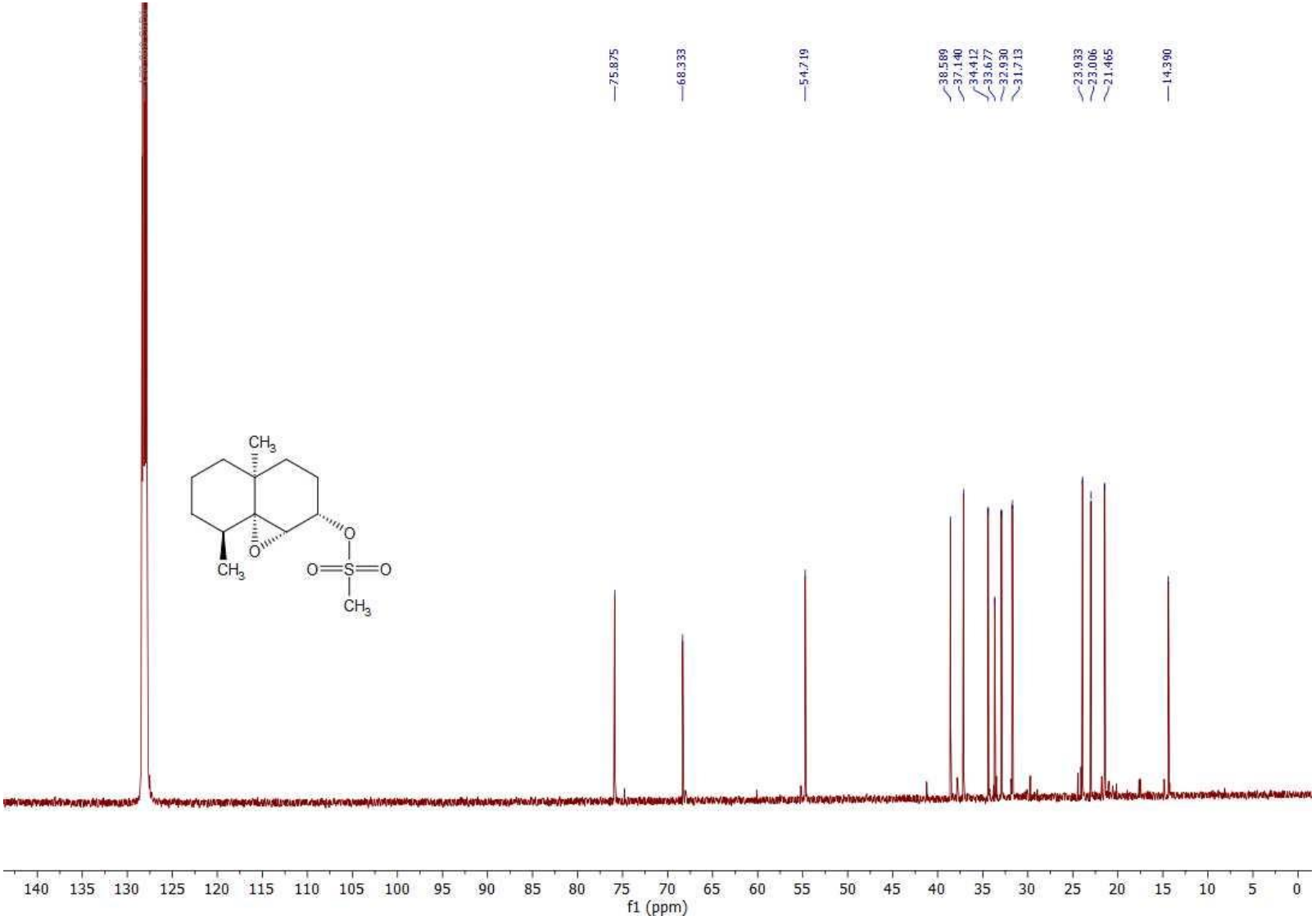

Figure S34. ^{13}C-NMR spectrum of synthetic **21** (126 MHz, C_6D_6).

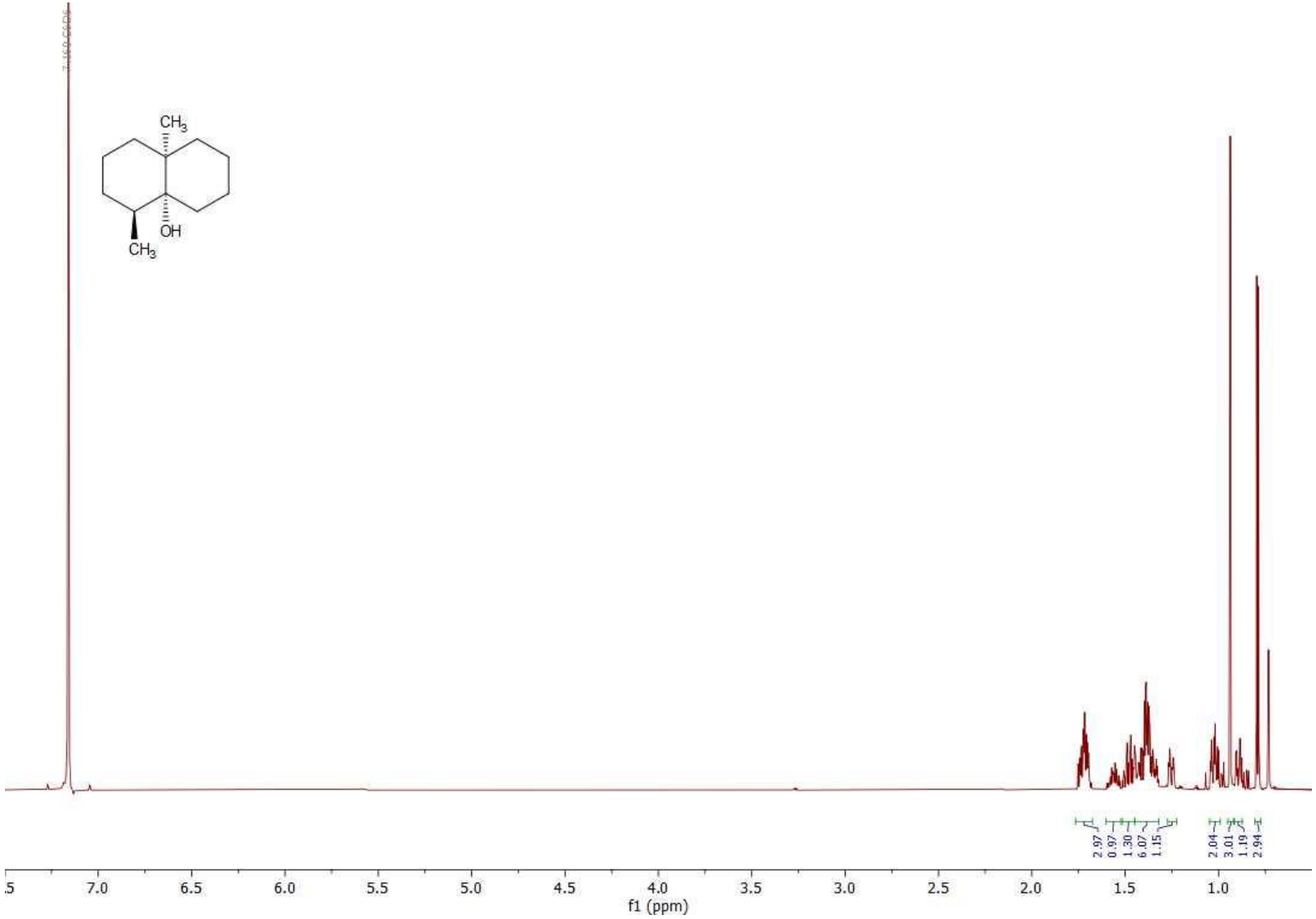

Figure S35. ^{1}H-NMR spectrum of synthetic **22** (700 MHz, C_6D_6).

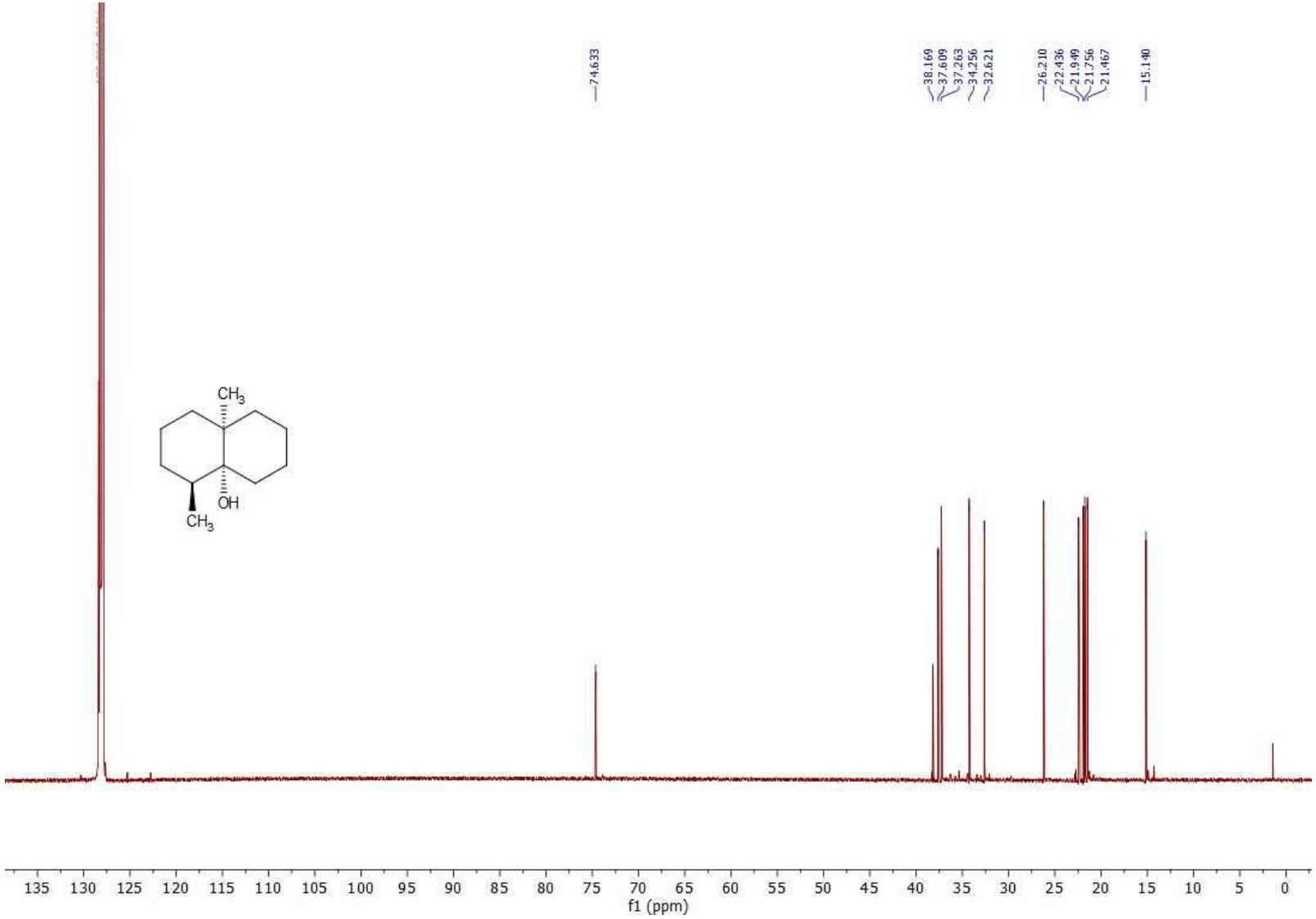

Figure S36. ^{13}C-NMR spectrum of synthetic **22** (176 MHz, C_6D_6).

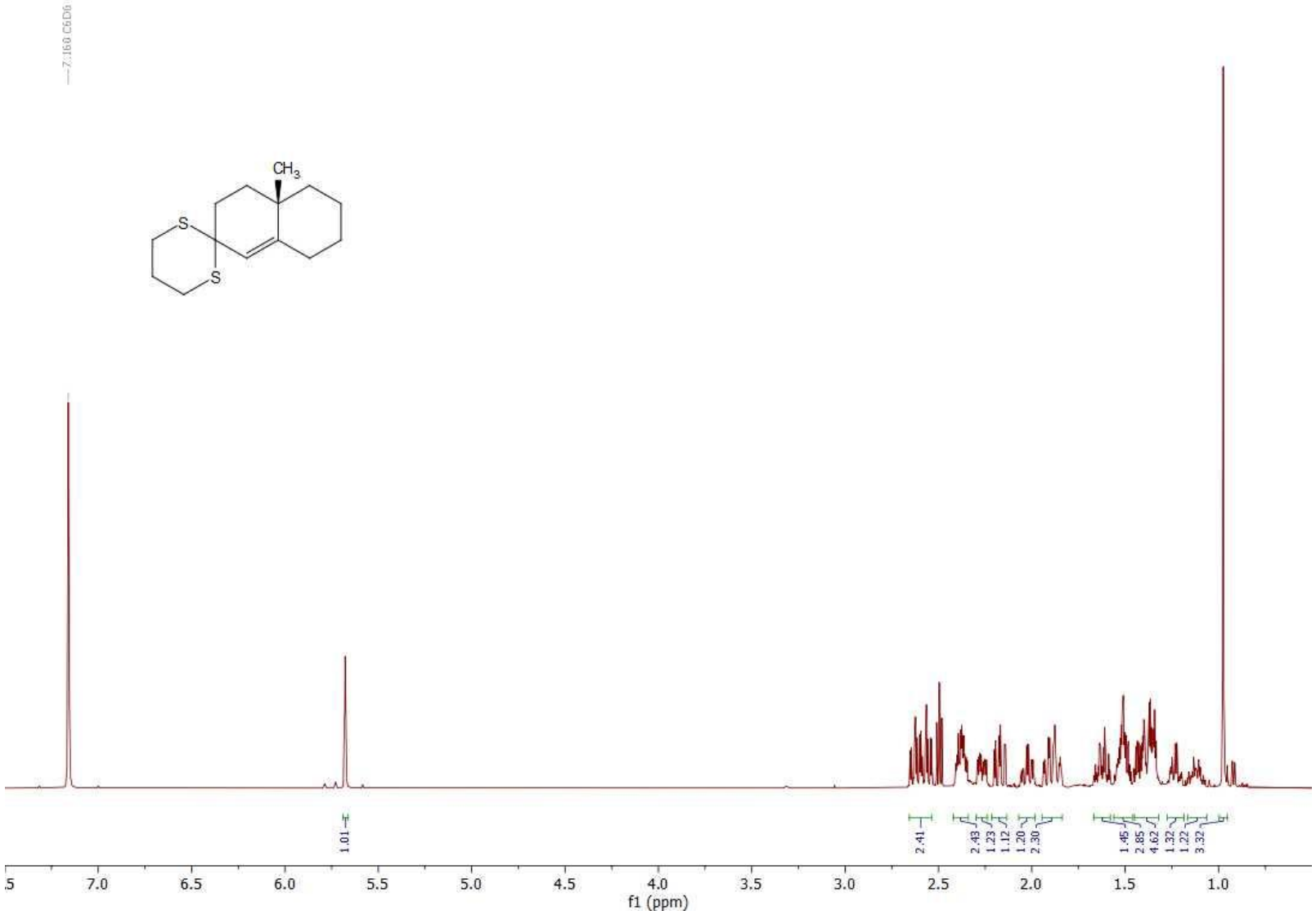

Figure S37. ^{1}H-NMR spectrum of synthetic **24** (500 MHz, C_6D_6).

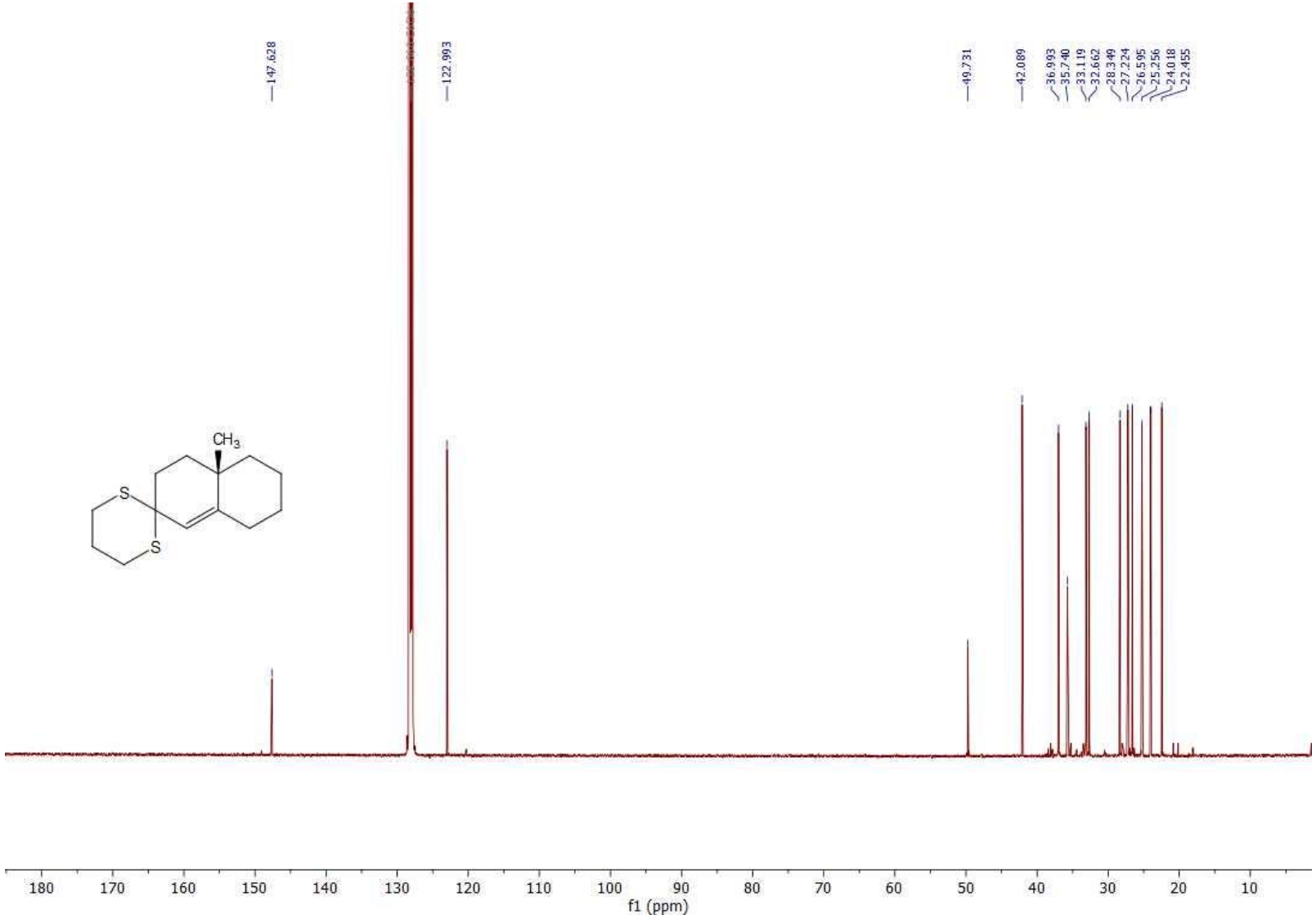

Figure S38. ^{13}C-NMR spectrum of synthetic **24** (126 MHz, C_6D_6).

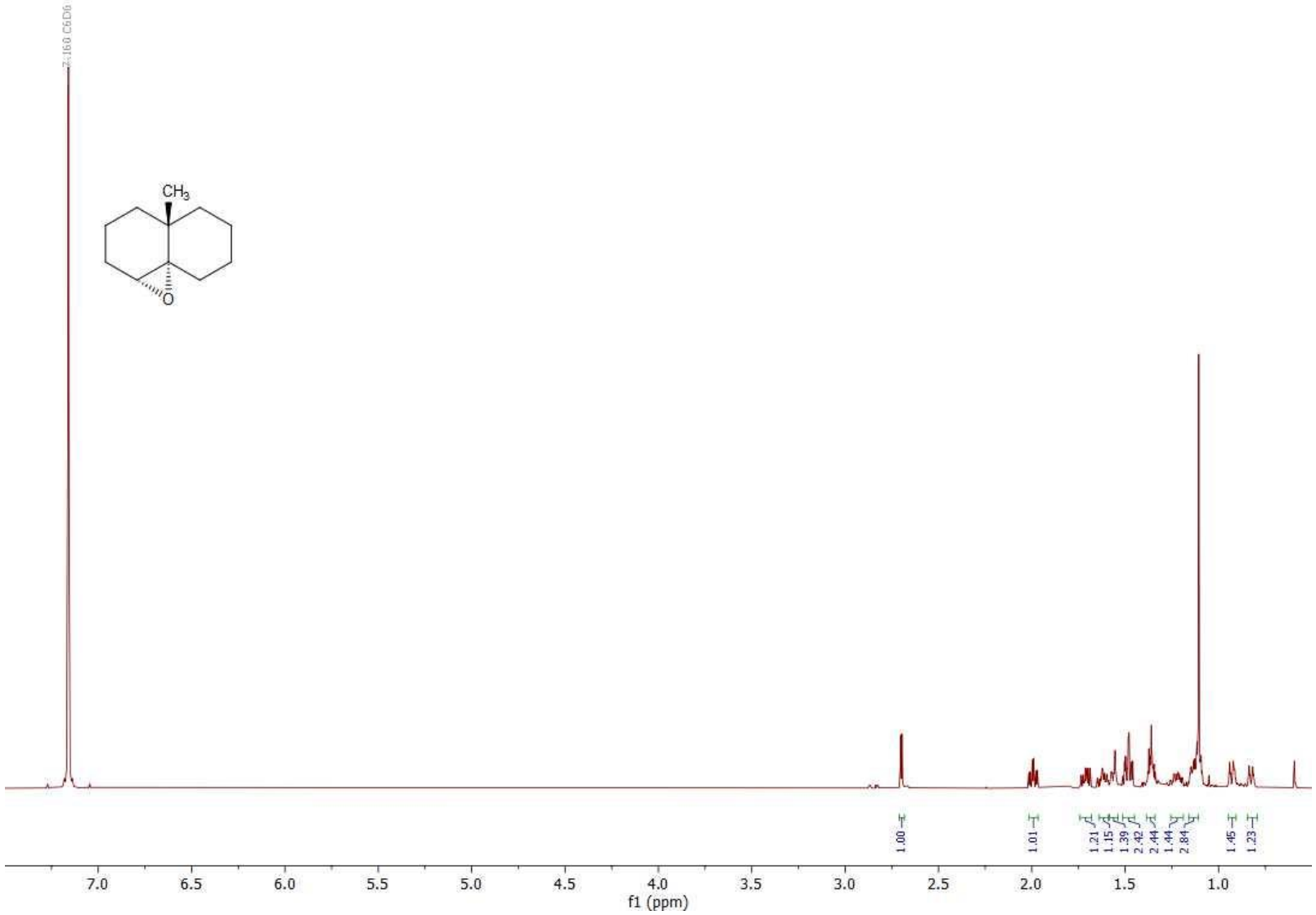

Figure S39. ^{1}H-NMR spectrum of synthetic **26a** (700 MHz, C_6D_6).

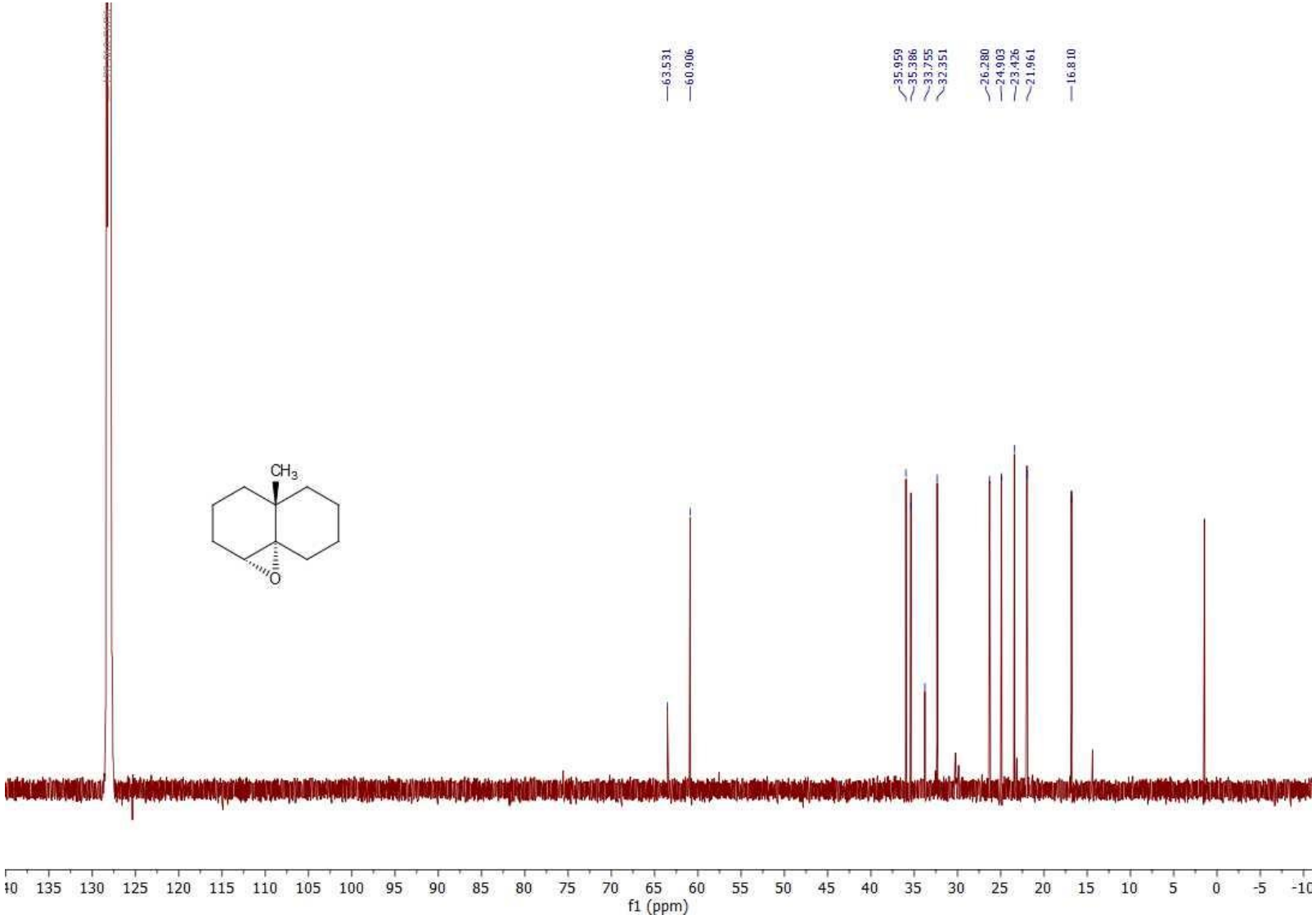

Figure S40. ^{13}C-NMR spectrum of synthetic **26a** (176 MHz, C_6D_6).

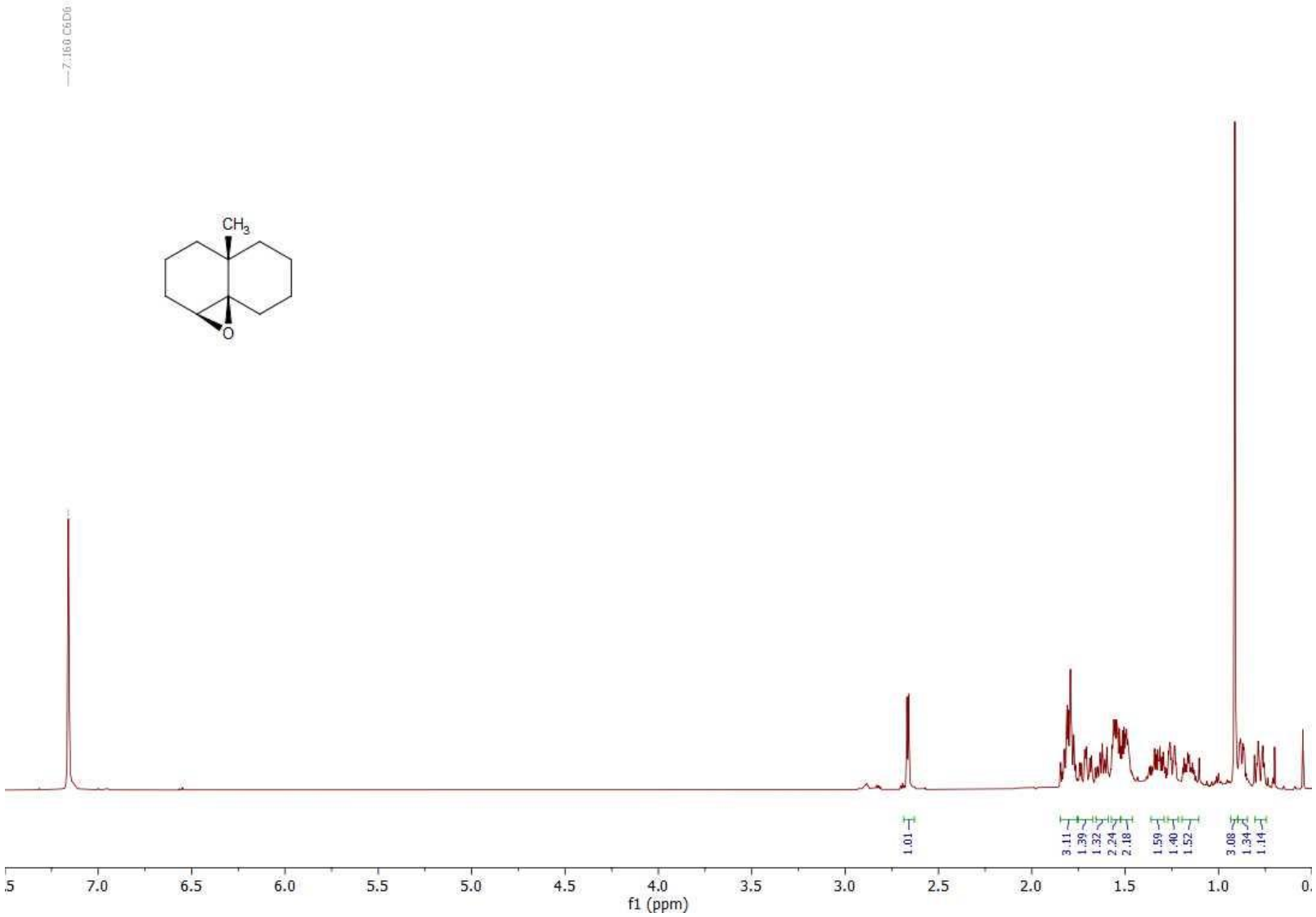

Figure S41. ^{1}H-NMR spectrum of synthetic **26b** (500 MHz, C_6D_6).

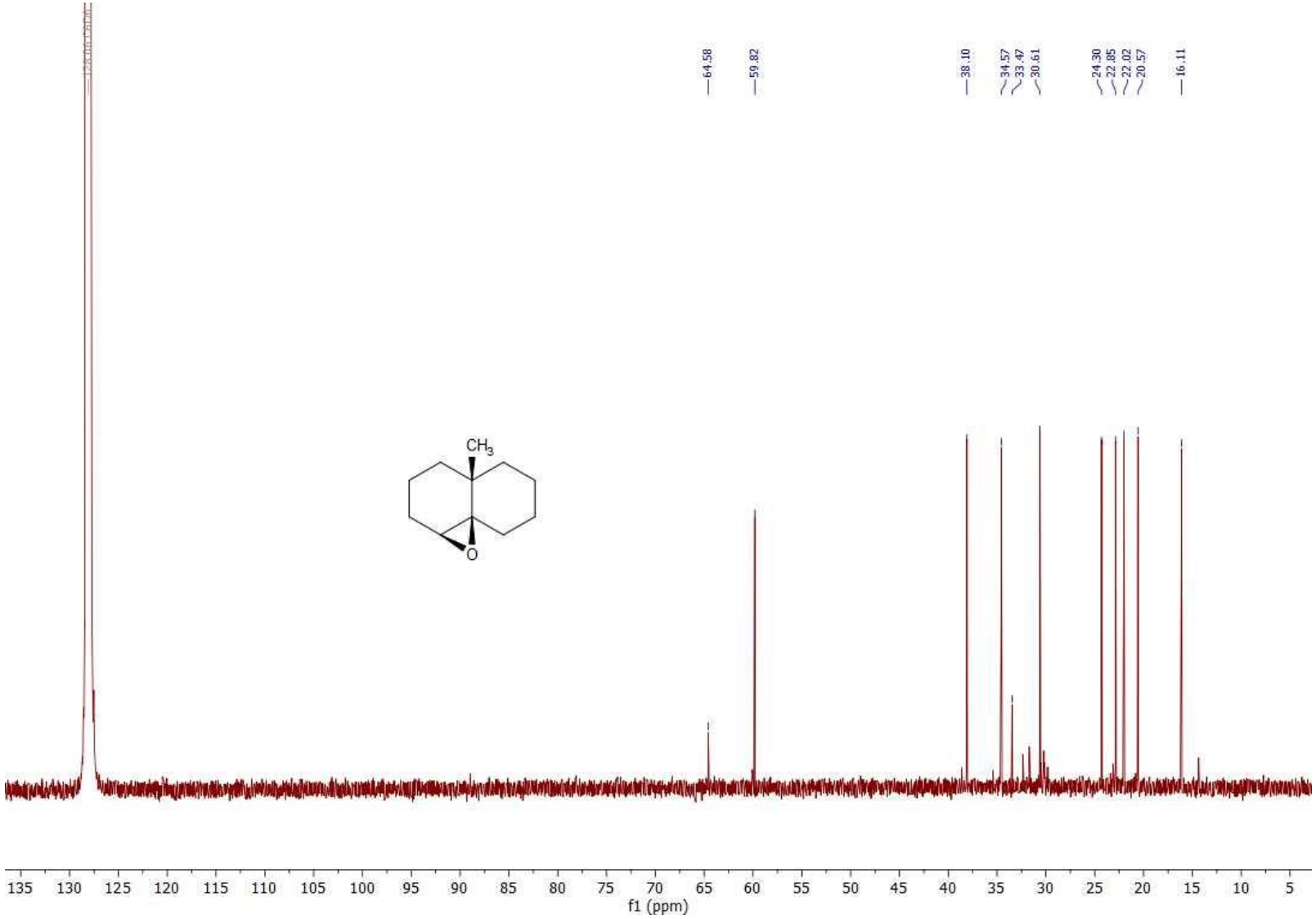

Figure S42. ^{13}C-NMR spectrum of synthetic **26b** (126 MHz, C_6D_6).

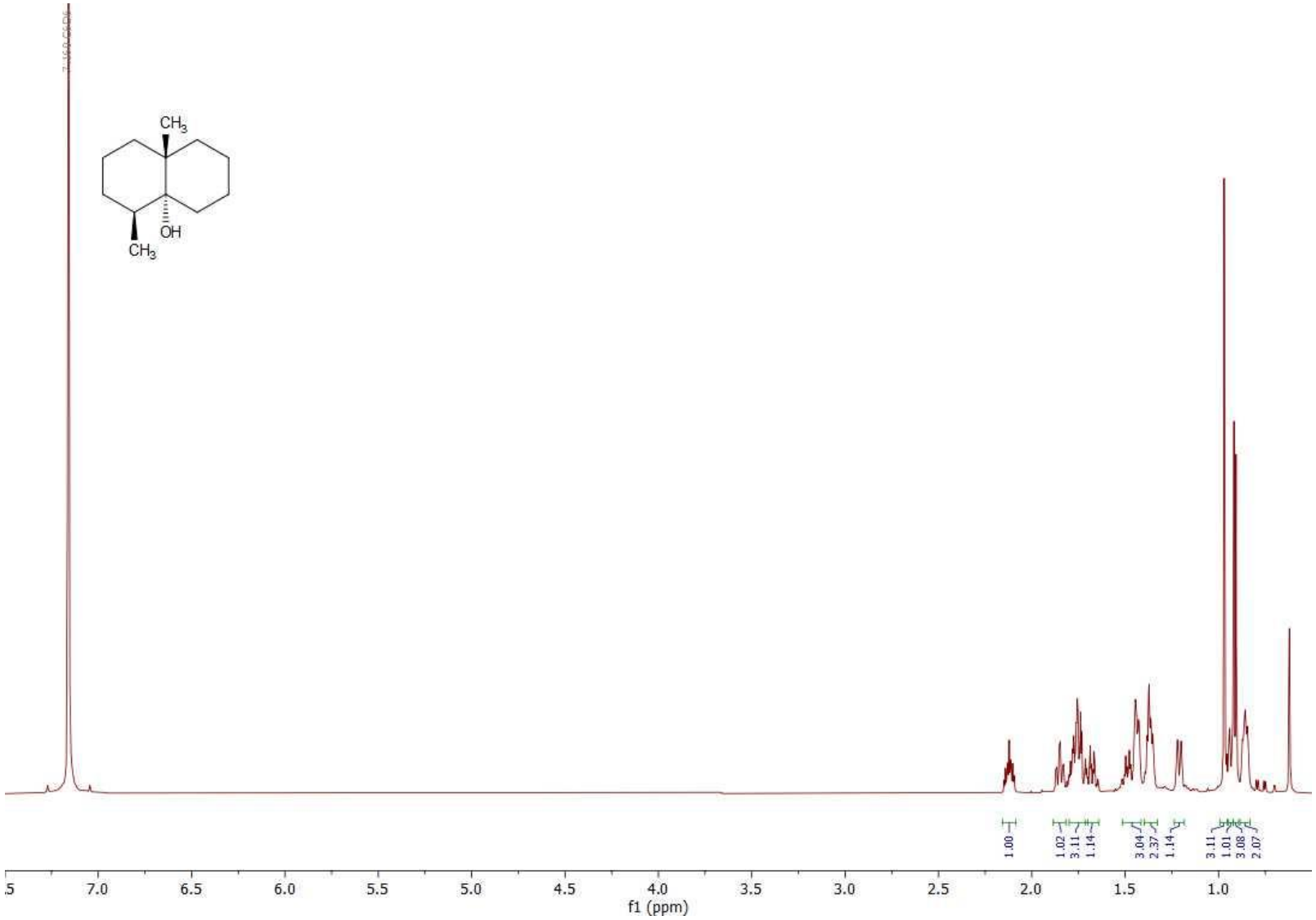

Figure S43. ^{1}H-NMR spectrum of synthetic **27** (700 MHz, C_6D_6).

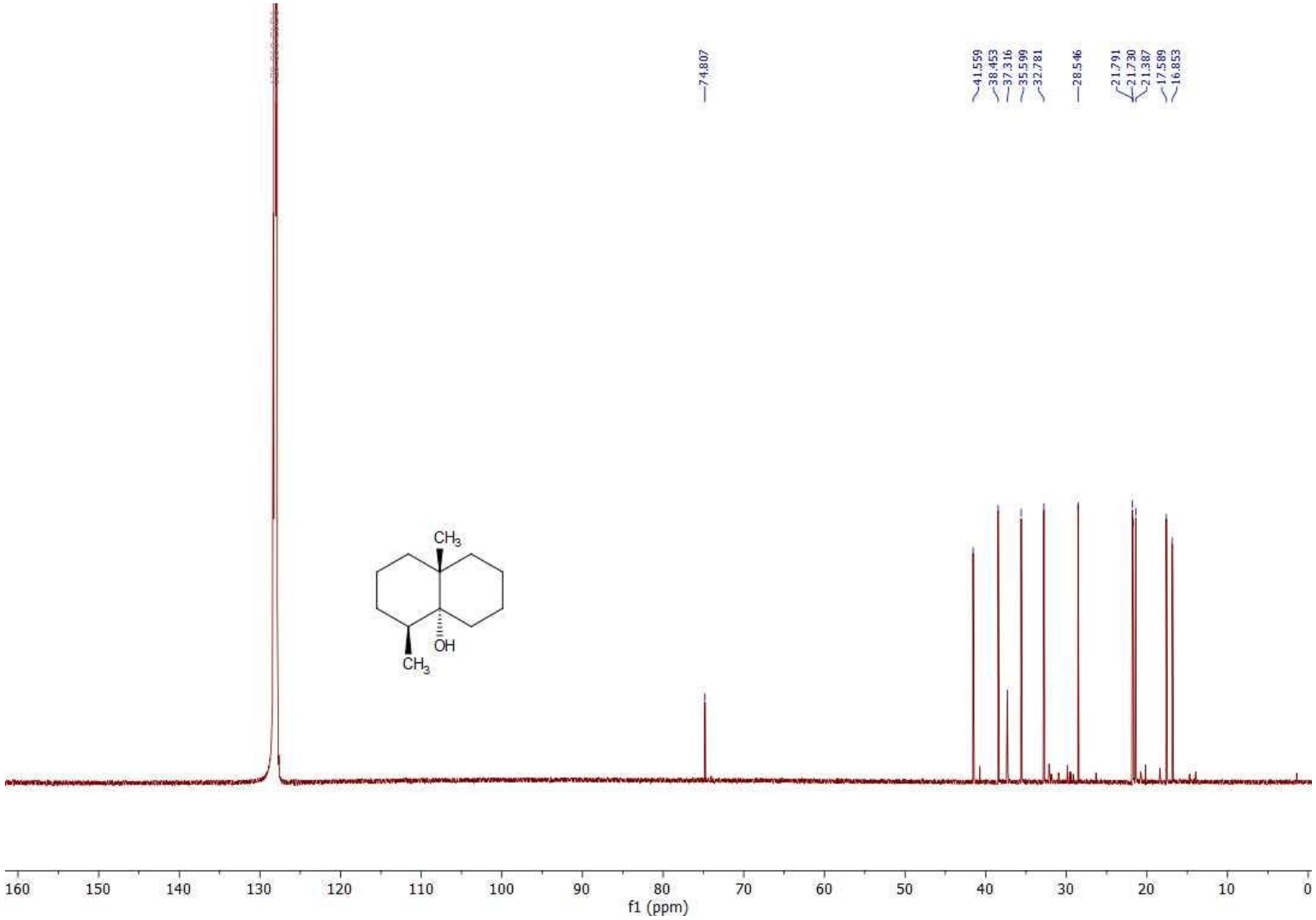

Figure S44. ^{13}C-NMR spectrum of synthetic **27** (176 MHz, C_6D_6).

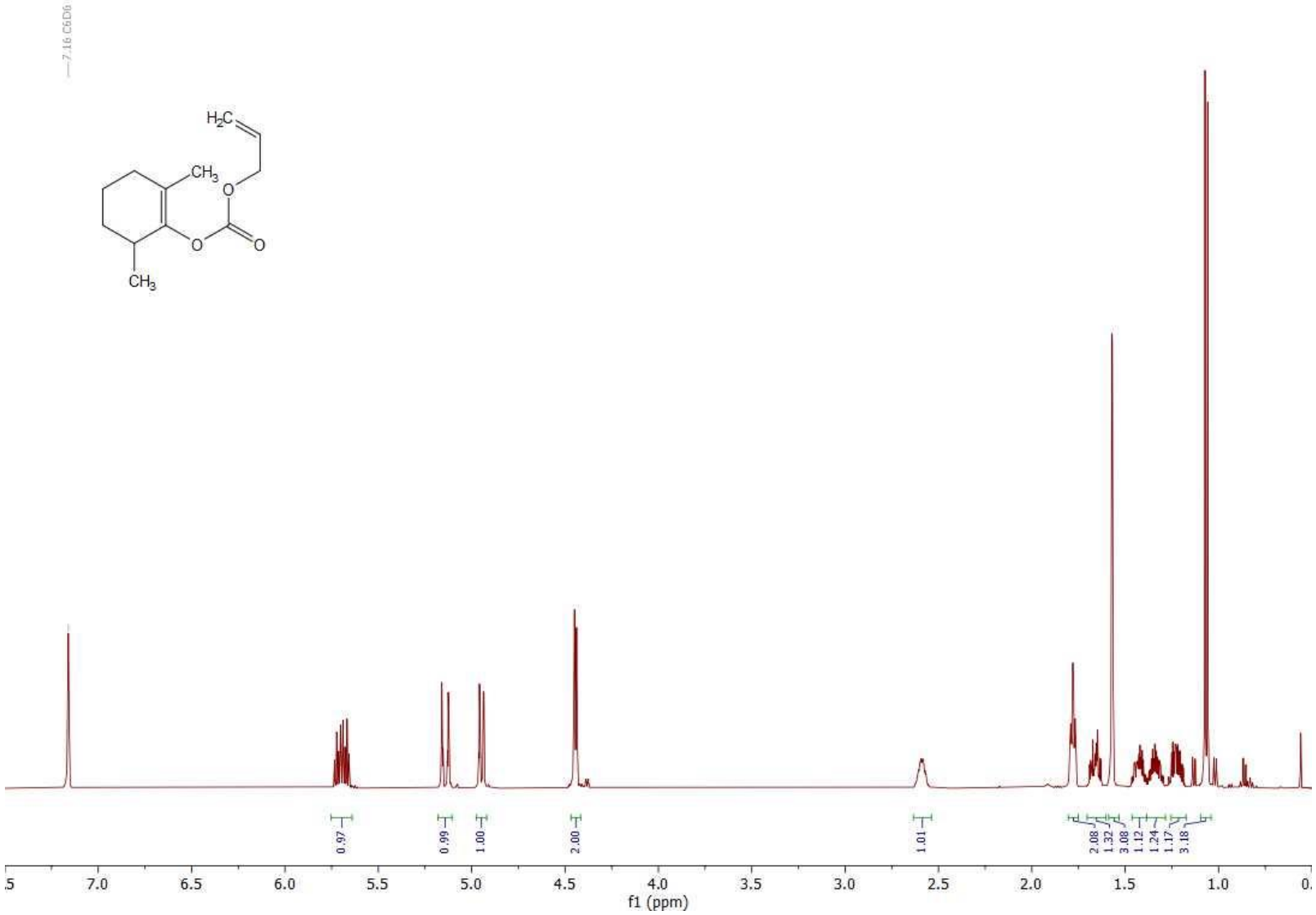

Figure S45. ^{1}H-NMR spectrum of synthetic **29** (500 MHz, C_6D_6).

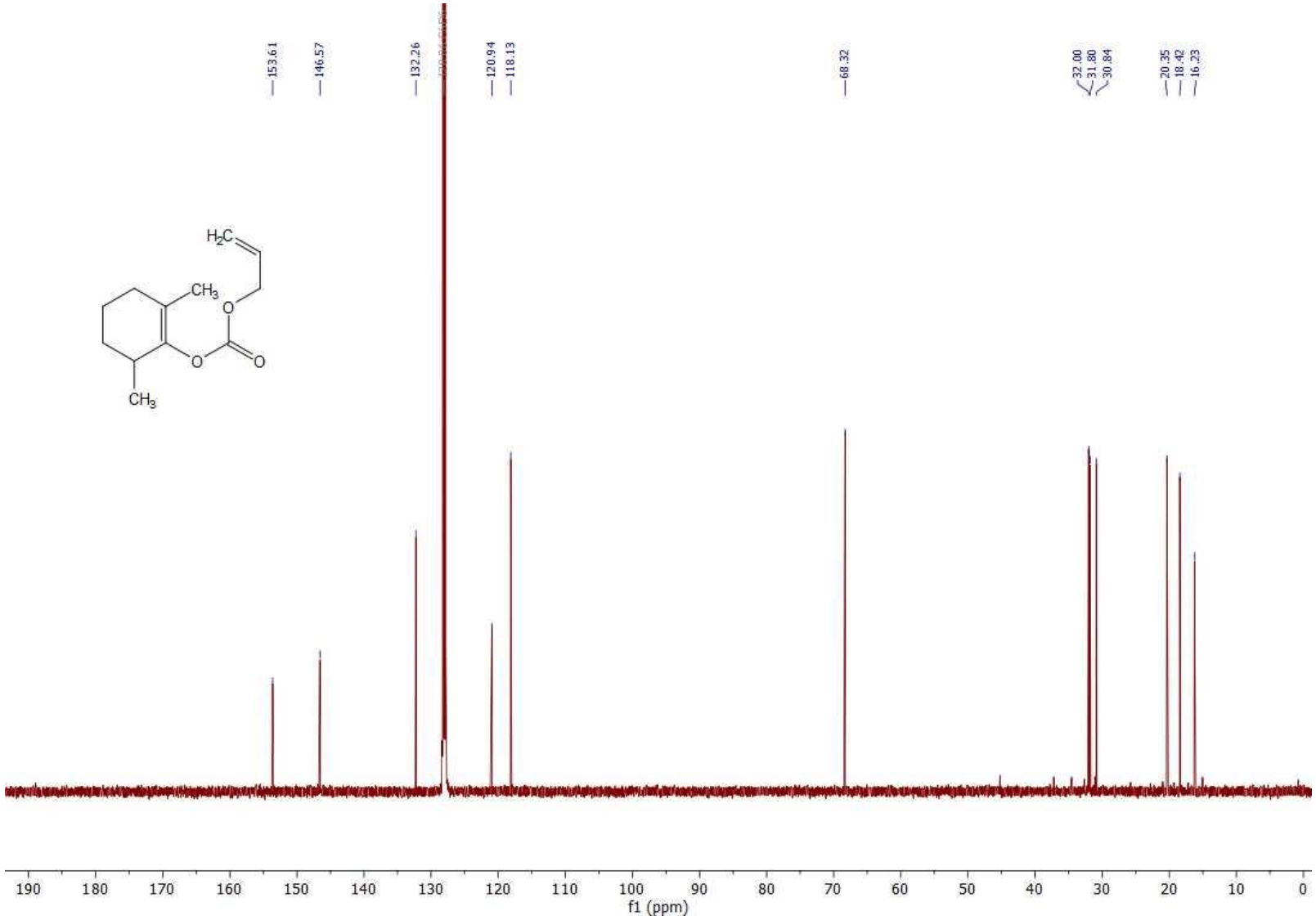

Figure S46. ^{13}C-NMR spectrum of synthetic **29** (126 MHz, C_6D_6).

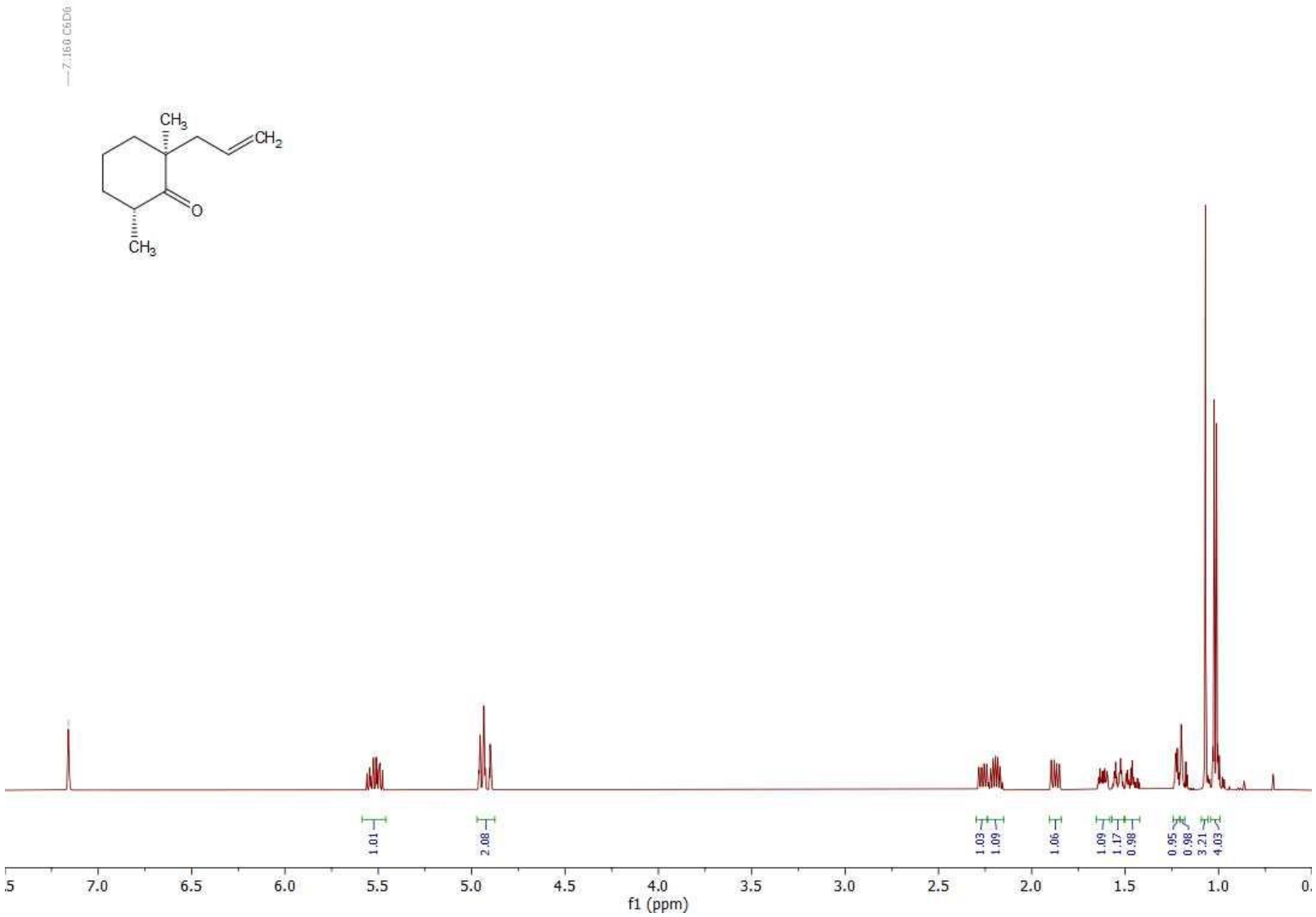

Figure S47. ^{1}H-NMR spectrum of synthetic **31a** (500 MHz, C_6D_6).

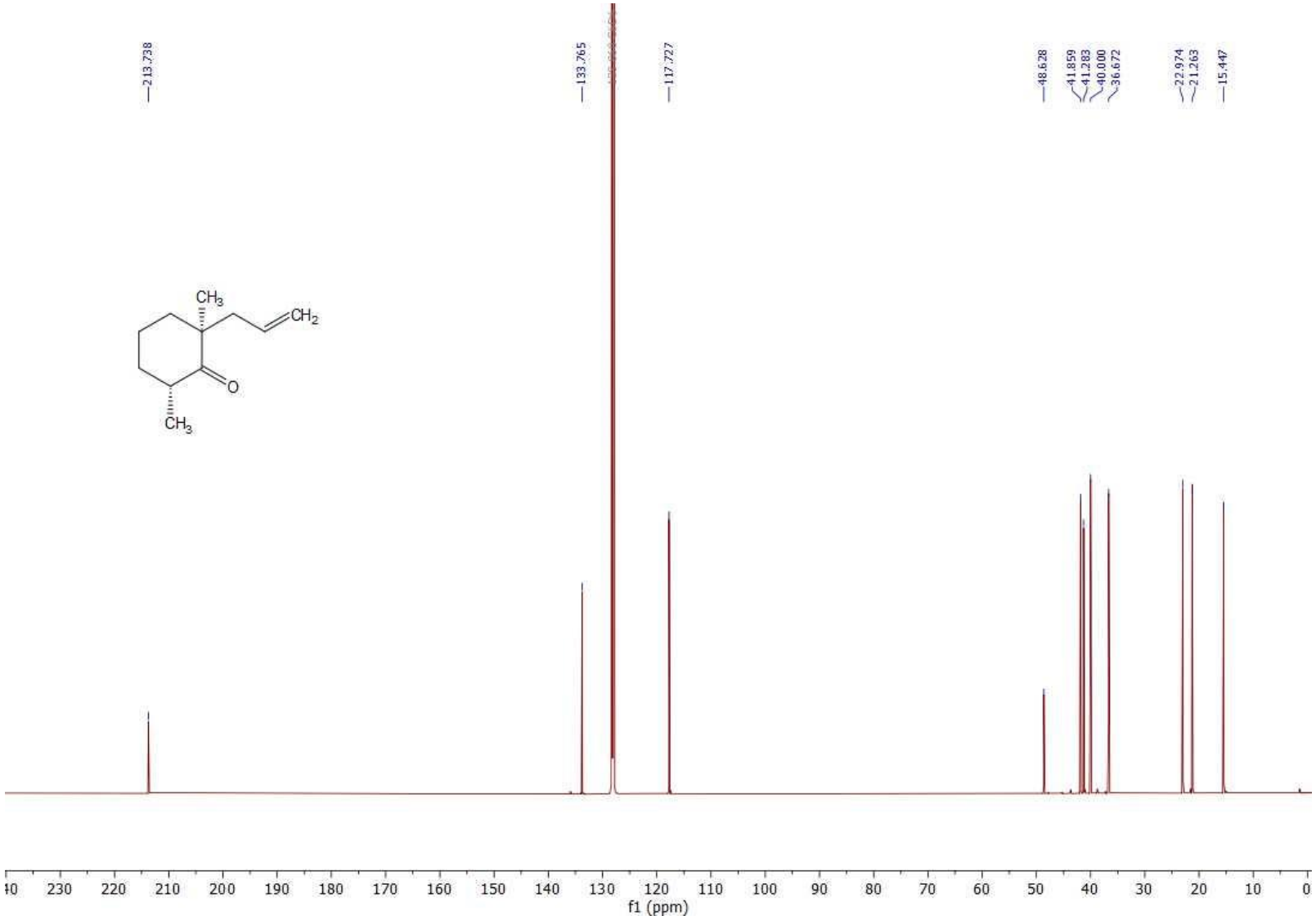

Figure S48. ^{13}C-NMR spectrum of synthetic **31a** (126 MHz, C_6D_6).

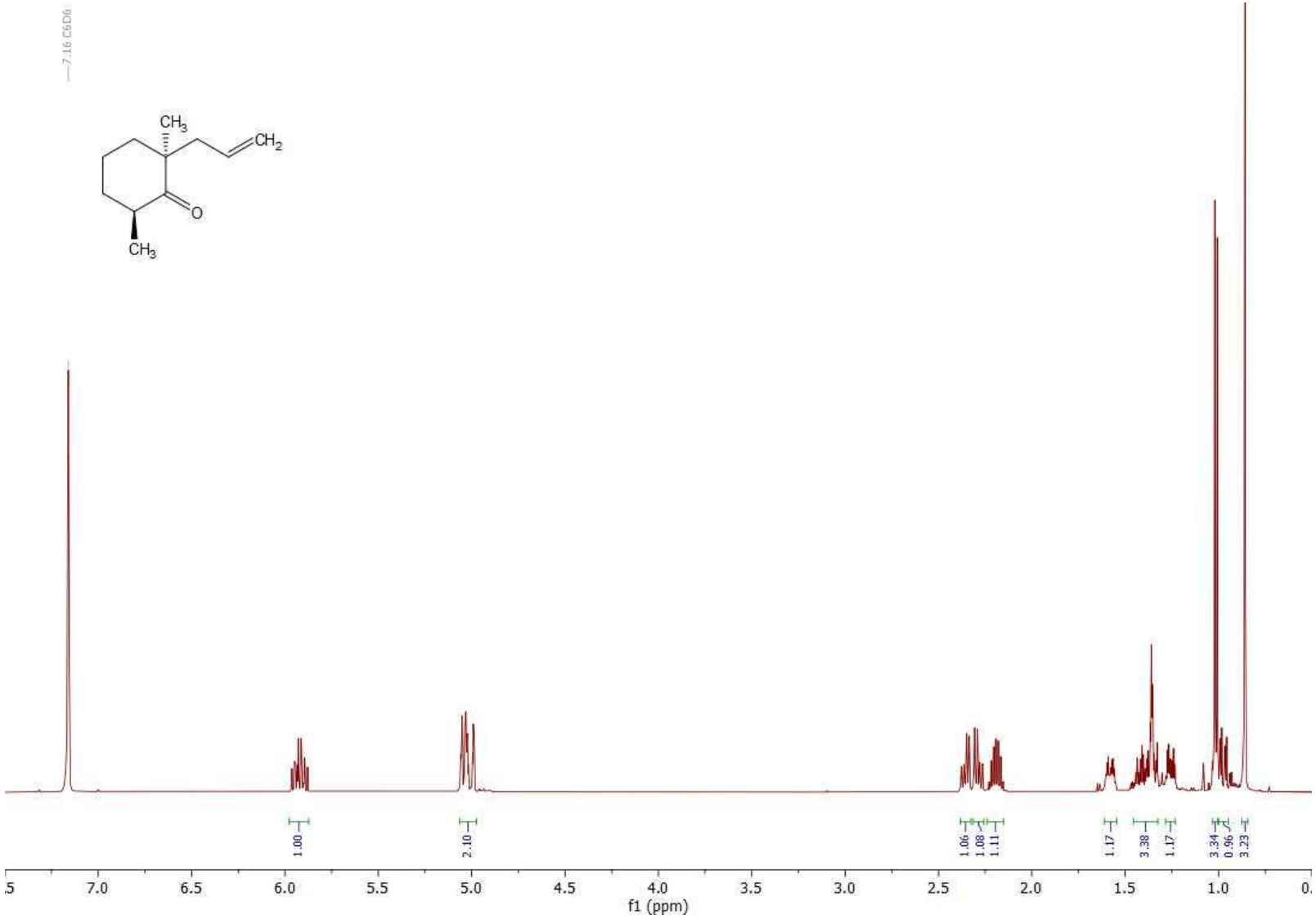

Figure S49. ^{1}H-NMR spectrum of synthetic **31b** (500 MHz, C_6D_6).

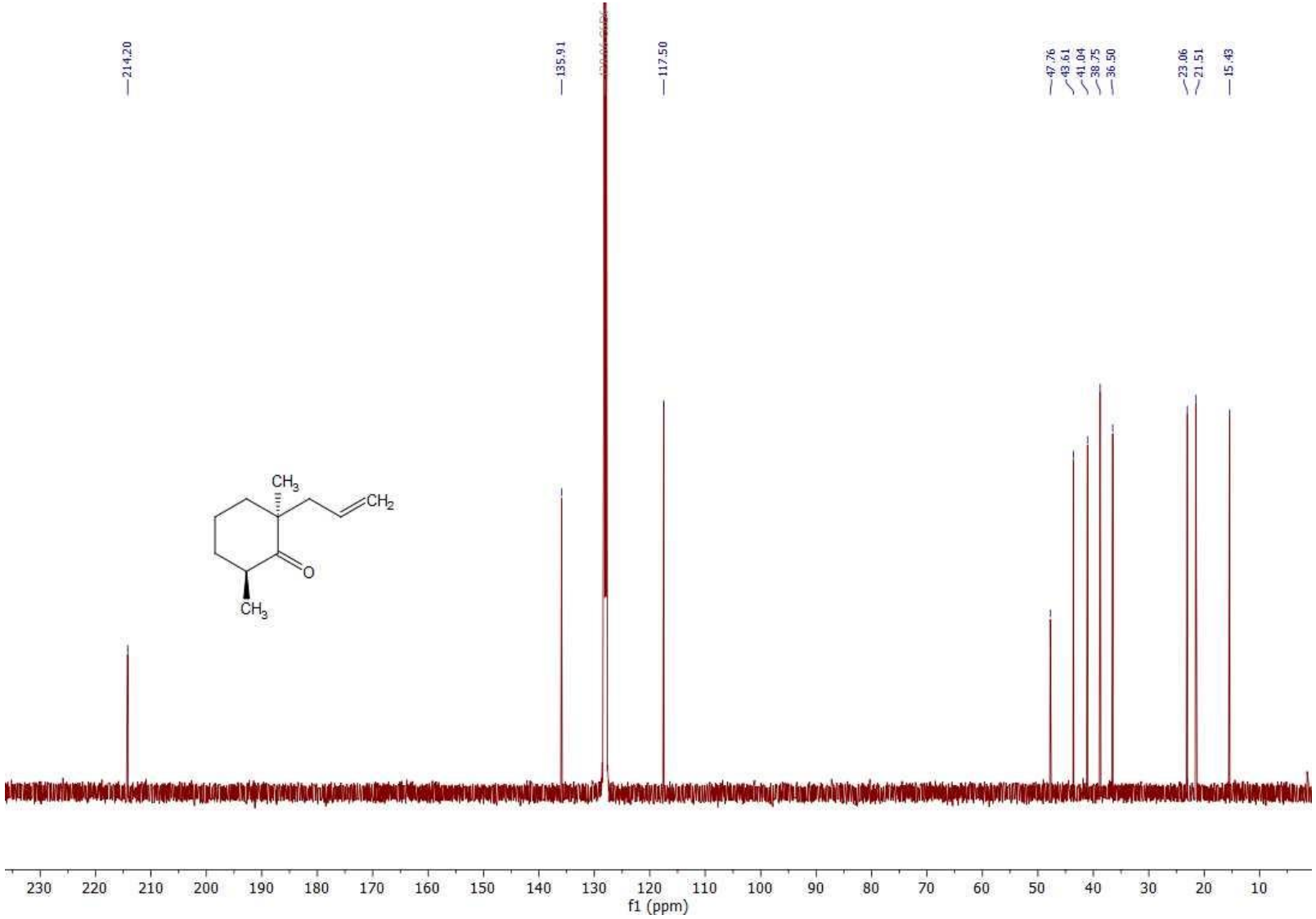

Figure S50. ^{13}C-NMR spectrum of synthetic **31b** (126 MHz, C_6D_6).

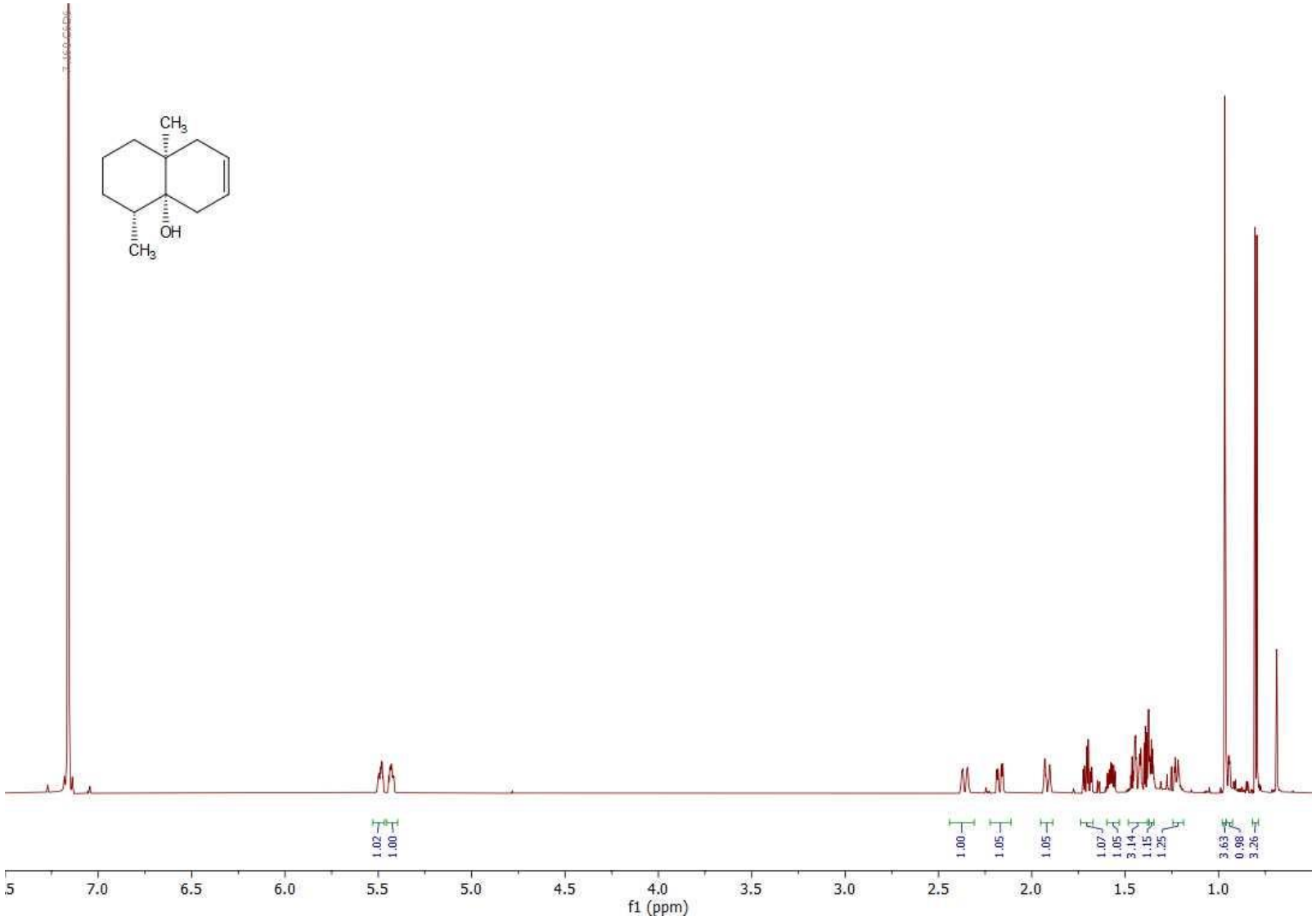

Figure S51. ^{1}H-NMR spectrum of synthetic **33a** (700 MHz, C_6D_6).

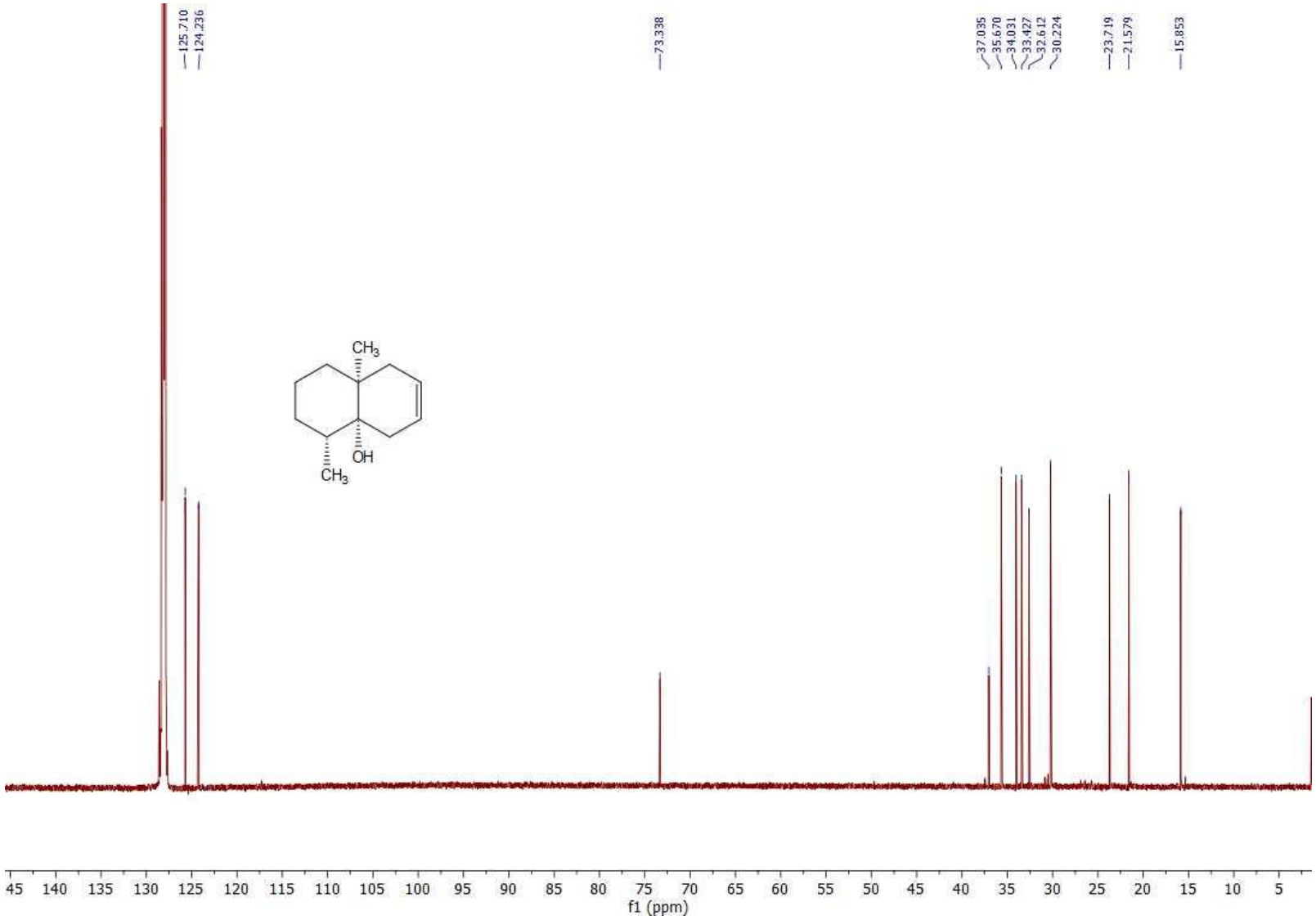

Figure S52. ^{13}C-NMR spectrum of synthetic **33a** (176 MHz, C_6D_6).

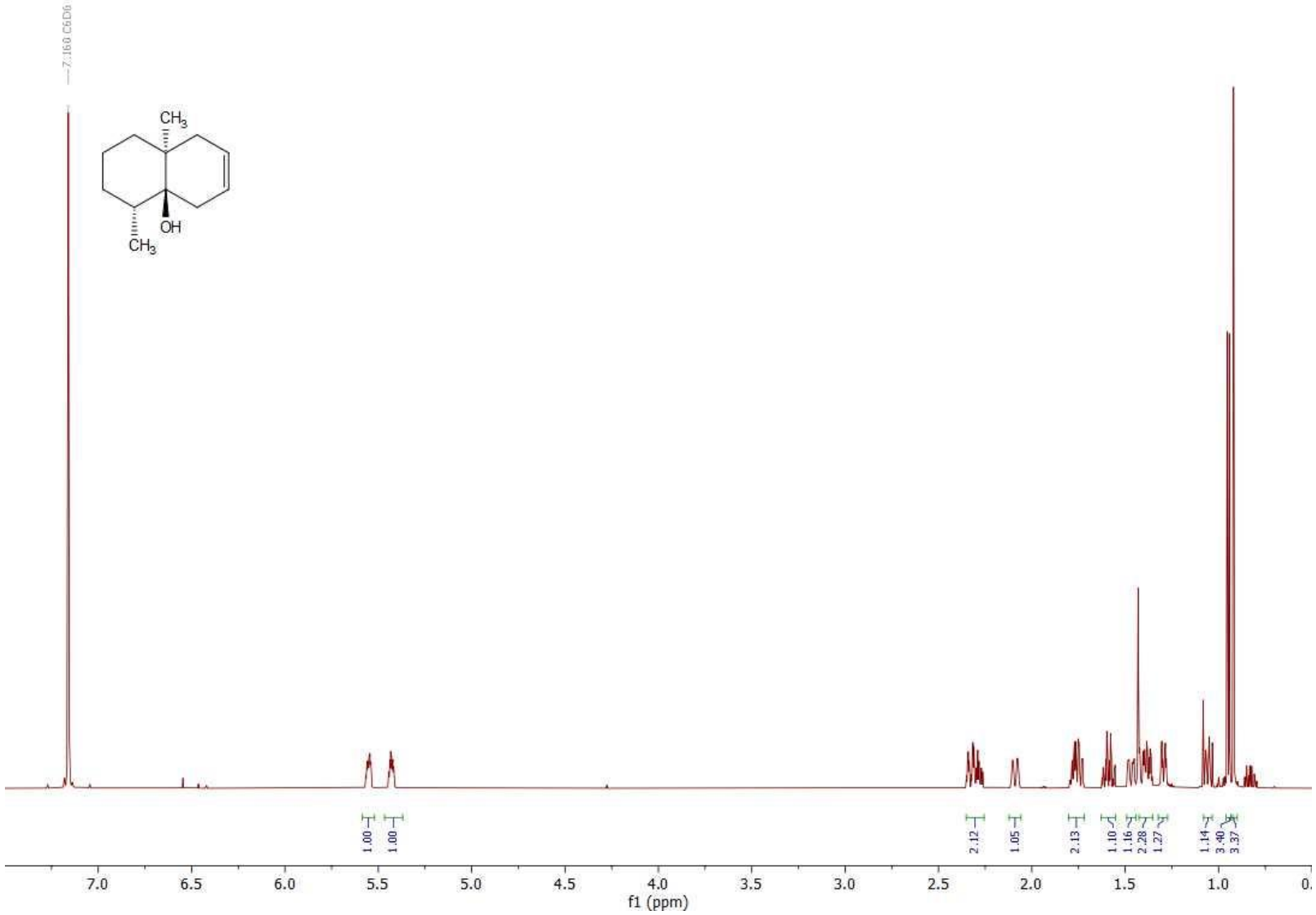

Figure S53. ^{1}H-NMR spectrum of synthetic **33b** (700 MHz, C_6D_6).

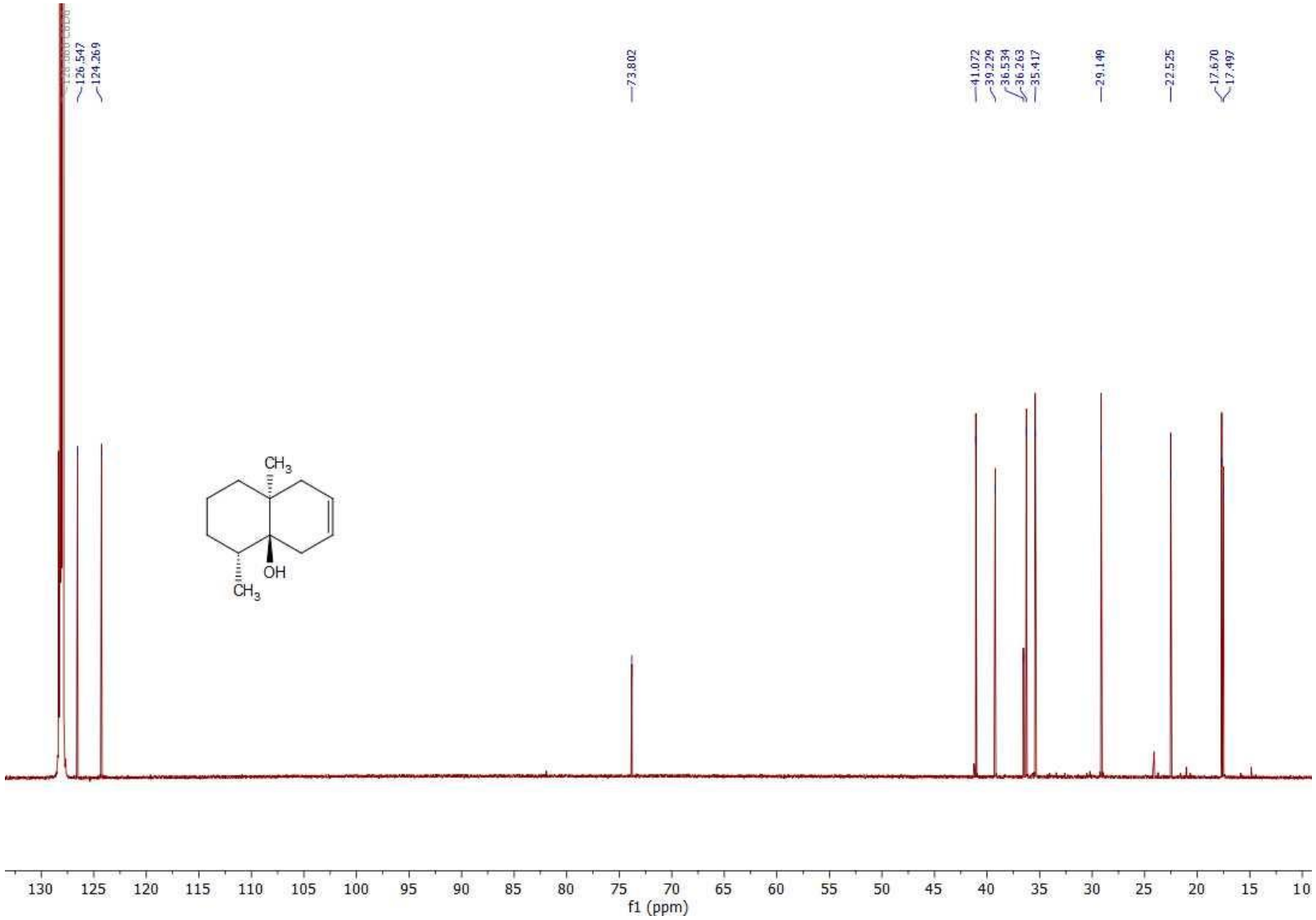

Figure S54. ^{13}C-NMR spectrum of synthetic **33b** (176 MHz, C_6D_6).

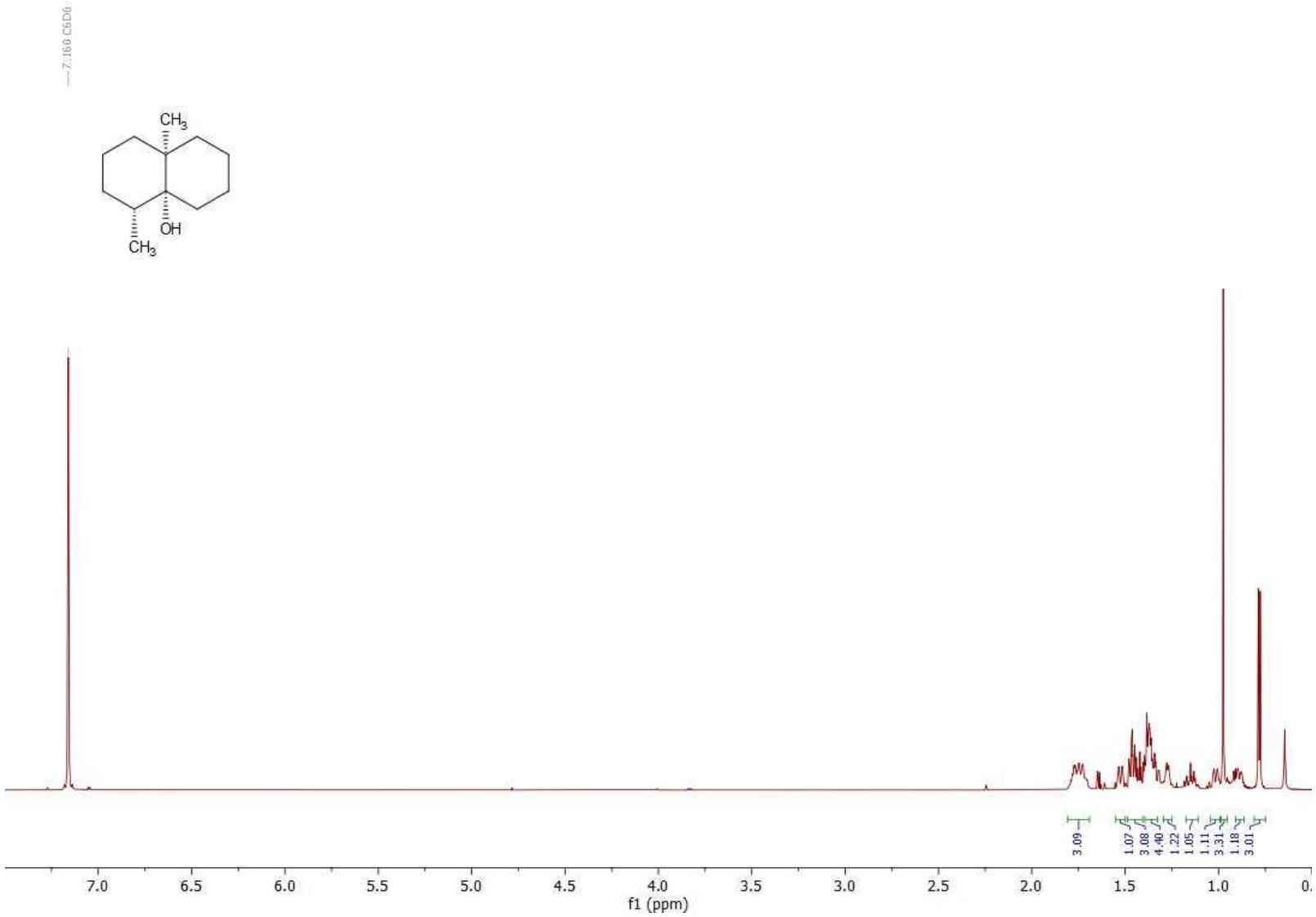

Figure S55. ^{1}H-NMR spectrum of synthetic **34** (700 MHz, C_6D_6).

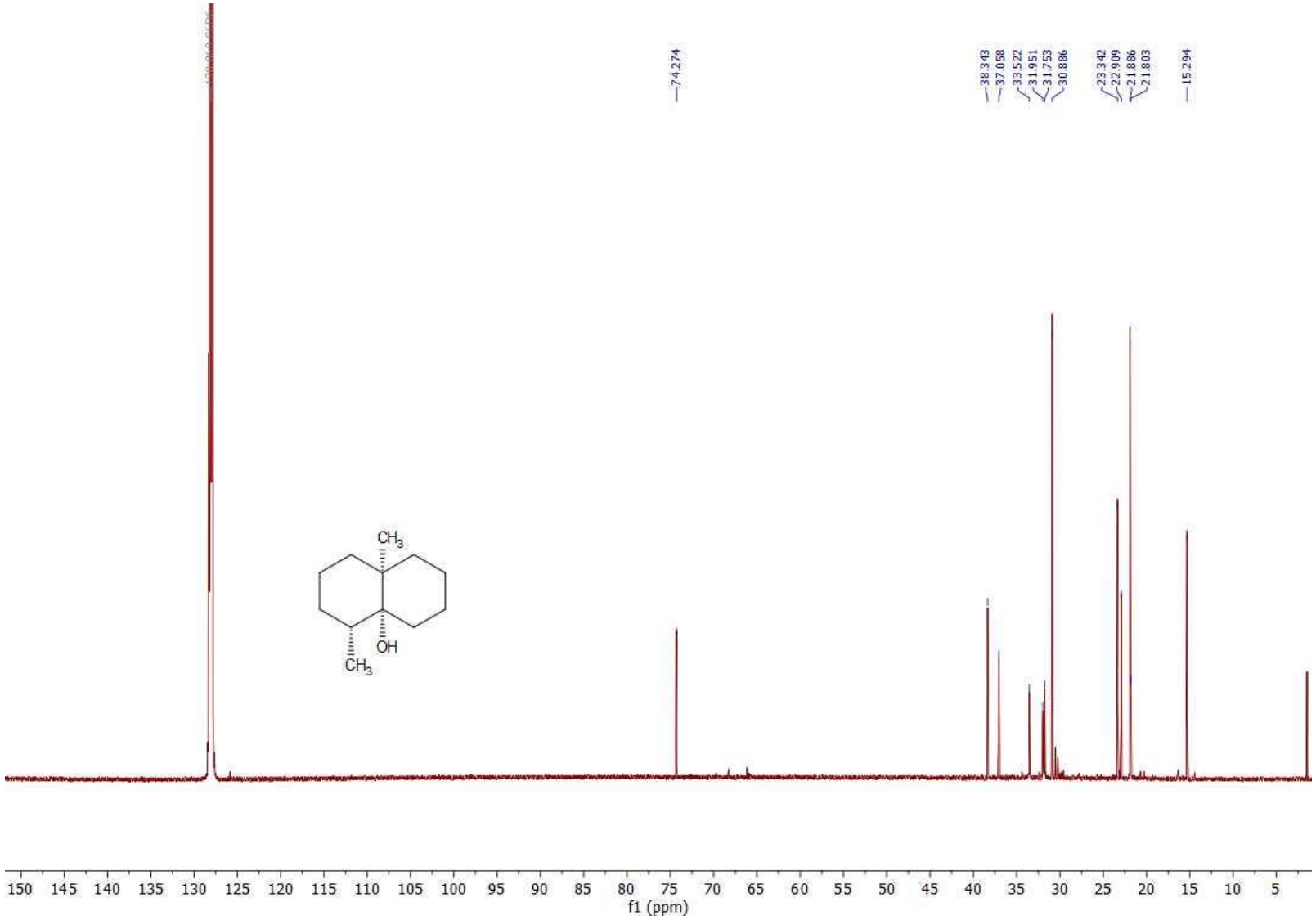

Figure S56. ^{13}C-NMR spectrum of synthetic **34** (176 MHz, C_6D_6).

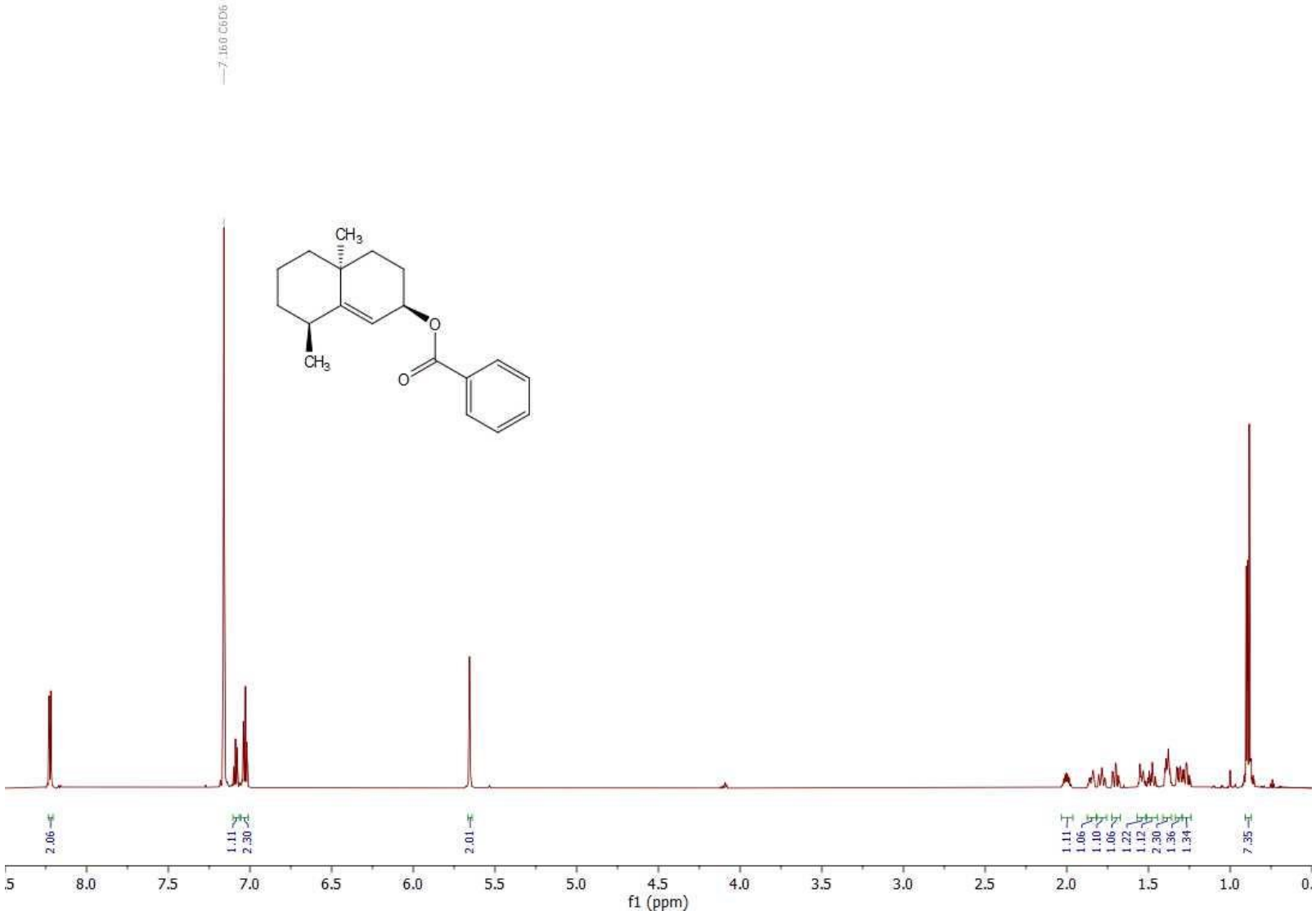

Figure S57. ^{1}H-NMR spectrum of synthetic **35** (700 MHz, C_6D_6).

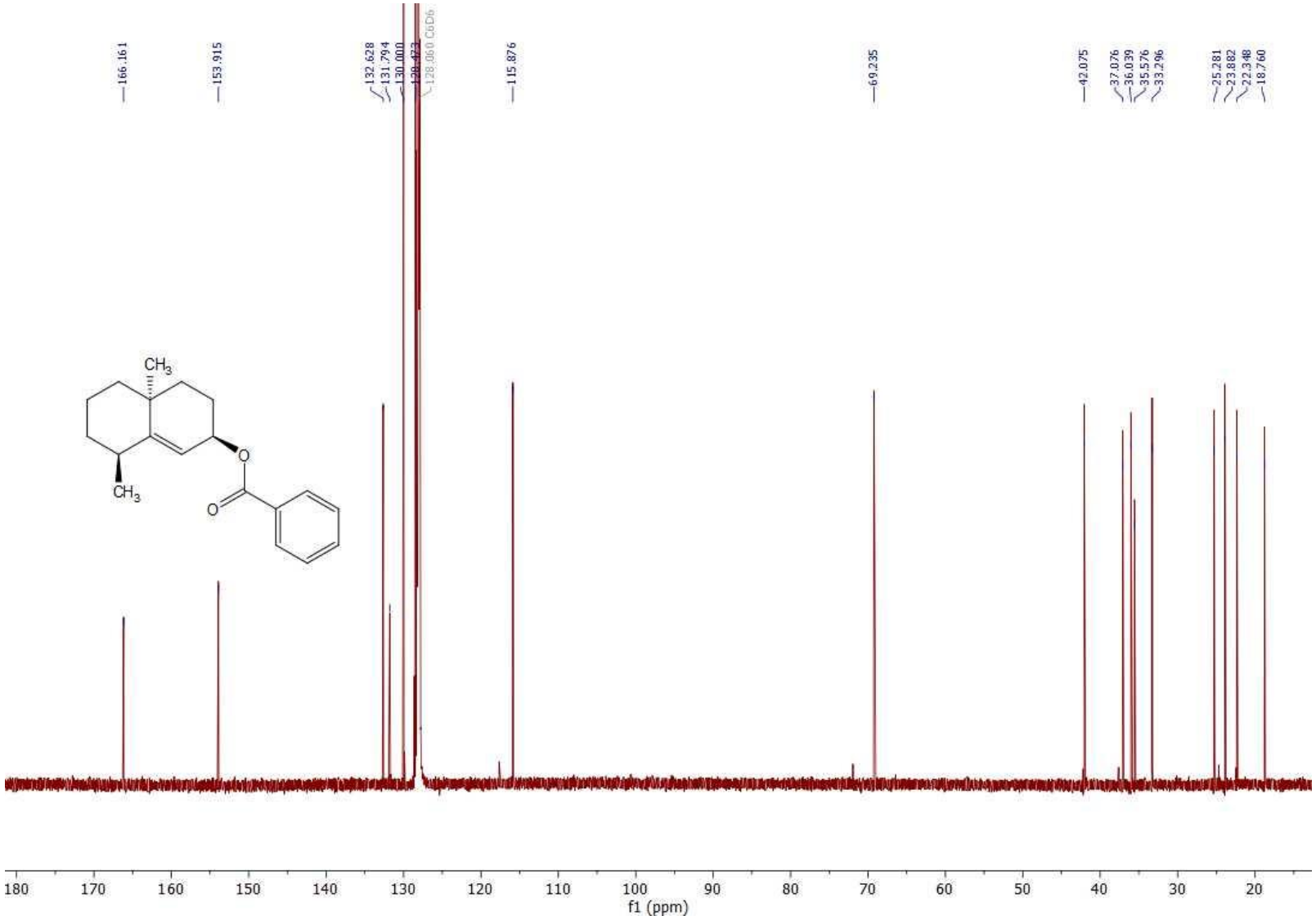

Figure S58. ^{13}C-NMR spectrum of synthetic **35** (176 MHz, C_6D_6).

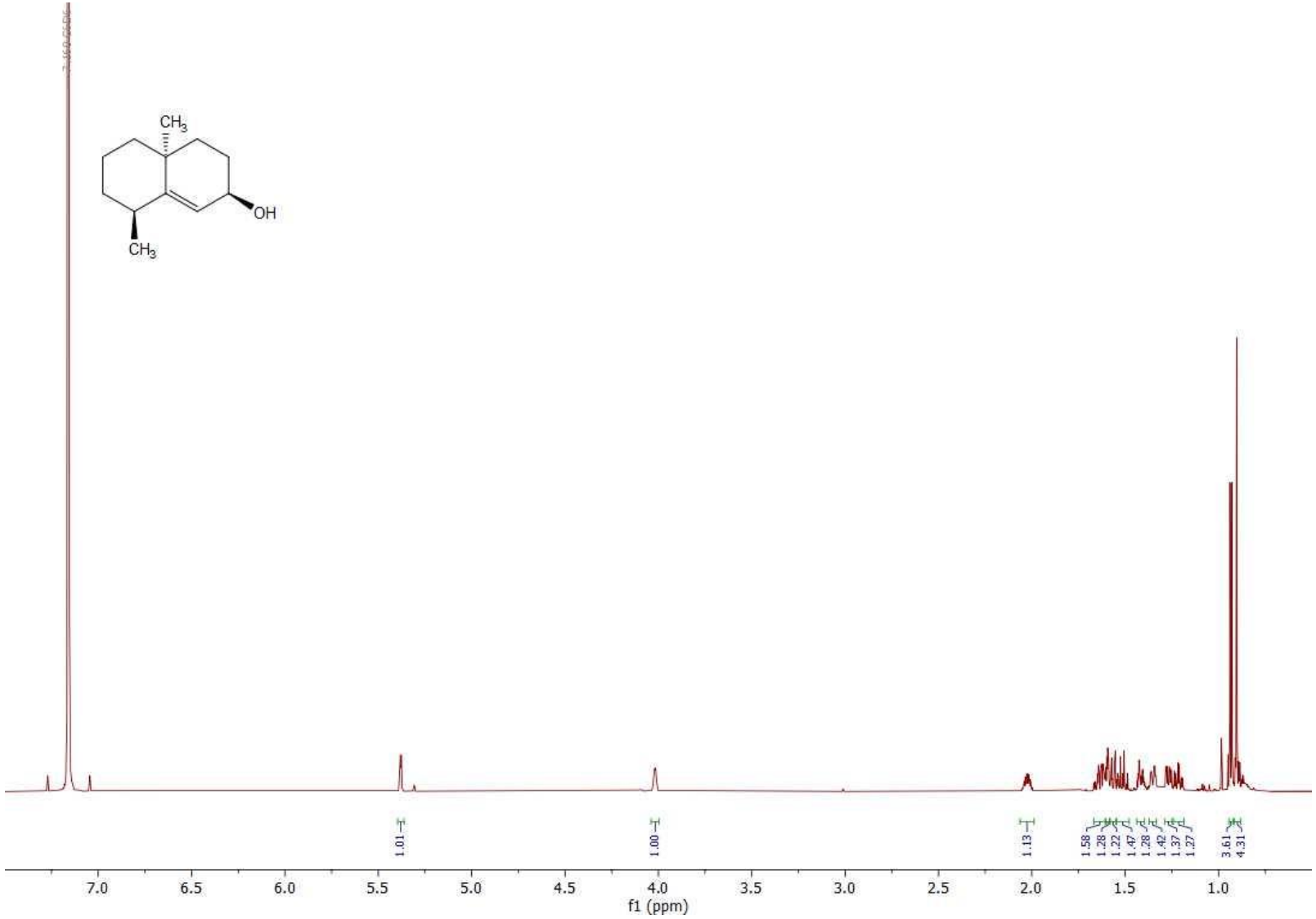

Figure S59. ^{1}H-NMR spectrum of synthetic **36** (700 MHz, C_6D_6).

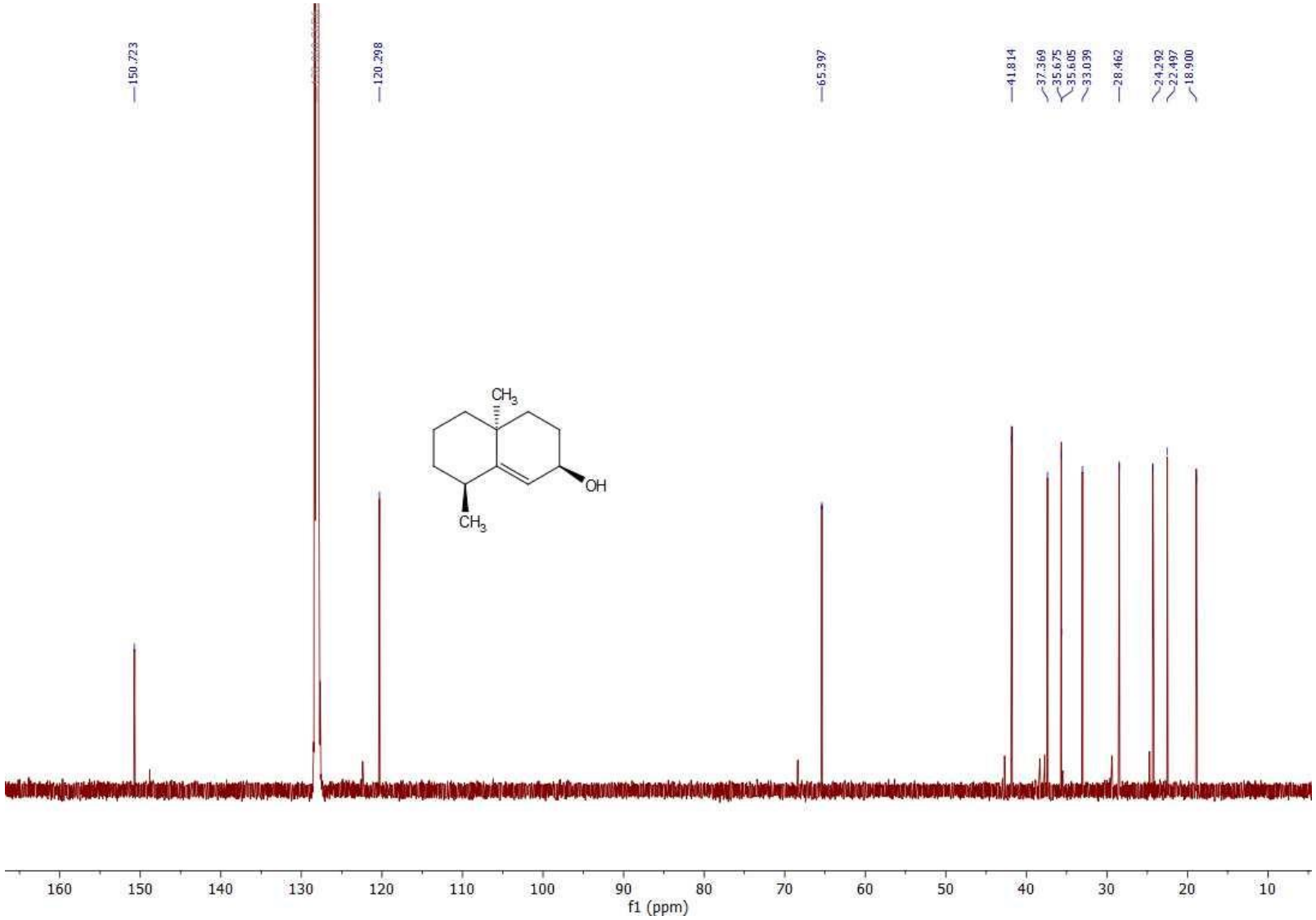

Figure S60. ^{13}C-NMR spectrum of synthetic **36** (176 MHz, C_6D_6).

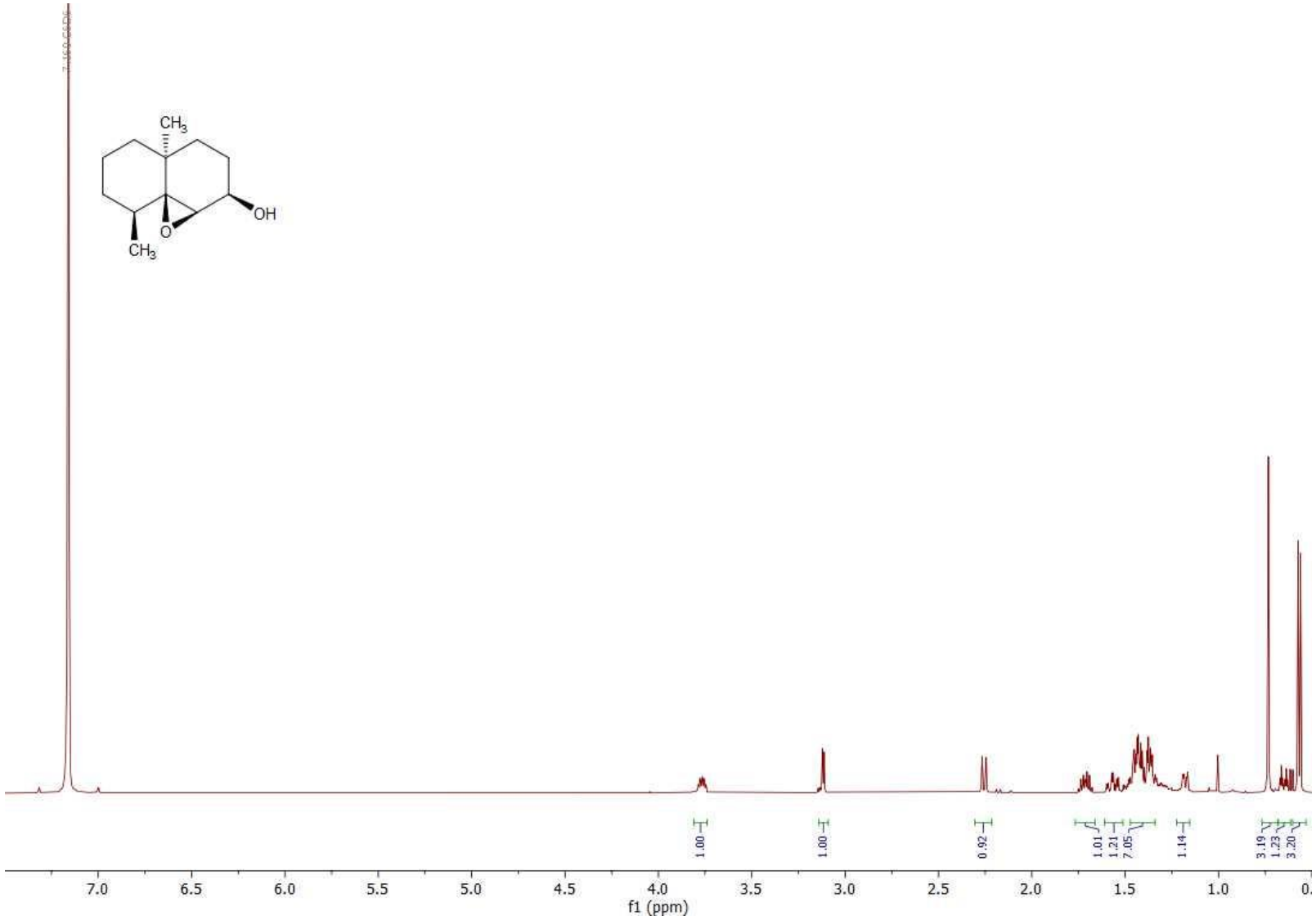

Figure S61. ^{1}H-NMR spectrum of synthetic **37a** (500 MHz, C_6D_6).

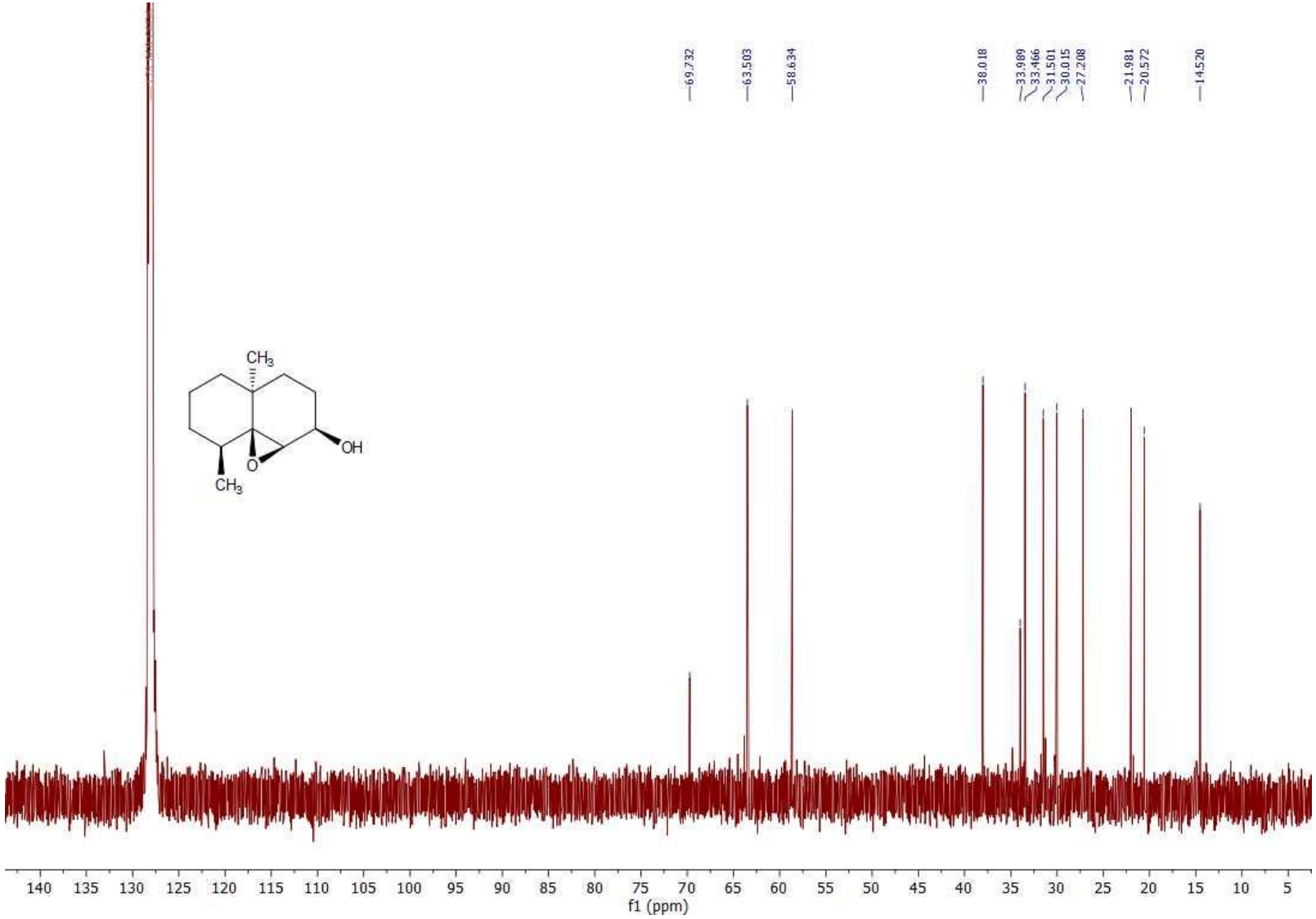

Figure S62. ^{13}C-NMR spectrum of synthetic **37a** (126 MHz, C_6D_6).

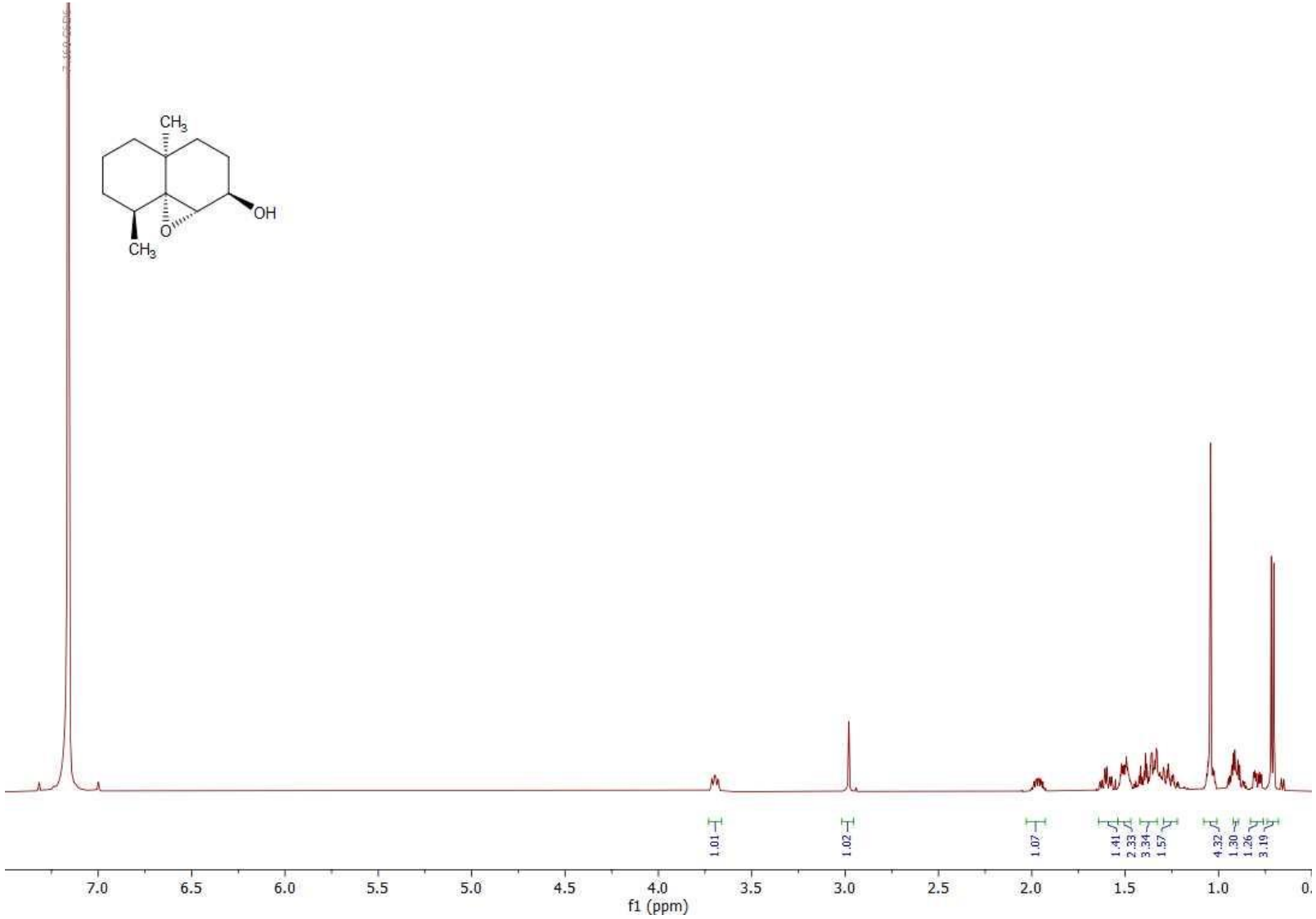

Figure S63. ^{1}H-NMR spectrum of synthetic **37b** (500 MHz, C_6D_6).

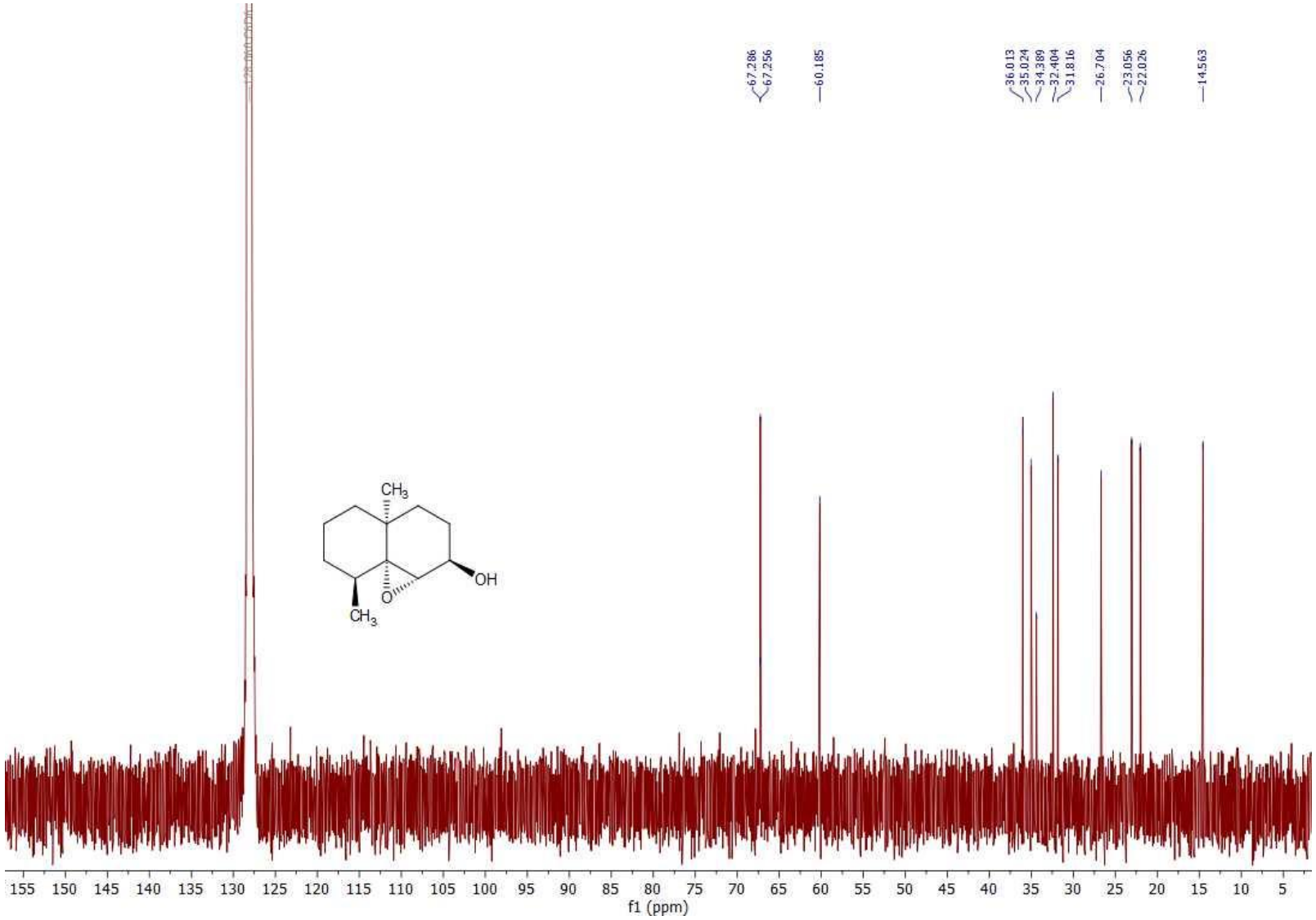

Figure S64. ^{13}C-NMR spectrum of synthetic **37b** (126 MHz, C_6D_6).

References

1. G. R. Fulmer, A. J. M. Miller, N. H. Sherden, H. E. Gottlieb, A. Nudelman, B. M. Stoltz, J. E. Bercaw and K. I. Goldberg, *Organometallics*, 2010, **29**, 2176-2179.
2. J. Koziskova, F. Hahn, J. Richter and J. Kozisek, *Acta Chimica Slovaca*, 2016, 9, 136-140.
3. G. M. Sheldrick, *Acta Crystallogr. A Found. Adv.*, 2015, **71**, 3-8.
4. G. M. Sheldrick, *Acta Crystallogr. C*, 2015, **71**, 3-8.
5. O. V. Dolomanov, L. J. Bourhis, R.J. Gildea, J. A. K. Howard and H. Puschmann, *J. Applied. Cryst.*, 2009, **42**, 339-341.
6. L. Ding and C. Hertweck, *J. Nat. Prod.*, 2020, **83**, 2207-2211.
7. K. Grob and F. Zürcher, *J. Chromatogr. A.*, 1976, **117**, 285-294.
8. J. Jiang, X. He and D. E. Cane, *J. Am. Chem. Soc.*, 2006, **128**, 8128-8129.
9. J. S. Dickschat, K. A. K. Pahirulzaman, P. Rabe and T. A. Klapschinski, *ChemBioChem* 2014, **15**, 810-814.
10. H. Xu and J. S. Dickschat, *ChemBioChem*, 2023, **24**, e202300101.
11. M. M. Bradford, *Anal. Biochem.*, 1976, **72**, 248-254.